Development and application of an analytical method for the determination of total atmospheric biogenic non-methane organic carbon

Dissertation

zur Erlangung des Grades
„Doktor der Naturwissenschaften“
im Promotionsfach Chemie

am Fachbereich Chemie, Pharmazie und Geowissenschaften
der Johannes Gutenberg-Universität
in Mainz

Julia Regnery
geboren in Trier
Mainz, August 2012

„Bazinga“

Dr. Sheldon Cooper

Zusammenfassung

Ein wesentlicher Anteil an organischem Kohlenstoff, der in der Atmosphäre vorhanden ist, wird als leichtflüchtige organische Verbindungen gefunden. Diese werden überwiegend durch die Biosphäre freigesetzt. Solche biogenen Emissionen haben einen großen Einfluss auf die chemischen und physikalischen Eigenschaften der Atmosphäre, indem sie zur Bildung von bodennahem Ozon und sekundären organischen Aerosolen beitragen. Um die Bildung von bodennahem Ozon und von sekundären organischen Aerosolen besser zu verstehen, ist die technische Fähigkeit zur genauen Messung der Summe dieser flüchtigen organischen Substanzen notwendig. Häufig verwendete Methoden sind nur auf den Nachweis von spezifischen Nicht-Methan-Kohlenwasserstoffverbindungen fokussiert. Die Summe dieser Einzelverbindungen könnte gegebenenfalls aber nur eine Untergrenze an atmosphärischen organischen Kohlenstoffkonzentrationen darstellen, da die verfügbaren Methoden nicht in der Lage sind, alle organischen Verbindungen in der Atmosphäre zu analysieren. Einige Studien sind bekannt, die sich mit der Gesamtkohlenstoffbestimmung von Nicht-Methan-Kohlenwasserstoffverbindung in Luft beschäftigt haben, aber Messungen des gesamten organischen Nicht-Methan-Verbindungsaustauschs zwischen Vegetation und Atmosphäre fehlen. Daher untersuchten wir die Gesamtkohlenstoffbestimmung organische Nicht-Methan-Verbindungen aus biogenen Quellen. Die Bestimmung des organischen Gesamtkohlenstoffs wurde durch Sammeln und Anreichern dieser Verbindungen auf einem festen Adsorptionsmaterial realisiert. Dieser erste Schritt war notwendig, um die stabilen Gase CO, CO_2 und CH_4 von der organischen Kohlenstofffraktion zu trennen. Die organischen Verbindungen wurden thermisch desorbiert und zu CO_2 oxidiert. Das aus der Oxidation entstandene CO_2 wurde auf einer weiteren Anreicherungseinheit gesammelt und durch thermische Desorption und anschließende Detektion mit einem Infrarot-Gasanalysator analysiert. Als große Schwierigkeiten identifizierten wir (i) die Abtrennung von CO_2 aus der Umgebungsluft von der organischen Kohlenstoffverbindungsfaktion während der Anreicherung sowie (ii) die Widerfindungsraten der verschiedenen Nicht-Methan-Kohlenwasserstoff-verbindungen vom Adsorptionsmaterial, (iii) die Wahl des Katalysators sowie (iiii) auftretende Interferenzen am Detektor des Gesamtkohlenstoffanalysators. Die Wahl eines Pt-Rd Drahts als Katalysator führte zu einem bedeutenden Fortschritt in Bezug

auf die korrekte Ermittlung des CO_2-Hintergrund-Signals. Dies war notwendig, da CO_2 auch in geringen Mengen auf der Adsorptionseinheit während der Anreicherung der leichtflüchtigen organischen Substanzen gesammelt wurde. Katalytische Materialien mit hohen Oberflächen stellten sich als unbrauchbar für diese Anwendung heraus, weil trotz hoher Temperaturen eine CO_2-Aufnahme und eine spätere Abgabe durch das Katalysatormaterial beobachtet werden konnte. Die Methode wurde mit verschiedenen leichtflüchtigen organischen Einzelsubstanzen sowie in zwei Pflanzenkammer-Experimenten mit einer Auswahl an VOC-Spezies getestet, die von unterschiedlichen Pflanzen emittiert wurden. Die Pflanzenkammer-messungen wurden durch GC-MS und PTR-MS Messungen begleitet. Außerdem wurden Kalibrationstests mit verschiedenen Einzelsubstanzen aus Permeations-/Diffusionsquellen durchgeführt. Der Gesamtkohlenstoffanalysator konnte den tageszeitlichen Verlauf der Pflanzenemissionen bestätigen. Allerdings konnten Abweichungen für die Mischungsverhältnisse des organischen Gesamtkohlenstoffs von bis zu 50% im Vergleich zu den begleitenden Standardmethoden beobachtet werden.

Abstract

A major fraction of organic carbon which is present in the atmosphere is found as volatile organic compounds (VOCs) that are dominantly emitted by the biosphere. These biogenic emissions have a major impact on the chemical and physical properties of the atmosphere by contributing to the formation of tropospheric ozone and secondary organic aerosol (SOA). In order to better understand the ozone and aerosol formation processes in the atmosphere the technical ability to accurately measure the sum of these volatile organics is necessary. Frequently used methods focus on the detection of specific non-methane organic compounds (NMOC). However, adding these single compound based concentrations might only represent a lower limit of atmospheric carbon concentrations, since the available methods are not capable to analyze all organic compounds present in the atmosphere. A few studies are known that report on total NMOC concentration analysis in ambient air but measurements of the total NMOC exchange between vegetation and the atmosphere are missing. Therefore, we investigated the limits of a total NMOC concentration analysis by collecting VOC compounds on a solid adsorbent material for subsequent total carbon analysis. This first step was necessary to separate the stable gases CO, CO_2 and CH_4 from the volatile NMOC fraction. The NMOC compounds were desorbed and converted to CO_2 by passing an oxidation unit. The CO_2 resulting from oxidation was collected on a second preconcentration unit followed by thermal desorption and detection by an infrared gas analyzer. As major difficulties we identified the (i) separation of ambient CO_2 from the NMOC fraction on the solid adsorbent unit, (ii) recovery rates of the different NMOC compounds from the solid adsorbent unit, (iii) the choice of the catalytic material and (iiii) major interferences on the detector of the analyzer. The choice of a Pt-Rd wire as a catalyst led to a major progress concerning the correct determination of the CO_2 background signals. This was necessary as CO_2 was also collected in small amounts on the NMOC solid adsorbent unit. Catalytic materials with high surfaces appeared to be impractical for this application because of CO_2 storage and release even at high temperatures. The method was tested with different single VOC compounds as well as within two plant chamber experiments comprising a variety of major VOC species emitted from a mixture of plant species. The plant chamber measurements were accompanied by GC-MS and PTR-MS analysis of single VOC species. Furthermore,

calibration tests were performed with single compounds derived from permeation/diffusion devices. The total NMOC analysis confirmed the diurnal course of plant emissions. However, discrepancies for the total carbon mixing ratios of up to 50% could be observed in comparison to the accompanying default methods.

Contents

1. General introduction

Carbon is the molecular basis of all life on earth. It circulates in a biogeochemical cycle exchanging among the biosphere, the pedosphere, the geosphere, the hydrosphere, and the atmosphere of the Earth. Figure 1 shows an overview of the global carbon cycle. It can be divided into two categories: the geological cycle, which operates over large time scales (millions of years), and the biological/physical cycle, which operates at shorter time scales (days to thousands of years).[1] The carbon is stored in so called reservoirs that can hold the carbon for long periods of time. The deep oceans and fossil fuel reserves represent such major carbon reservoirs. Normally they do not contribute to the shorter carbon cycling time scales.

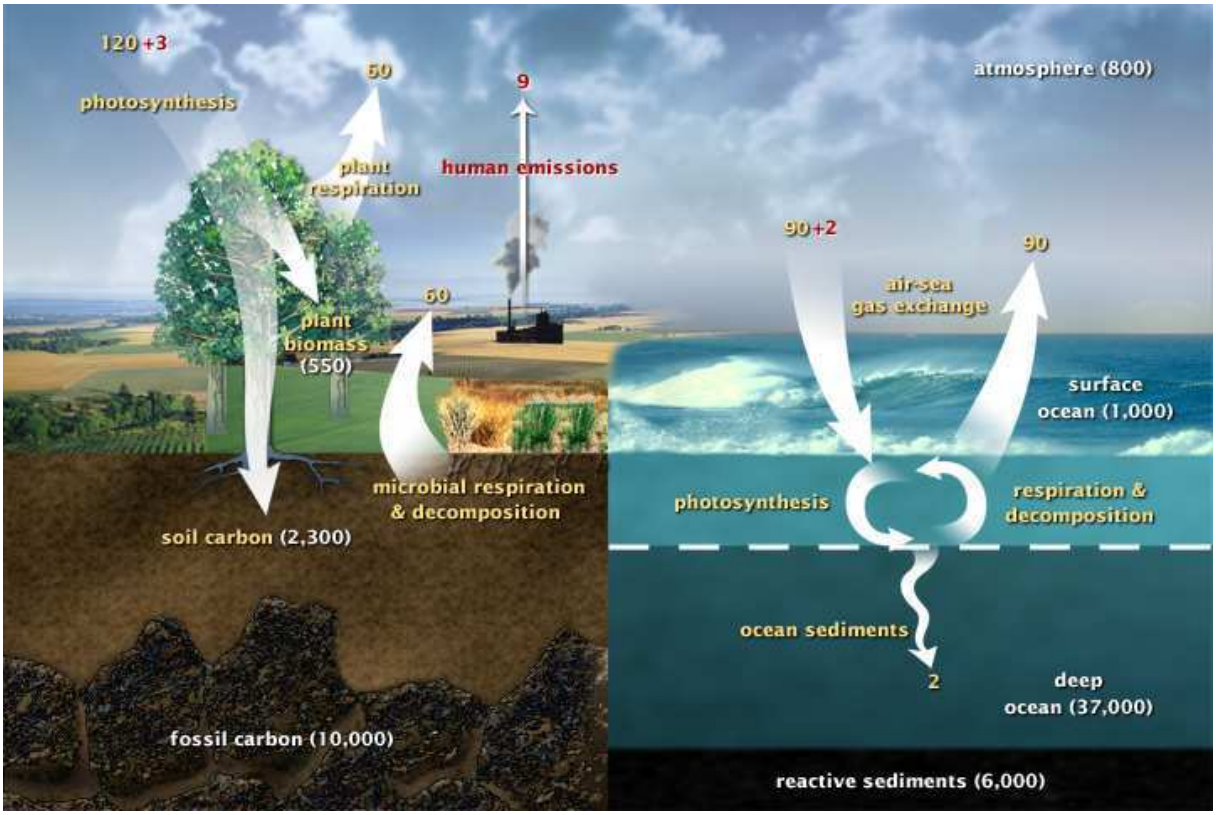

Figure 1: The biological/physical carbon cycle and the circulation of carbon between the atmosphere, land, and oceans in gigatons of carbon per year. Yellow numbers indicate natural fluxes, red numbers are human contributions and white numbers represent carbon storages.[2]

[1] http://earthobservatory.nasa.gov/Features/CarbonCycle/carbon_cycle2001.pdf
[2] http://earthobservatory.nasa.gov/Features/CarbonCycle/?src=eoa-features

However, human influence and the usage of combustible fossil fuels leads to a transfer of carbon from the long term reservoirs to the short term cycle which results in a permanent carbon increase on the short time scales. In comparison to the major carbon reservoirs, the atmosphere and the terrestrial biosphere represent a smaller carbon reservoir. Nevertheless next to the oceans these carbon pools play a substantial role on the short term cycle of carbon. About half of the CO_2 which is emitted by anthropogenic sources is absorbed by terrestrial and marine environment (see Figure 1, red numbers). Therefore, this carbon uptake is limiting the extent of atmospheric and climatic change, but its long-term nature remains uncertain (Schimel *et al.* 2001). The balance of the carbon exchanges between the different reservoirs is referred to as the global carbon budget. This global carbon budget is crucial for the understanding of climate change as the CO_2 increase influences the atmosphere. CO_2 absorbs infrared radiation, which influences the climate and leads to global warming. Therefore, it has become a focal topic in various disciplines because of the observed increase in levels of atmospheric CO_2 (from 280 ppm in 1800 to 315 ppm in 1957 to 356 ppm in 1993 (Schimel 1995) to 380 ppm in 2006 (Fowler *et al.* 2009, IPCC 2007)) due to anthropogenic influences. A detailed knowledge about the processes and influences within the carbon cycle are necessary for future climate predictions. In the past decades the knowledge of the global carbon cycle has increased. Balancing the carbon budget definitely requires the terrestrial biosphere, which acts as a sink for the anthropogenic CO_2 (Fung *et al.* 1997). Plants are able to use the atmospheric CO_2 and fixate it through photosynthesis as carbohydrates. However, the vegetation can also act as a source for carbon and has an important contribution to the trace gas exchanges. Many of the major theoretical issues regarding the regulation of trace gas exchange at the scale of leaves and whole plants, have been successfully addressed and major progress has been made in linking these scales for CO_2 (Lerdau and Gray 2003, Malmstrom *et al.* 1997, Randerson *et al.* 1999). Additionally to the CO_2 exchange the biosphere emits a considerable amount of volatile organic compounds (VOC) into the atmosphere (Kesselmeier and Staudt 1999). With regard to the carbon budget of the terrestrial biosphere, a release of these carbon compounds is regarded as a loss of photosynthetically fixed carbon (Kesselmeier *et al.* 2002). Whilst CO_2 exchange between the biosphere and the atmosphere is thought to be well understood, the impact of the vegetation on the trace gas exchange of volatile organic compounds

needs to be investigated further. Due to the complex processes of carbon storage, the manifold diversity of vegetation and the impact on land use and land management, it is difficult to quantify the role of the terrestrial biosphere in the global carbon cycle.

1.1 VOCs in the atmosphere

The composition of the atmosphere consists of the main constituents N_2 (78%), O_2 (21%) and Ar (0.9%). The remaining gaseous constituents, the trace gases, represent less than 1% of the atmosphere. The carbon that is present in the atmosphere belongs to this group of trace gases and is mainly found as inorganic compounds like carbon dioxide (CO_2) and carbon monoxide (CO). Their mixing ratios are approximately ~390 ppm for CO_2 (Wolff 2011) and ~1 ppm for CO (Finlayson-Pitts 2000, Seinfeld 1997). Methane (CH_4) is the most abundant volatile organic compound in the atmosphere with mixing ratios of ~1.7 ppm (Park 2001). In contrast to the mixing ratio of CH_4 the amount of other volatile organic compounds (VOC) represents a much smaller pool of organic carbon in the atmosphere. Nevertheless, these volatile organic compounds play a major role in atmospheric chemistry, as the VOCs are more reactive and more diverse in their structure (e.g. saturated and non-saturated hydrocarbons or oxygenated volatiles (Kesselmeier and Staudt 1999)). Volatile organic compounds (VOC) (Fehsenfeld *et al.* 1992, Kesselmeier and Staudt 1999) is the most frequently used term for the description of organic carbon compounds with a low vapor pressure. The inorganic compounds CO_2 and CO are excluded from this denotation. However, there is no uniform definition of which compound is actually included into this denotation. Some definitions include information on the actual vapor pressure[3,4] while others define the term VOC on the atmospheric photochemical reactivity of the compounds[5,6,7]. In some definitions certain organic substances are explicitly excluded from the VOC definition. Methane due to its long atmospheric lifetime is frequently excluded and the terms non-methane volatile organic compound (NMVOC) (Chung Myeong Y. *et al.* 2010, Lanz

[3] http://toxics.usgs.gov/definitions/vocs.html
[4] http://www.bmu.de/files/pdfs/allgemein/application/pdf/richtlinie_emission.pdf
[5] http://eur-lex.europa.eu/LexUriServ/site/de/com/2005/com2005_0447de01.pdf
[6] http://toxics.usgs.gov/definitions/vocs.html
[7] http://www.epa.gov/ttn/naaqs/ozone/ozonetech/def_voc.htm

et al. 2009, Sidiropoulos and Tsilingiridis 2007), non-methane hydrocarbons (NMHC) (Baker *et al.* 2011, Choi *et al.* 2011, von Schneidemesser *et al.* 2011) or non-methane organic compound (NMOC) (Blanchard *et al.* 2011, Shreffler 1993, Yung-Chen *et al.* 2009) are used. A variety of other terms also apply. As VOCs can have their origin in anthropogenic and biogenic sources another important term for the distinction is needed – biogenic volatile organic compound (BVOC) (Kesselmeier and Staudt 1999, Kim Leesun *et al.* 2011a, Kim S. *et al.* 2011b, Simpraga *et al.* 2011). Biogenic VOCs include the isoprenoids (isoprene and monoterpenes), as well as alkanes, alkenes, carbonyls, alcohols, esters, ethers, and acids (Kesselmeier and Staudt 1999). Emissions from the biosphere are versatile and a huge number of different NMOC species have been identified by now. The great diversity of the biogenic volatile organics indicates a major problem concerning their determination. The versatile number of different compounds is linked to an equivalent number of problems which include sampling and analysing techniques, understanding the biological metabolisms and the biological emission/deposition regulations, and describing and modelling the exchange as well as the atmospheric chemistry of all these compounds (Kesselmeier and Staudt 1999). Biogenic VOC emissions exceed anthropogenic emissions on a global scale by far. Estimates of current fluxes amount to 700-1100 x 10^{12} g of organic carbon per year, which get emitted by the biosphere (Guenther *et al.* 1995, Laothawornkitkul *et al.* 2009). In comparison, on a global scale, only approximately 150 x 10^{12} g of carbon are emitted from anthropogenic sources (Lindfors and Laurila 2000, Müller 1992). However, emissions occur locally. Biogenic emissions emerge mainly in the tropics, in the northern midlatitudes and the boreal regions during summer (IPCC 2001). Anthropogenic VOC emissions mostly appear in industrial regions in the northern hemisphere. Together with emitted nitrogen oxide compounds (NO_x) they have a substantial impact on the regional air chemistry. Nevertheless, due to the high VOC emissions from the biosphere, they largely effect the atmospheric composition. That implies that VOCs influence the chemical and physical properties of the atmosphere. Figure 2 shows an overview of the chemical processes in the troposphere involving VOC emissions.

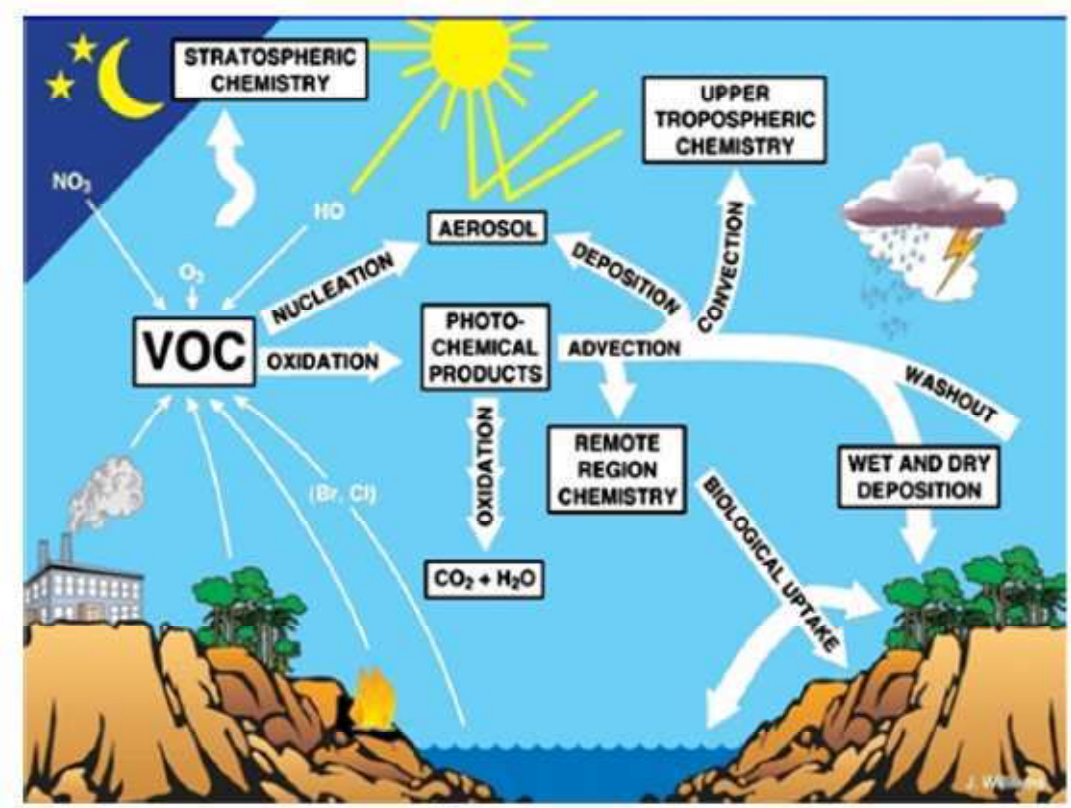

Figure 2: Schematic overview of tropospheric chemistry (Monks *et al.* 2009).

A major decomposition reaction of VOCs in the atmosphere is with OH radicals. Additionally, reactions with NO_3 radicals during night time and O_3, as well as with Cl and Br atoms in coastal areas are possible (Atkinson and Arey 2003). Another transformation process of VOCs in the atmosphere originates from photolysis at wavelengths > 290 nm. Which degradation mechanism applies is dependent on the volatile organic compound. In most cases the reaction mechanism involves formation of an alkyl or substituted alkyl radical or oxoalkyl (Atkinson and Arey 2003). Several products can be formed from the different reactions. The diversity of the reaction products from degradation processes is a typical characteristic of atmospheric chemistry. Considering the reaction of the monoterpene compound α–pinene with O_3, more than 30 reaction products can be formed (Dindorf 2006). Furthermore, many reaction products are less volatile than their precursors and promote the formation of secondary organic aerosol (SOA). Biogenic volatile organic compounds are much more reactive than VOCs emitted by anthropogenic sources. With their short lifetimes they influence the chemistry of the atmosphere significantly. Table 1 gives an overview of estimated atmospheric lifetimes of selected biogenic volatile organic compounds.

Table 1: Estimated atmospheric lifetimes of selected biogenic VOCs (Atkinson and Arey 2003, Hewitt *et al.* 2011).

Biogenic VOC	Lifetime by reaction with		
	OH[(a)]	O_3[(b)]	NO_3[(c)]
Isoprene	1.4 h	1.3 day	1.6 h
C10 monoterpenes			
Alpha-pinene	2.6 h	4.6 h	11 min
Beta-pinene	1.8 h	1.1 day	27 min
Limonene	49 min	2 h	5 min
Alpha-terpinene	23 min	1 min	0.5 min
C15 sesquiterpenes			
β-caryophyllene	42 min	2 min	3 min
Longifolene	2.9 h	>33 day	1.6 h
Oxygenated VOCs			
Linalool	52 min	55 min	6 min
Acetone	61 day	>4.5 y	>8 y
Methanol	12 day	>4.5 y	2 y
Cis-3-hexen-1-ol	1.3 h	6.2 h	4 h

[(a)]Assuming 12-h daytime average OH radical concentration of 2×10^6 molecules/cm^3.
[(b)]Assuming 24-h average O_3 concentration of 7×10^{11} molecules/cm^3.
[(c)]Assuming 12-h nighttime average NO_3 radical concentration of 2.5×10^8 molecules/cm^3.

Nitrogen oxides (NO_x) are also emitted into the troposphere or are produced by precursors in it. Natural sources are soils and fires as well as the in situ formation in the troposphere from lightning. However NO_x are also emitted from anthropogenic combustion processes. The estimated worldwide emissions of NO_x (including formation from lightning) are 10 million t yr^{-1} (as N) from biogenic or natural sources and 40 million to yr^{-1} (as N), respectively, from anthropogenic sources (Atkinson 2000). The combination of VOC and NO_x emissions leads to the formation of photochemical air pollution, which occurs mainly in urban areas with a lot of industrial influence. The most known compound which is formed due to these photochemical reactions is ozone. In general, the net photochemical formation of O_3 results in a photoequilibrium. No ozone is formally lost or formed. A schematic overview of the ozone formation is shown in Figure 3. The photolysis of NO_2 leads to the formation of ozone. The formed O_3 however, rapidly reacts with NO. The ratio between NO, NO_2 and O_3 is balanced (Figure 3 A). In the presence of nitrogen oxide, the degradation of the VOCs leads to intermediate alkyl peroxy (RO_2) and hydroperoxide (HO_2) radicals. The reactions of these radicals with NO result in NO_2, as well as hydroxyl (OH) and alkoxy (RO) radicals. Furthermore, the formed NO_2 photolyzes and leads to the formation of ozone (Figure 3 B). As a consequence, a net production of ozone occurs. However, atmospheric reactions are versatile and a variety of other factors play an important part for the chemical processes in the troposphere.

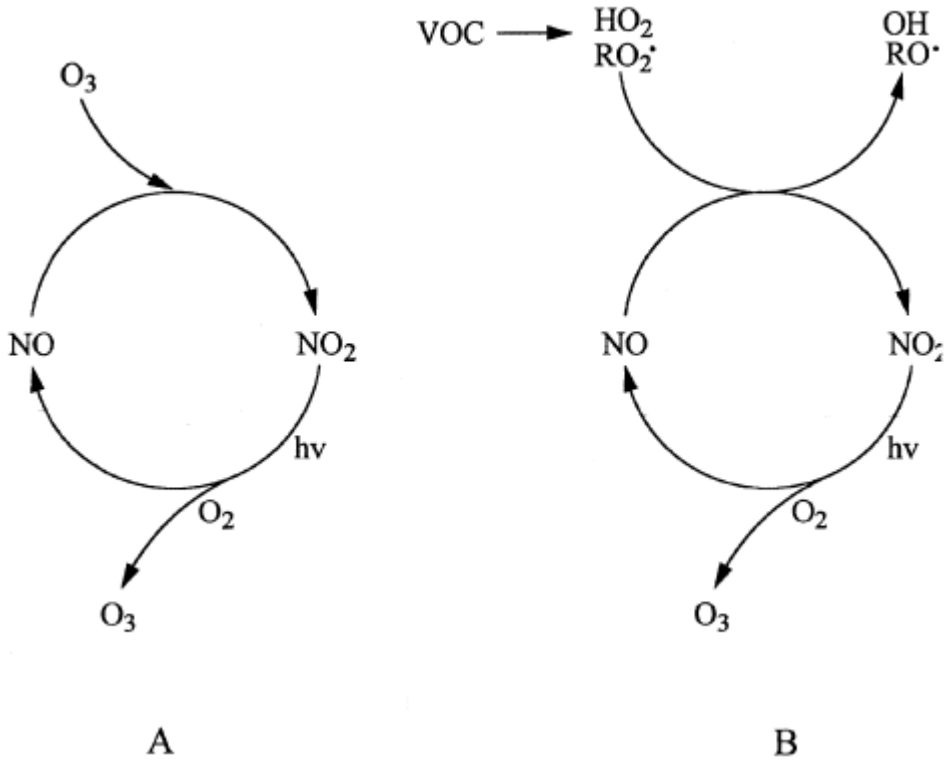

Figure 3: Scheme of ozone formation without VOC influence (A) and with VOC influence (B) (Atkinson 2000).

In view of the dominant contribution of biogenic VOC fluxes, their understanding is crucial for atmospheric chemistry processes and future climate predictions. However, estimates of global fluxes of biogenic VOCs are uncertain. Changes in land use and factors influencing the emission of VOCs from terrestrial plants lead to high uncertainties for global models, which try to predict future atmospheric scenarios.

1.2 VOC exchange by the biosphere

The dominant source for atmospheric VOCs is the biosphere. The annual global natural VOC flux (excluding methane) is estimated to be 1150 Tg of carbon, which is composed of 44% isoprene, 11% monoterpenes, 22.5% other reactive VOCs, and 22.5% other (relatively unreactive) VOCs (Guenther *et al.* 2006, Guenther *et al.* 1995). This composition includes compounds like terpenoids (e.g. isoprene and monoterpenes), alcohols, esters, carbonyls and acids, as well as alkanes and alkenes. Plants produce a large number of volatiles based on many secondary plant metabolic pathways (Laothawornkitkul *et al.* 2009). Their purposes are not always

understood, but it is assumed that VOCs are important as signalling agents and as protectants against biotic and abiotic stresses (Hewitt C.N. *et al.* 2011, Laothawornkitkul *et al.* 2009).

As it became clear in the latter paragraph, biogenic VOCs affect the air quality and the climate. The biosphere-atmosphere interactions are of great importance. Therefore, quantifying the biogenic VOC emission rates and determining their impact on atmospheric chemistry became a research focus in the past decades. Isoprene is the most predominant compound emitted by biogenic sources, followed by monoterpenes. Terpene compounds like sesquiterpenes were also recognized in the past, especially because of their potential to form SOA. The terrestrial vegetation also emits a variety of non-terpenoid compounds. They implement oxygenated VOCs such as alcohols, ketones, aldehydes and esters but also non-oxygenated VOCs like alkenes, alkanes and aromatics. The oxygenated VOCs are the most dominant non-terpeniod compounds emitted by the biosphere (Seco *et al.* 2007). Recent studies indicate that alkenes are also emitted in considerable amounts, whereas alkanes and aromatics only make a very small contribution to biogenic VOC fluxes (Kirstine *et al.* 1998, Monks *et al.* 2009). Table 2 gives an overview of the major classes of volatile organic compounds.

Table 2: The major classes of biogenic volatile organic compounds, the major group of BVOC emitting plants and estimates of current and future BVOC fluxes into the atmosphere adapted from Laothawornkitkul *et al.* 2009 and further information added from Dindorf *et al.* (2006), Kesselmeier and Staudt (1999), Rottenberger *et al.* (2008).

BVOC species	Present estimated annual global emission (10^{12} g C)	Future estimated annual global emission (10^{12} g C)	atmospheric lifetimes (d)	Example	Major emitting plants
Total	700-1000	1251-1288			
Isoprene	412-601	638-689	0.2		Populus, Salix, Platanus, Cocos, Elaeis, Casuarina, Picea, Quercus and Eucalyptus
Monoterpene	33-480	265-316	0.1-0.2	β-pinene, α-pinene, limonene	Lycopersicon, Quercus, Cistus, Fagus, Malus, Pinus and Trichostema
Other reactive BVOCs	~260	~56-159 (only for acetaldehyde and formaldehyde)	< 1	Acetaldehyde, 2-methyl-3-buten-2-ol and hexenal family	Grassland (mix of C_3 plants), Vitis, Brassica, Secale, Betula and flooded plants
Other less reactiv BVOCs	~260	~292-514 (only for methanol, acetone, formic acid and acetic acid)	> 1	Methanol, ethanol, formic acid, acetic acid and acetone	Grassland (mix of C_3 plants), Vitis, Brassica, Secale, Betula and flooded plants
Ethylene	8-25		1.9		

The diversity of the VOC compounds emitted by plants, leads to a large number of problems for sampling and analysis techniques. The choice of the sampling method for the determination of VOC emissions has to be adapted to the special compounds or measurement surroundings. Research applications can vary from the leaf and

branch scale to earth observations (Figure 4). The major challenges of sampling VOCs is a short sampling time as VOC emissions are influenced by a variety of different factors like light, temperature, wounding, CO_2 concentration and humidity. The applied sampling method has to consider these factors, despite the difficulties entailed. The second challenge is the chemical and physical characteristics of the different VOCs. They vary in properties like reactivity, adsorption behavior or solubility in different mediums. As shown in Figure 4, research focuses on different studies that include laboratory measurements, field studies and earth observations which are used to determine the biosphere atmosphere interaction.

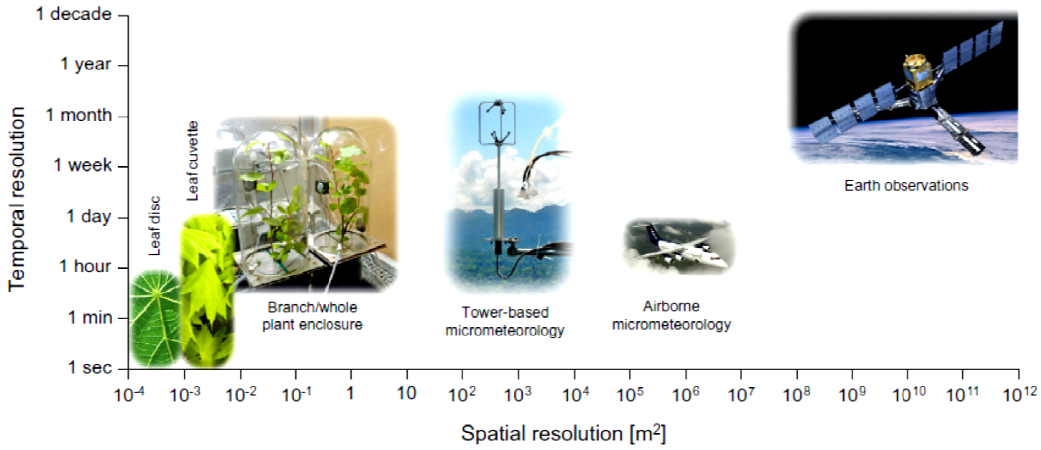

Figure 4: Biogenic VOC sampling approaches and their spatial and temporal scales (Hewitt C.N. *et al.* 2011).

A multitude of different analytical techniques is applied to quantify VOC emissions from the biosphere to the atmosphere. Flux measurements of ambient air at canopy scale are quite often difficult, as biogenic VOCs are very reactive and have only low atmospheric concentrations. Alternatively leaf- and branch-level enclosure techniques can be used to determine biogenic VOC fluxes of reactive and low-volatile compounds. These quantitative leaf-or branch-level emission rates can be used as input data for models. With additional information of site-specific biomass and meteorological parameters, the results obtained from enclosure measurements can be scaled to canopy fluxes. However, it is a challenging task as present technologies do only allow estimates for the VOC emissions on a large scale. The major method to obtain global estimates for biogenic VOC emissions are chemistry and transport models that require time dependent regional emission estimates as an input. Uncertainties corresponding to measurements of biogenic emissions are subject to

the spatial and temporal scales used, but they also depend on the compound. Global annual isoprene emissions are believed to be known within an uncertainty factor of 2. However, the uncertainty for the emissions for a specific time and location can exceed a factor of five (Guenther *et al.* 2006, Monks *et al.* 2009). Moreover, for other biogenic compounds like monoterpenes, sesquiterpenes and oxygenated VOCs the uncertainties for the VOC emissions are much higher. Estimations of uncertainties of biogenic VOC emissions are predicted on the comparison of available databases. Variables like temperature, solar radiation, leaf area index, and vegetation type are necessary for the estimated VOC emissions on a leaf scale. As these variables already contain uncertainties, large errors occur for the resulting VOC emission estimates. Nevertheless, estimations of biogenic VOC emissions have improved as measurement techniques and the understanding of controlling factors has improved. However, natural emissions of VOC are very sensitive to changes in land cover (e.g. vegetation type and density), soil moisture, temperature and solar radiation (Monks *et al.* 2009). This must also be considered for future emission prediction. The functions of VOC emissions in plant metabolism, reproduction, growth, communication, protection and defence will evidently be influenced by the changes arising from global and climate changes, and as a result of these alterations, the structure and the functioning of organisms, communities and ecosystems might therefore change significantly (Penuelas and Staudt 2010). Figure 5 gives an overview of the effects and possible interactions of global climate changes on BVOC emissions. It indicates that various environmental factors are linked to the biogenic VOC emissions. Hence, climate change is likely to result in an increase of VOC emissions. A better knowledge of the controls and influences of these environmental factors is necessary for future emission predictions.

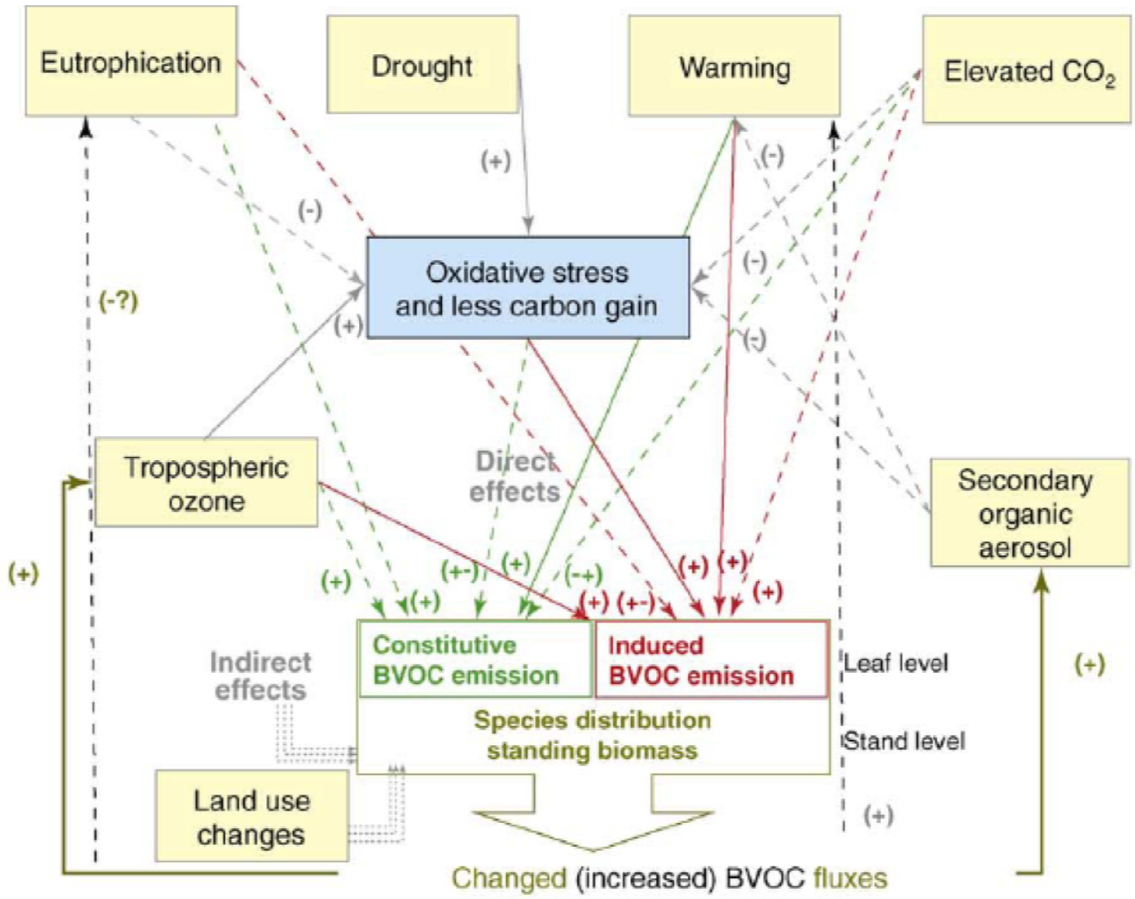

Figure 5: Effects and possible interactions of global changes in climate and atmospheric composition on BVOC emissions adapted from Penuelas and Staudt (2010).

Good progress was made in the past for the measuring of biogenic VOC fluxes. However, measurement techniques and modelling attempts result in high uncertainties due to the high diversity of compounds emitted by the biosphere and thus, the difficulty in quantifying the VOC emissions. Furthermore, changes in land use and also climate changes have to be considered for future BVOC flux predictions.

1.3 Biosynthesis of VOCs

Plants synthesize volatile organic compounds for a range of factors. These include growth, defence, reproduction and communication (within plant communities and between plants and insects). Changes to the environment, due to anthropogenic influences and climate change, may lead to varying emission rates from biogenic sources. The pathways of biogenic VOC synthesis within plants are relatively well known nowadays (Laothawornkitkul *et al.* 2009). A lot of secondary plant product

synthesis pathways are involved by producing volatile intermediates or end products. These include isoprene, monoterpenes, sesquiterpenes, green leave volatiles (e.g. C_6 compounds like hexenal or hexenol), diterpenes, methyl salicylate (MeSA), benzylbenzoate, phenylethylbenzoate, methyl jasmonate (MeJA) and ethylene, ethanol, acetaldehyde, acetone, methanol and formaldehyde. Laothawornkitkul et al. 2009 gives a compilation of the metabolic pathways of the biosynthesis of biogenic volatile organic compound. There are three major biochemical routes which are responsible for the synthesis of most biogenic volatile organic compounds: the isoprenoid, the lipoxygenase or the shikimic acid pathway (Dudareva *et al.* 2006, Feussner and Wasternack 2002, Kesselmeier and Staudt 1999, Laothawornkitkul *et al.* 2009, Lichtenthaler 1999, Matsui 2006, Qualley and Dudareva 2008, Xiang *et al.* 2007). Isoprenoids represent the largest group of biogenic volatile organic compounds. The substructure for all isoprenoid compounds is the isopentenyl pyrophosphate (IPP) which is also called “active isoprene” and has a C_5 structure. The different isoprenoids arise from the condensation of IPP with its reactive isomer dimethylallyl-diphosphate (DMAPP). This represents a fusion of C_5 units. From the number of C_5 structure units, the resulting isoprenoids are divided into groups: hemiterpenes (C_5 structure), monoterpenes (C_{10} structure), sesquiterpenes (C_{15} structure), diterpenes (C_{20} structure), triterpenes (C_{30} structure), tetraterpenes (C_{40} structure), and polyterpenes ($>C_{40}$ structure). The precursor IPP can be synthesized by two different metabolic pathways. The classical pathway is taking place in the cytosol and the endoplasmatic reticulum, where IPP is synthesized from primary metabolite acetyl CoA with mevalonic acid as an intermediate. It is called the mevalonate pathway. Sesquiterpenes, triterpenes and polyterpenes are synthesized via this route. The second pathway is called the DOXP- or MEP-pathway termed after the resulting intermediates in this pathway. It is happening in the plant’s chloroplasts. Isoprene, monoterpenes, diterpenes, and tetraterpenes are synthesized in this sub cellular compartment. These isopreniod compounds are synthesized from primary metabolite pyruvate and glyceraldehyde-3-phosphate (GAP). 1-Deoxy-D-xylulose-5-phosphate (DOXP) and 2-C-Methyl-D-erythritol-4-phosphate (MEP) are formed as intermediates at this pathway. The IPP synthesis via the DOXP- or MEP-pathway seems more efficient as 6 carbon atoms, 20 ATP and 14 $NADPH_2$ are consumed. In contrast to this are 9 carbon atoms, 24 ATP, and 14 $NADPH_2$ units for the production of IPP via the mevalonate pathway (Sharkey and Yeh 2001). Nevertheless, IPP might

also be exchanged between the plastidic and cytosolic compartment (Bartram *et al.* 2006). Besides the predominant group of isoprenoids, a number of other VOCs is also emitted by the biosphere. These compounds include alkenes, organic acids, carbonyls, alcohols, aldehydes, alkanes and esters. A prominent representative of the group of alcohols is methanol. The production of this compound is related to plant growth and development (Bracho Núnez 2010). Methanol is produced by plants in significant amounts during seed growth and maturation, cell expansion in roots, stems, leaves and fruits, cell wall degradation and the formation of intercellular air spaces and leaf abscission and senescence of plant tissues (Kreuzwieser *et al.* 1999). Ethene as an important compound from the group of alkenes is emitted in response to several stress effects like injury or in response to the impact of extreme temperatures (Kimmerer and Kozlowski 1982, Yang and Hoffman 1984). Stress effects like root flooding were discussed to be involved with acetaldehyde emission (Holzinger *et al.* 2000, Kimmerer and Kozlowski 1982, Kreuzwieser *et al.* 1999, Rottenberger *et al.* 2008). Most biochemical synthesis pathways are well studied today. However, the regulation and function of most VOCs is not well understood. For quite a long time monoterpenes were considered as compounds, which are always released from storage pools within the plants, whereas isoprene was distinguished as a non-storing VOC which is directly synthesized and released. However, several authors also reported an immediate light-dependent monoterpene emission (Kesselmeier *et al.* 1996, Kesselmeier *et al.* 1998, Kesselmeier *et al.* 1997, Kuhn *et al.* 2002, Rinne *et al.* 2002). This indicates that monoterpenes are not only emitted from storages, but released directly, reacting to a changing factor in the current environment. The emission of biogenic VOCs is influenced by abiotic factors. Major environmental parameters are temperature and light, but also droughts and flooding can influence the emission rate. Not only abiotic factors are involved in the emission rates of biogenic VOCs, but also biotic factors. These include for example defense, growth and communication.

1.4 Aim of this work

In the past decades it became clear that biogenic VOC play a major role in the earth system. Figure 6 gives an overview of the importance of these research studies for the understanding of the biosphere-atmosphere interactions. This understanding

supports estimating biogenic VOC emissions on a global scale, though with high uncertainties. A reason for these high uncertainties is the lack of ability to accurately measure the whole amount of biogenic VOC emission.

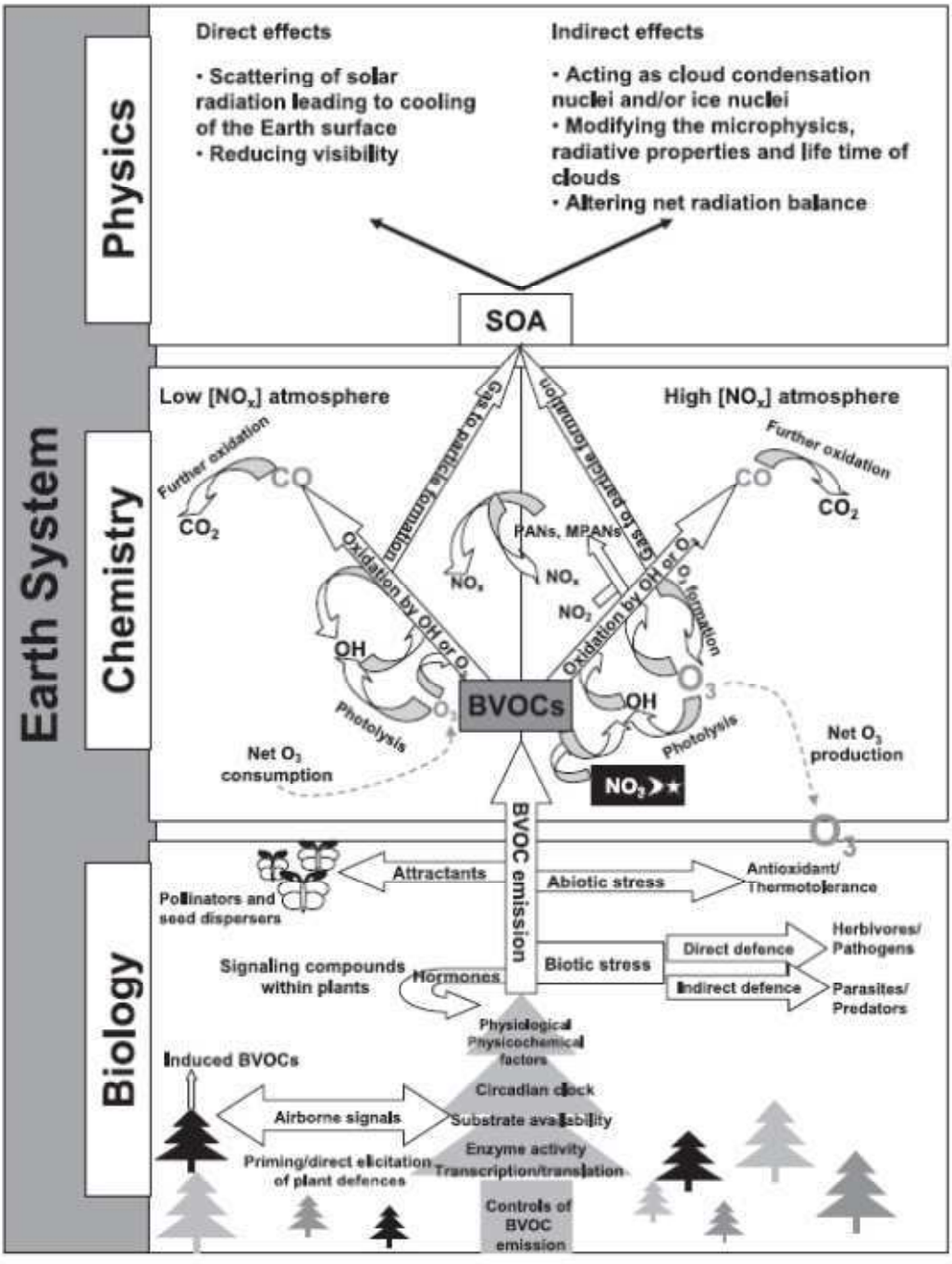

Figure 6: Schematic diagram showing the current understanding of biogenic volatile organic compounds (BVOCs) in the Earth system. BVOCs are involved in the biological, chemical and physical components (Laothawornkitkul *et al.* 2009).

Current and especially future predictions about the biogenic VOC emissions and their influence on the atmosphere are vague. Not only the disability to measure the exact carbon amount which is exchanged between the biosphere and the atmosphere also the regulations of the BVOC synthesis and their influence on environmental factors is not well understood.

Different analytical techniques like PTR-MS (Proton Transfer Reaction-Mass Spectrometry), GC-MS (Gas Chromatography-Mass Spectrometry) or GC-FID (Gas Chromatography-Flame Ionisation Detection) have been developed in the past and enable the measurement of specified VOCs. However, due to the wide variety of biogenic volatile organic compounds the carbon amounts determined with these instruments might only represent a share of the total organic carbon which is exchanged. Summing up the concentrations of each measured single compound might only represent a lower fraction of atmospheric organic carbon, since none of these methods is able to analyse all organic compounds that are present. Unknown compounds from primary emission or resulting from oxidation processes could account for a large proportion of missing organic carbon. Hence, only a few studies can be found for the measurement of total NMOC which concentrate on studies of ambient air (Chung M. Y. *et al.* 2003, Maris *et al.* 2003, Roberts *et al.* 1998). Biosphere – atmosphere interaction studies observing the exchange of total organic carbon between the vegetation and the atmosphere are missing. For the determination of total NMOC concentrations in ambient air, studies by Roberts *et al.* 1998 and Maris *et al.* 2003 attempted to separate CO, CO_2, and CH_4 from the VOC fraction after or during the NMOC preconcentration step. The preconcentration step is realized by cryogenic collection of the NMOCs. CO, CO_2, and CH_4 were either separated from the NMOC fraction during the cryogenic collection on fused silica beads where CO, CO_2, and CH_4 were only co-collected in low amounts (Maris *et al.* 2003) or by a chromatographic column that was operated alternatively in a flush- and backflush mode (Roberts *et al.* 1998). The total NMOC fraction was catalytically converted to CO_2 and in a second step reduced to methane to obtain an equal FID sensitivity. The total NMOC compound was calculated from the methane signal obtained by the FID detector. Although the systems gave good mixing ratio results in the lower ppb range (5 and 35 ppb), both instruments had difficulties with water interference using a FID. Furthermore, two conversion steps are needed for the detection of the total NMOC concentration with a FID.

There are also commercially available total hydrocarbon analyzers which are available from different manufacturers (e.g. J.U.M. Engineering, Germany; Environment S.A, France; Baseline-Mocon Inc., USA). They are based on a continuous flow FID device that responds to methane and NMOCs. In general these instruments catalytically remove all NMOC compounds and measure the methane signal. The NMOC amount is then determined by the difference of the methane signal and the total CH_4 + NMOC response. Large uncertainties are related with this technique, since atmospheric methane concentrations exceed the atmospheric NMOC mixing ratios by far. Despite an easy and comfortable handling, a differentiation between methane and NMOCs is not possible. Moreover, a different carbon response for several functional groups is also affecting the measurement.

Accurate data on total carbon amounts from leaf- or branch-enclosure or even from atmospheric flux measurements are desirable. The aim of this work was the development of an analytical method to determine the total NMOC amount from plant emission. The analyzer setup is described and the essential parts of the instrument are characterized. Improvements to the analyzer were realized, minimizing the size of the instrument, and allowing a better performance concerning recovery rate and oxidation efficiency, respectively. The instrumental setup was tested in the laboratory with calibrated single volatile organic compounds. Plant chamber experiments accomplished by two frequently used methods for monitoring biogenic VOC emissions were carried out. The results of the total NMOC analyzer were compared to the conventional methods in terms of qualitative and quantitative aspects.

2. Material and methods

2.1 Total NMOC analyzer

The following chapter describes the instrument setup of a total NMOC analyzer developed for the measurement of biogenic VOCs from plant enclosure experiments to investigate the exchange of total NMOC between plants and the atmosphere. The instrument is based on the general methodologies of elementary analysis and the techniques developed by Roberts *et al.* (1998) and Maris *et al.* (2003). The main components of the analyzer are:

- a solid adsorbent unit for the preconcentration and adsorption of volatile organic compounds and their separation from CO, CO_2 and CH_4,
- an oxidation unit for the conversion of these VOCs to CO_2, and
- a CO_2 preconcentration unit followed by an infrared gas analyzer for the detection of the previously formed CO_2 (Dindorf 2006).

The basic setup of the present NMOC analyzer was already described by Dindorf (2006). However, changes were made to the previous analyzer, which is further discussed in this work. Figure 7 shows the schematic setup of the present analyzer. The system was operated with helium as a carrier gas (He 6.0, Linde AG, Unterschleissheim). To avoid background signals from CO_2 or H_2O, the helium was purified by application of purifier cartridges (1+2). The cartridges contained NaOH coated carrier material (sodium hydroxide on support, granulated 0.8-1.6 mm, for elementary analysis, Merck, Germany) and Sicapent (phosphorous pentoxide with indicator, Merck, Germany). The materials were separated and immobilized by quartz wool. One purifier cartridge was located prior to the carrier- and dilution gas inlet and one prior to the reference cell of the detector. The helium gas passed through three 6-way-2-postion valves (calibration-, sample-, and oxidation valve) (model ET46 UWE, ViciAG, Gamma Analysen Technik GmbH). Accordingly the carrier gas was directed to a dryer cartridge (4) (filled only with Sicapent) which removed excessive water from the gas stream. Subsequently, the gas was either directed via two 3-way-2-position bypass valves (model SP764.0282, Elementar Analysensysteme GmbH) immediately to the detector or via the CO_2 preconcentration unit. The CO_2

preconcentration unit was necessary to avoid peak broadening during the detection by using a trapping system filled with a CO_2 adsorbent material. Through thermal desorption the CO_2 was released and resulted in a Gaussian formed peak at the infrared gas analyzer.

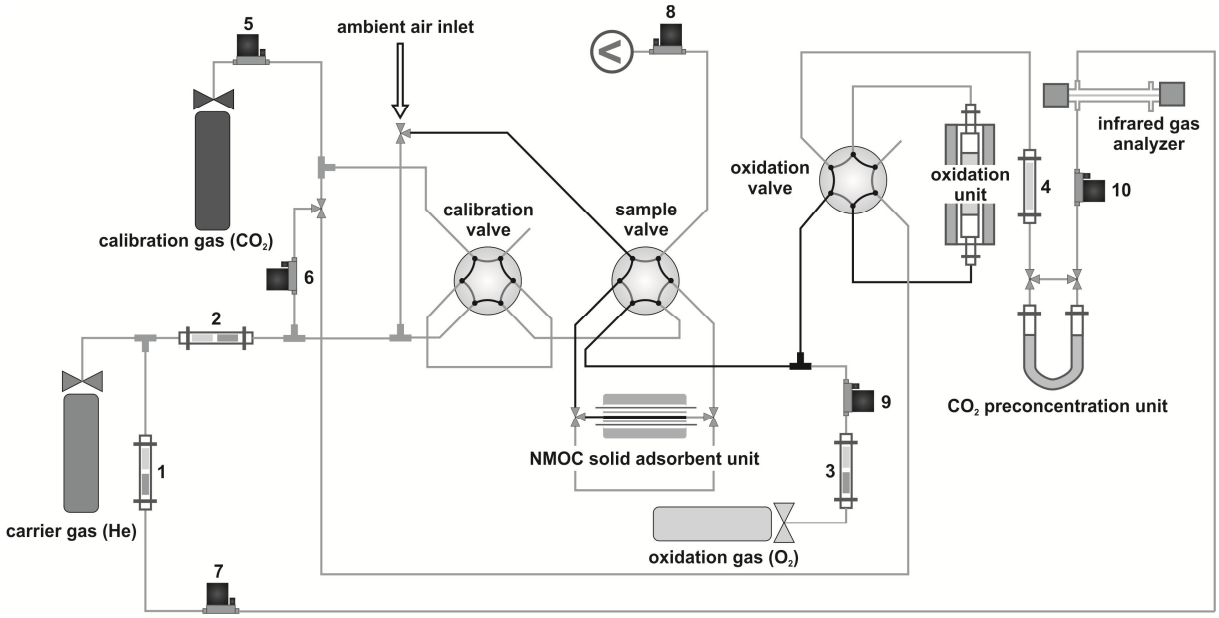

Figure 7: Instrument setup of the total NMOC analyzer. (1) purifier cartridge for reference gas, (2) purifier cartridge for carrier and dilution gas, (3) purifier cartridge for oxidation gas, (4) dryer cartridge, (5) CO_2 calibration gas flow controller, (6) dilution gas flow controller, (7) reference gas flow controller, (8) sample gas flow controller, (9) oxidation gas flow controller, (10) carrier gas flow controller. Stainless steel tubing is indicated by light grey lines, Silicosteel tubing by black lines. The controller unit and the external immersion cooler of the NMOC adsorbent unit are not shown.

Measurements of NMOC samples were implemented by a NMOC solid adsorbent unit, which was connected to the sample valve of the instrument. This unit allowed the sampling of volatile organic compounds at different flow rates and temperatures. The special properties of the solid adsorbent material (Carbograph 1 and Carbograph 5, LARA, Italy) enabled to a great extent a separation of the stable gases CO, CO_2, and CH_4 from the volatile NMOC fraction. After the sample collection the NMOC solid adsorbent unit was flushed with helium (helium flush volume) to eliminate excessive air. Through thermal desorption in backflush mode, the volatiles were introduced into the analyzer and directed into the oxidation unit. The oxidation unit consisted of a catalyst which was kept at 500°C. It was constantly flushed with helium and could be bypassed with the different settings of the oxidation valve. Pure oxygen (O_2 5.5, Linde AG, Unterschleissheim) was added to the catalyst to assure the entire

oxidation of all compounds. The gas flows of the instrument were adjusted by various flow controller units (MKS Instruments), controlling the carrier gas flow (10) (size: 500 sccm), the CO_2 calibration gas flow (5) (size: 10 sccm), the dilution gas flow (6) (size: 100 sccm), the sample gas flow (8) (size: 500 sccm), the oxidation gas flow (9) (size: 50 sccm) and the reference gas flow (7) (size: 500 sccm). To prevent contamination with ambient CO_2 and to ensure the impermeability of the system, the instrument was under overpressure. The majority of the tubing material was made from 1/8" stainless steel (Figure 7: indicated by light grey lines). To avoid adsorption effects of volatile organics within the analyzer, the tubing between the air inlet and up to the oxidation unit was made from Silicosteel® tubing (1/8", RESTEK) (Figure 7: indicated by black lines). Furthermore, this tubing and all valves coming into contact with the NMOCs were heated to 50°C by an external heating tape (model BC8028 HBST, 5 m, 250 W, Horst GmbH). Small Teflon filters (Zeflour Teflon filters, 2 µm pore size, Gelman Science) were fitted within several stainless steel reducer units. These filters prevented a contamination of the instrument from small particles emerging from the usage of quartz wool in the purifier cartridges and the NMOC solid adsorbent unit. The filters were located in the stainless steel units of each purifier and dryer cartridge, as well as in the NMOC adsorbent unit. Most units were controlled by an external controller device. Typical run times for the measurements were 17 min for one calibration file and 35 min for the sampling of ambient air or the corresponding CO_2 amount. A detailed description of the main components of the NMOC analyzer is given in the following chapters.

To determine the total NMOC amount the integral of the CO_2 background signal ($area_{CO2Sample}$) and the integral of the total NMOC signal ($area_{NMOCSample}$) (see also formula 2.7.9 and 2.7.11) had to be measured. For the total NMOC signal the sample air which was directed into the analyzer via the sampling valve had to pass through the oxidation unit. The resulting CO_2 is collected on the preconcentration unit and subsequently detected with the infrared analyzer. The signal consisted of the sampled NMOC plus the additionally collected CO_2. For the $area_{CO2Sample}$ value which represented the CO_2 amount that was also collected on the solid adsorbent unit the oxidation unit was bypassed. The preconcentrated and analyzed CO_2 from this measurement had to be subtracted from the $area_{NMOCSample}$ value to obtain the NMOC concentration.

2.1.1 External controller device

An external controller device (V25) was the core of the total NMOC analyzer. It was built and programmed by the electronic department of the Max Planck Institute for Chemistry. By means of the controller device the analyzer valves (6-way-2-position and 3-way-2-position), the flow controller units (see Figure 7: 5-10), the NMOC solid adsorbent unit, the CO_2 preconcentration unit, the detector temperature and the pump for ambient air sampling could be controlled. Furthermore the device was storing the various temperature measurements and the detector signals in 1 s intervals. The data was saved onto a flash disk memory card (PCMCIA). The resulting file was a log file. Table 3 gives an overview of all parameters.

Table 3: Overview of the parameters that are saved on the flash disk of the controller unit.

Parameters	Flow Controller	Valve	Temperature
Date	carrier gas flow	calibration	detector
Time	reference gas flow	sample	NMOC adsorbent unit
CO_2 detector signal	dilution gas flow	oxidation	oxidation unit
H_2O detector signal	oxidation gas flow	bypass NMOC adsorption	CO_2 preconcentration unit
	CO_2 calibration gas flow	bypass CO_2 preconcentration	ambient
	sample flow	ambient air inlet/flush NMOC	heating tape intern
		dilution calibration/flush oxidation	heating tape extern

The controller device could be operated independently with a small display and a keypad that allowed access to several functions of the analyzer. Input and output signals were checked and calibrated with a test box device (Max Planck Institute for Chemistry, electronic department) that was connected to the controller. A connection to an external computer was also possible. Therefore a RS-232 interface was available. With the RPC700 (remote PC) software (Max Planck Institute for Chemistry, electronic department) the controller device was operated by the computer. The main commands for the functions and settings for the single subunits of the total NMOC analyzer were accomplished by a configuration file. This file also defined the menu structure. Together with the configuration file a parameter file which contained temperature and flow controller settings was generally needed. The measurement procedure of the NMOC analyzer (e.g. variations in valve or flow controller status) was operated by individual program files. A method file which

defined the sequence of the program files was also required. With a so called “loop” function the sequence within the method file was continuously repeated. All of these files had to be stored either on the internal memory or on a flash disk memory card that also stored the resulting data. An overview of the different files can be found in Appendix D. Another important property of the configuration file was the integration of the CO_2 detector signal. A mathematical calculation was embedded in the file. With this process a data file (spc) was produced and stored on the flash disk, which included only the date and time together with the detector signal for CO_2 and H_2O with five data points per second. The integrals resulting from the spc data files of the CO_2 detector signal were summarized in a so called dat file. Next to the CO_2 integration value, the dat file included the name of the corresponding program file with start-, end time and the duration but also the start- and end time of the integration duration and the number of data points taken. With the earlier mentioned log file and the spc- and dat files, the data of the measurements can be evaluated. Thus, no separate chromatographic software was required.

2.1.2 Detector

For the detection of the carbon amount resulting from NMOC oxidation reaction, a commercially available infrared gas analyzer (model Li 6262, Li-COR) was used. The detector was based on non-dispersive infrared gas analysis (NDIR). Figure 8 shows the schematic setup of the detector. The CO_2 mixing ratio was determined by the differential measurement of infrared radiation passing through two gas sampling cells – the reference and the sample cell. The reference cell was purged with a gas with a known CO_2 concentration, the sample cell with an unknown one. The difference in the absorption between the two cells was proportional to the output of the analyzer. The infrared radiation was emitted by a vacuum sealed infrared source and was alternately transmitted to the reference and the sample cell by a chopping shutter.

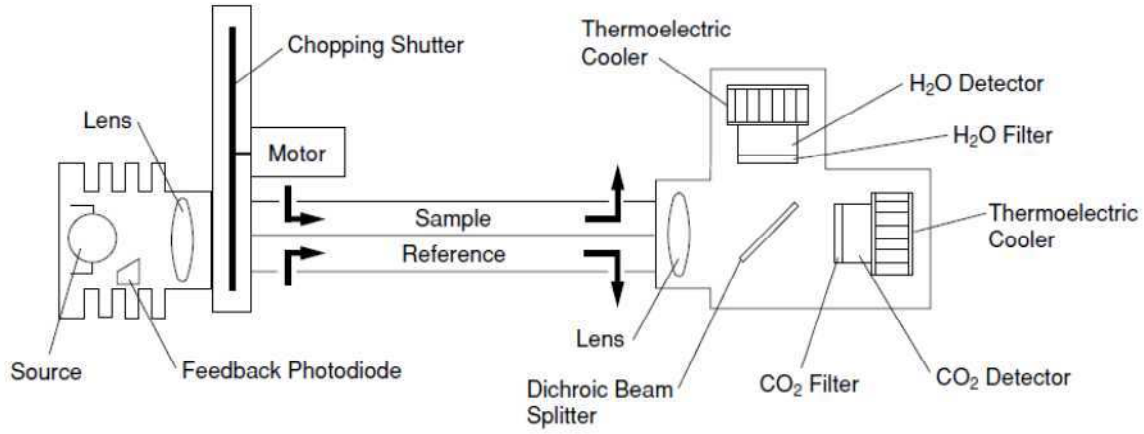

Figure 8: Schematic setup of the infrared gas analyzer.[8]

The detection of CO_2 was achieved at a wavelength of 4.26 µm. Flow rates to the sample and the reference cell were adjusted to 50 ml min^{-1} or 100 ml min^{-1} by utilization of the corresponding flow controller (see Figure 7: 7+10). Since water vapor can influence infrared detection of CO_2, the NMOC instrument setup was provided with purifier and drying cartridges (see Figure 7: 1, 2, 3, 4), that took up all the water present in the system. Hence, cross sensitivities due to water vapor were unlikely. Dilution and pressure broadening corrections were not required (function 76 = off).

Dindorf (2006) showed in her work that the detector response increased linear with increasing detector temperature. A maximum was reached at 35°C. At higher detector temperatures the response curve followed a saturation trend. For this reason constant detector temperatures of 38°C were adjusted. This was achieved by placing the analyzer in a temperature controlled aluminium box, preventing signal fluctuations induced by the detector's temperature sensitivity. Temperature control was achieved by using the heat output of the IRGA (infrared gas analyzer), supported by two ventilator units (24 V, 2.4 W), which were controlled by the external controller device.

With the CO_2 gas standard and the helium carrier gas, the detector was regularly calibrated following the default procedure. The CO_2 released by the CO_2 preconcentration unit corresponded to a chromatographic peak, which was recorded and evaluated by the external controller device.

[8] ftp://ftp.licor.com/perm/env/LI-6262/Manual/LI-6262_Manual.pdf

2.1.3 CO_2 preconcentration unit

The CO_2 preconcentration unit prior to the infrared gas analyzer was kindly provided by Elementar Analysensysteme GmbH, Germany. Figure 9 shows a schematic illustration of the unit. The device was constructed from an U-shaped copper tubing (diameter: 8 mm, terminal connection: 1/4” stainless steel) which was filled with 7 g of modified silica (silica type 175, 0.5–1 mm, Elementar Analysensysteme GmbH) and quartz wool at both ends. It was attached to a support frame. A ventilator (24 V, 0.15 A) mounted at the back panel of the support frame enabled cooling of the unit to ambient temperatures. On the surface of the copper tubing, a heating coil was attached. It allowed the heating-up of the CO_2 preconcentration unit, which was necessary for the thermal desorption of the collected CO_2. The power supply of the heating coil was generated by a transformer unit (in: 230 V, out: 24 V, 5.43 A). Temperature control was achieved by a thermocouple attached to the outer surface of the tubing. Both, transformer unit and thermocouple were controlled via the external controller unit. The CO_2 preconcentration unit was connected via 1/4” to 1/8” reducer units to the NMOC analyzer. It could be bypassed by two 3-way-2-position valves. Generally a heating time of 3 min up to a temperature of 200°C was adjusted but varied depending on the experiment.

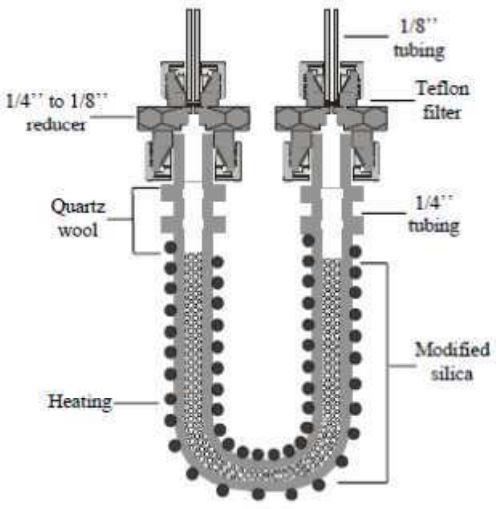

Figure 9: Schematic illustration of the CO_2 preconcentration unit. Support frame, ventilator and thermocouple are not shown (Dindorf 2006).

2.1.4 Oxidation unit

The oxidation unit is an important part of the analyzer because it must be ensured that all NMOCs are converted to CO_2. Various catalytic materials are available. Most commonly used are porous materials or ceramics with a high surface area, which are covered with noble metals like platinum or palladium. Other materials can be quartz wool or wire coated with noble metals. However, it was important that the material properties match the experiment. The original setup of the oxidation unit was built from a quartz glass tube (length 360 mm, external diameter 28 mm), which was filled with 250 g CuO (copper oxide, wire fine, 0.65-3 mm, for elementary analysis, surface CuO, core Cu_2O, ≤ 0.002% total carbon, Elementar Analysensysteme GmbH) and quartz wool. It was placed in a vertical tube furnace which was kept at 800°C. Connection of the quartz glass tube to the instrument was realized by utilization of quartz to metal seals (model GMQS050TE, ½" OD, Kurt J. Lesker Company Ltd) and stainless steel reducer units. Other tube materials and fitting types resulted in high CO_2 background signals when reaching higher temperatures. Further details can be found in Dindorf (2006). To support the oxidation process, oxygen (5.5, Linde AG, Unterschleissheim) was added prior to the oxidation unit (see Figure 7). The catalyst could be included into the carrier gas stream, but also be bypassed by utilization of two 3-way-2-position valves (shown in Dindorf (2006)). In case the bypass was active in the original setup, the oxidation unit was cut off from any gas flow. Extensive tests were carried out with the oxidation unit which resulted in multiple changes of the catalytic material and the whole setup of the oxidation unit. The present oxidation unit was downsized to a much smaller quartz glass tube (length 80 mm, external diameter 11 mm). It was manufactured by the glass blower workshop of the Research Centre in Jülich. Instead of quartz wool, which was used to stop the catalytic material from shifting around within the tube and resulting in cavities and dead volume, the glass tube was equipped with a glass frit (porosity P=1) at the outlet of the oxidation unit. For the connection of the oxidation unit to the instrument, the quartz to metal seals, which were also used for the original oxidation tube, were utilized. Due to the size reduction of the glass tube, smaller quartz to metal adapters were implemented (model GMQS025TE, 1/4" OD, Kurt J. Lesker Company Ltd). The vertical tube furnace was eliminated and replaced by a heating wire coil, surrounding the quartz glass tube. Figure 10 shows the schematic setup of the new oxidation unit.

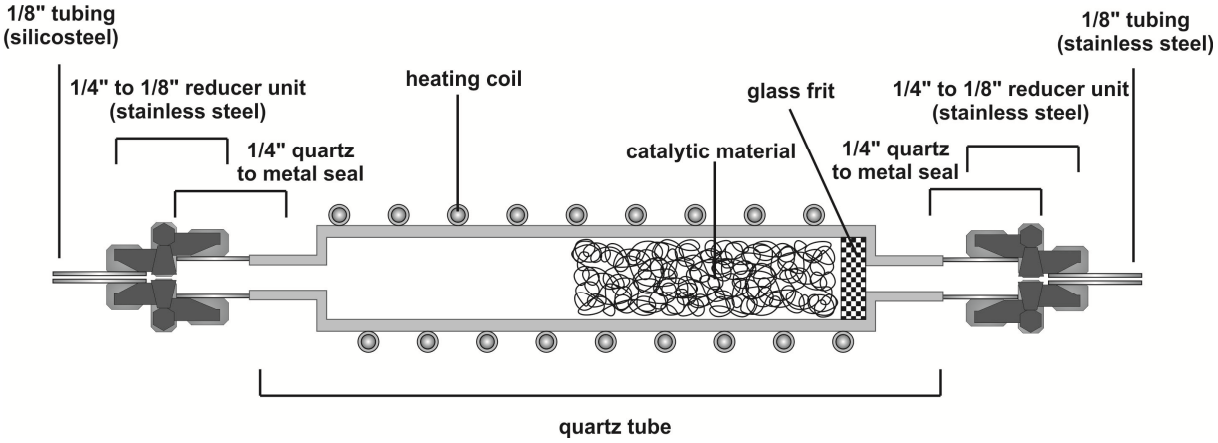

Figure 10: Schematic figure of the new oxidation unit. Thermocouple, power supply and insulation material are not shown.

Insulation material was wrapped around the tube-heating coil construction. On the surface of the glass tube a thermocouple was attached, which was connected to the external controller device recording the actual oxidation unit temperature. The power supply of the heating coil was generated by a commercially available laboratory power supply unit. The temperature was controlled through voltage settings. Due to the size reduction of the oxidation unit, the flow rate of the carrier gas was decreased to 50 ml min^{-1} to allow the longest possible contact time of the NMOCs with the catalytic material. The two 3-way-2-position oxidation bypass valves of the original setup were eliminated and exchanged by a 6-way-2-position valve (see Figure 7: oxidation valve). This enabled a constant flushing of the catalyst to minimize any possible CO_2 background that might be released from the catalytic material. Four different catalytic materials were examined in various tests. Required properties for this instrument setup were a low CO_2 background signal, efficient oxidation of all compounds to CO_2 and no surface interaction of the resulting CO_2 with the catalytic material (e.g. adsorption of CO_2). Details to the various experiments with the different catalytic materials can be found in chapter 3.2.

2.1.5 NMOC solid adsorbent unit

The sampling and measuring of VOCs has been established to standard methods within the last decades. Besides the commonly used online technique of PTR-MS (see chapter 2.2), most other methods involve a preconcentration step to measure NMOC compounds. This preconcentration step is normally achieved by cryo-trapping

(Maris *et al.* 2003, Roberts *et al.* 1998) or by trapping the NMOCs on a solid adsorbent material. The latter method was applied for this instrument. The sampling and preconcentration of the NMOC compounds from ambient air was achieved by the NMOC solid adsorbent unit.

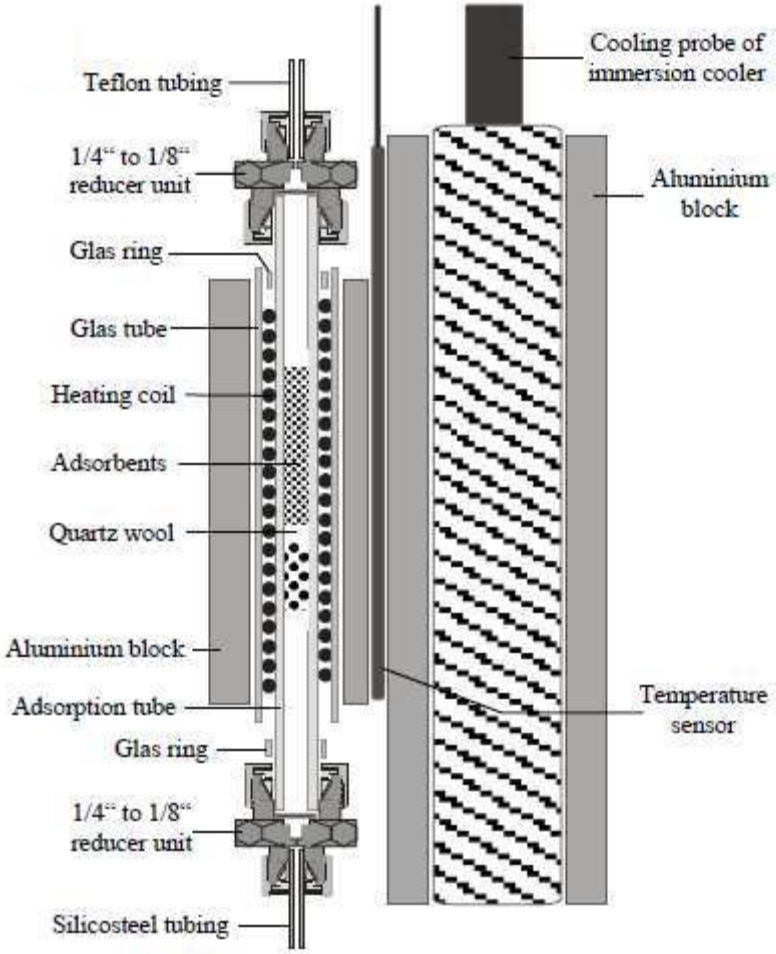

Figure 11: Schematic setup of the NMOC solid adsorbent unit (Dindorf 2006).

Figure 11 shows the schematic setup of the unit. Due to the properties of the solid adsorbent material, the largest share of CO_2, CO and CH_4 was separated from the NMOC fraction. The unit was constructed from a quartz glass tube (1/4" outer diameter, 240 mm length) which was filled with solid adsorbents. Dindorf (2006) mentioned in her work that the application of a glass tube provided better results than the Silicosteel® tubing. The glass tube was enclosed by a heating coil to enable heating for thermal desorption. A thermocouple was attached in between the outside of the glass tube and the heating coil. It was connected to the external controller device to enable temperature regulation of the NMOC solid adsorbent unit. Power

supply of the heating coil was generated by a connection to a transformer unit (in: 220 V, out: 30 V, 5.43 A). The heating coil was surrounded by another glass tube (16 mm outer diameter) to provide electrical insulation. This was essential as this whole construction was mounted on an aluminium block (length 190 mm, height 70 mm, width 50 mm). The aluminium block contained three different drilling holes. One was for the latter mentioned glass tube construction (12 mm in diameter). Another one hosted a cooling probe of an external commercially available immersion cooler (model CC-100 with cryotrol, Thermo Neslab) (32 mm in diameter). The last drilling hole contained the temperature sensor of the immersion cooler (5 mm in diameter). The immersion cooler kept the aluminium block at a preset temperature and thus allowed rapid cooling of the glass tube containing the adsorbent material. The NMOC solid adsorbent glass tube was coupled to the analyzer tubing by utilization of 1/4" to 1/8" reducer units made of stainless steel with Teflon ferrules. The unit was connected to the instrument via the sample valve (see Figure 7). Two 3-way-2-position valves (model SP764.0282, Elementar Analysensysteme GmbH) were mounted on the inlet and the outlet of the unit and created a bypass around the solid adsorbent unit. This enabled the flushing of the tubing with ambient air before collecting a sample. Air sampling was performed by utilization of a flow controller unit (size 500 sccm) connected to a small pump (model NMP30KNDC, 12 V, 0.5 A, KNF Neuberger). At the ambient air inlet a 3-way-2-position valve (model SP764.0282, Elementar Analysensysteme GmbH) was mounted, which was connected to the helium flow of the instrument, to allow the flushing of the NMOC solid adsorbent unit after air sampling. This was crucial for the removal of the excessive air, which was remaining in the sample tubing. It had to be flushed out of the adsorbent unit before thermally desorbing the sampled NMOC and introducing them into the analyzer. Carbograph 1 (90 m^2 g^{-1}, 20-40 mesh, LARA) and Carbograph 5 (560 m^2 g^{-1}, 20-40 mesh, LARA) served as solid adsorbent materials. 100 mg of Carbograph 1 and 200 mg of Carbograph 5 were filled in the glass tube separated by quartz wool. Quartz wool was also used to prevent any movement of the material due to the sample air or the helium flush flow. To avoid the formation of small air channels the adsorbent tube was arranged vertically. Ambient air was sampled at 35°C, with a flow of 300 ml min^{-1} for 10 min, resulting in a sampling volume of 3000 ml. The air was first passing the weaker adsorbent material Carbograph 1, which was efficiently collecting NMOC compounds with a carbon structure of C_6 – C_{15} and then Carbograph 5, which

collected efficiently from C_4 compounds upwards with an applied sampling volume of 3000 ml (Brancaleoni *et al.* 1999, Dindorf 2006). The excessive air was flushed out for 3 min with a helium flow of 750 ml min^{-1} (note that the flow controller is calibrated for N_2 – flow rates for helium were measured separately). Through switching the sample valve, the solid adsorbent unit was staged into the backflush mode and connected to the analyzer. In this mode the NMOCs were thermally desorbed for 8 min with a helium flow of 50 ml min^{-1} at a temperature of 250°C.

2.1.6 Calibration

The calibration of an analytical system is essential for evaluating the measured data. Regarding the total NMOC analyzer, a calibration based on VOC standards was quite difficult. Background signals, sampling and oxidation problems occured. Therefore, the calibration of the total NMOC analyzer was based on a detector calibration with a CO_2 standard gas (352ppm CO_2 in synthetic air, Air Liquide) since all VOCs were oxidized to CO_2 and detected with an infrared gas analyzer. Different CO_2 ratios were mixed in the calibration loop (1 ml) of the calibration valve with the dilution gas (helium 6.0). By switching the calibration valve, the CO_2/He mixture was led into the instrument. Through different valve positions, the gas flow was directed into the oxidation unit or onto the CO_2 preconcentration unit, depending on the experiment. Principally, for calibration the oxidation unit was bypassed but the CO_2 preconcentration unit was utilized.

Table 4 shows the different calibrations files. The carbon mixing ratios in ppb are already referred to the sampling volume of a measurement of 3000 ml. Calculations were based on the equations (2.7.8 and 2.7.10) in chapter 2.7. Errors were calculated via the Gaussian error propagation (formula 2.7.7) with experimentally determined or estimated errors of the single variables. Main errors were caused by the uncertainty of the CO_2 standard gas and the mass flow controllers that control the CO_2 ratio and the sampling volume.

Table 4: CO_2 content in helium (Cal1-Cal7) obtained by mixing CO_2 in synthetic air with helium with calculated errors (Δ). Cal8 represents only CO_2 in synthetic air.

[+] calculation based on a sampling volume of 3000 ml

[++] with temperature correction for a temperature of 30°C based on 1 ml calibration loop

	Cal1	Cal2	Cal3	Cal4	Cal5	Cal6	Cal7	Cal8
CO_2 ratio in %	0	9.1	16.7	20	25	33.3	50	100
ppb carbon[+]	0	10.7	19.6	23.5	29.3	39.1	58.7	117.3
Δppb carbon[+]	0	1.2	1.7	2.2	3	4.2	5.5	6.3
ng carbon[++]	0	15.5	28.3	34	42.5	56.7	85	170
Δng carbon[++]	0	1.3	2.3	2.7	3.2	4.1	5.5	9.1

Table 5 shows typical values and the corresponding errors. Due to changing values of the mass flow controller for the CO_2 flow and the helium dilution flow, the error of these mass flow controllers were estimated with 5% of the adjusted flow. The sampling volume was determined through a flow and a time interval. As the error of the flow was much higher than the one from the time measurement, the time error can be neglected.

Table 5: Systematic errors of the CO_2 standard gas, flow adjustments, volumes and temperature for the calibration.

variable	typical value	typical error	additional information
c_{CO2}	352 ppm	7 ppm	specification by manufacturer
FHe	0-50 ml min^{-1}	0-2.5 ml min^{-1}	5% of adjusted flow
FCO_2	0-10 ml min^{-1}	0.5 ml min^{-1}	5% of adjusted flow
FSample	300 ml min^{-1}	15 ml min^{-1}	3% of max. flow (=500 ml min^{-1})
V_{Loop}	1 ml	0.05 ml	estimated
T	30°C	0.1°C	estimated

Figure 12 shows typical calibration lines with a carrier gas flow of 50 ml min^{-1} (A and C) and 100 ml min^{-1} (B and D). They showed a good agreement in the CO_2/He mixtures.

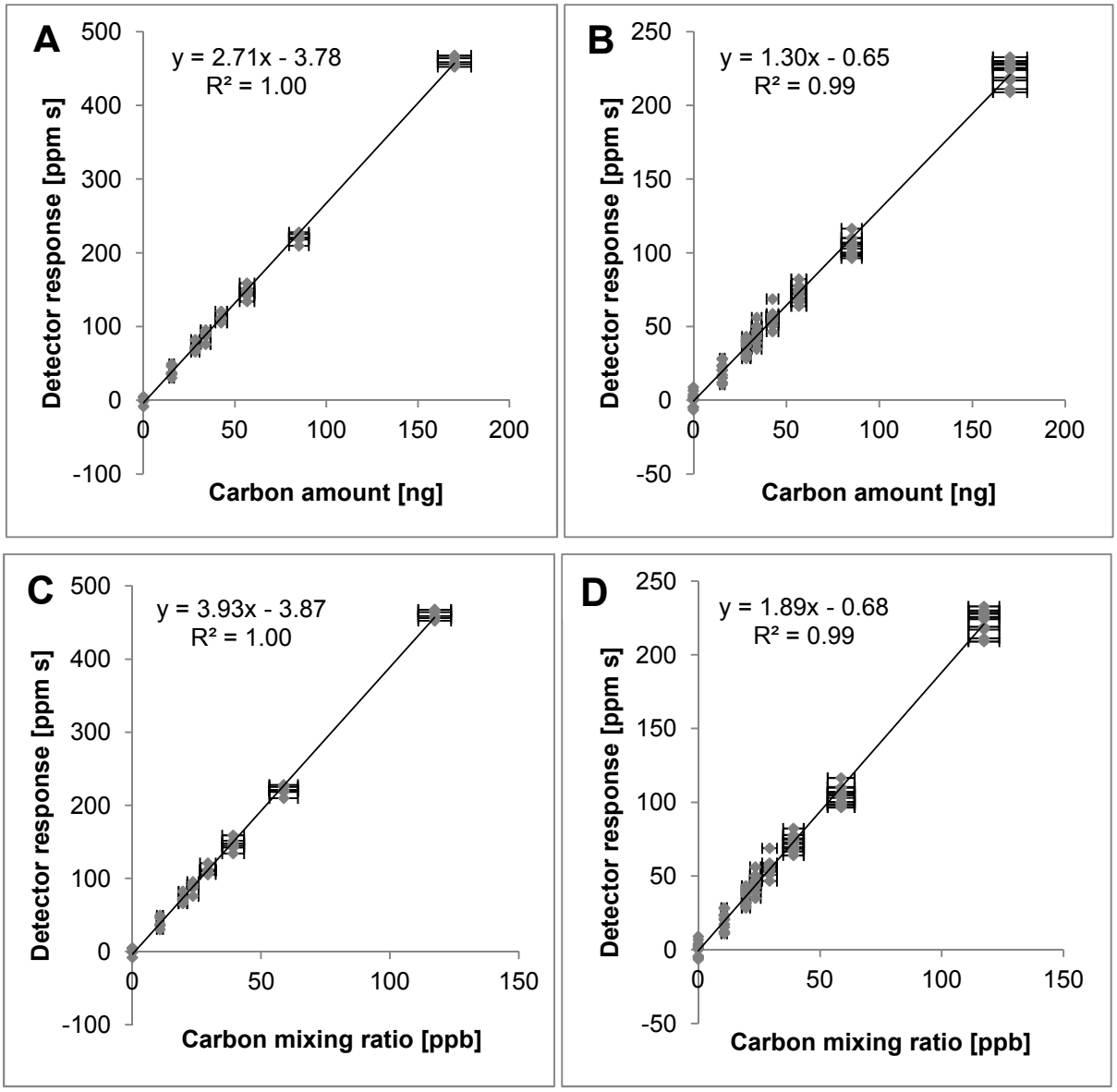

Figure 12: Calibration lines: A and B with amount of carbon in ng against detector response in ppm s with a carrier gas flow of 50 ml min-1 (A) and 100 ml min-1 (B); C and D with carbon mixing ratio in ppb (directly referred to a sampling volume of 3000 ml) against detector response in ppm s with a carrier gas flow of 50 ml min^{-1} (C) and 100 ml min^{-1} (D). The function of the linear fit and the coefficient of determination R^2 are included in each diagram.

The detector response was directly proportional to the carbon amount that was injected via the calibration loop into the analyzer, and resulted in an excellent coefficient of determination (R^2) ≥ 0.99. Furthermore it showed the directly proportional behavior of the detector response and the carrier gas flow caused by the different dilution.

2.2 Proton Transfer Reaction-Mass Spectrometer

Proton Transfer Reaction-Mass Spectrometry (PTR-MS) is a convenient on-line technique for the measurement and monitoring of VOCs. The instrument is widely used in a number of different applications. Besides from atmospheric chemistry, these applications include for example human breath analysis (Blake *et al.* 2009, Jordan *et al.* 1995, Karl *et al.* 2001, Lindinger *et al.* 1998, Warneke *et al.* 1996), monitoring of VOCs resulting e.g. from the decay of food (Blake *et al.* 2009, Boschetti *et al.* 1999, Lindinger *et al.* 1998) or vegetation (Blake *et al.* 2009, Lindinger *et al.* 1998, Warneke *et al.* 1999). The functional principle of the instrument was described in detail elsewhere (Hansel *et al.* 1995, Lindinger *et al.* 1998) and various reviews have been published (Blake *et al.* 2009, de Gouw and Warneke 2007, Hewitt C. N. *et al.* 2003). Figure 13 shows a schematic representation of the used PTR-MS. It is composed of three main units: a discharge ion source, a drift tube (reaction chamber) and a detection system.

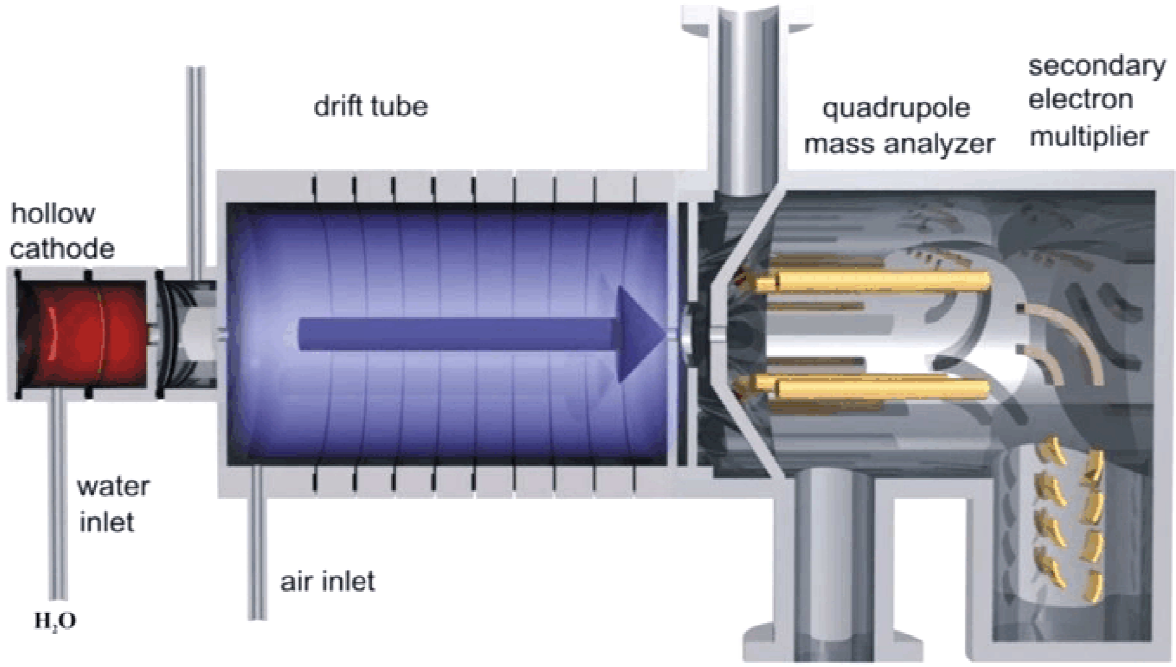

Figure 13: Schematic setup of the PTR-MS.[9]

[9] http://www.ionicon.com/technology/technology.html

The discharge ion source consists of a hollow cathode, which produces H_3O^+ ions that are transported into the drift tube under the influence of an electrical field. The sample air is introduced into the drift tube and collisions of the H_3O^+ ions with gaseous constituents can cause proton transfer reaction. Thereby, the major components of air undergo non-reactive collisions with H_3O^+ ions due to their relatively low proton affinities. They therefore act as a buffer gas. However, every collision with a component R that has a higher proton affinity than the one of water (~697 kJ mol^{-1}) results in a proton transfer reaction. This includes a great number of VOCs.

$$H_3O^+ + R \rightarrow RH^+ + H_2O$$

The protonated compounds (molecular mass + 1) are mass selected using a quadrupole mass analyzer (QMG 422) and detected by a Secondary Electron Multiplier (SEM). The instrument was operated at standard settings in selected ion-monitoring mode (E/N = 130 Td, E: electric field strength, N: buffer gas number density, 1 Td = 10^{-17} cm^2 V $molecule^{-1}$; drift tube pressure: 2.2 mbar, drift tube voltage: 600 V; mass dwell time: 1 s). The main masses detected were isoprene (69), monoterpenes (137, fragment on 81) and sesquiterpenes (205). The system was calibrated with the permeation/diffusion devices described in chapter 2.4. The identification of different species with the same mass, proton affinity and fragmentation cannot be distinguished by this method. Therefore, the measurement results always refer to the sum of monoterpenes and sesquiterpenes.

2.3 Gas Chromatography-Mass Spectrometer

Gas chromatography-mass spectrometry is a commonly used method for the measurement of hydrocarbons from air samples (Apel *et al.* 1999). The gas chromatography-mass spectrometer (GC-MS) system used was described in detail by Heiden *et al.* 1999. VOC samples were preconcentrated on solid adsorbents (Tenax TA 60/80 mesh: 110 mg Carbotrap 20/40 mesh 40 mg). The adsorbent materials were arranged according to their adsorptivity. During the enrichment, the sampling tube was heated to 30°C to prevent the condensation of water on the adsorbent material. Thermal desorption was achieved at 210°C with helium (6.0) in a

backflush mode (i.e. inverse to the sampling direction). The thermal desorption system (Gerstel online TDS G) was connected via a 6-position-2-way valve (Vici AG) to a cooled injection system (Gerstel CIS 3), where the samples were cryofocused on a tube filled with Tenax (Tenax TA 60/80, 22 mg) at -100°C with the help of liquid nitrogen. The substances were again thermally desorbed. Within 12s the cryotrap was heated up to 250°C before injecting the sample into a GC-MSD (mass spectrometric detector) -system (HP5890 Series II - HP5972A). The separation was realized with a BPX-5 column (DB5-MS, 60 m $\times$ 0.25 mm $\times$ 0.5 µm, 10m retention gap). The time resolution of one measurement was about 70 min. During each chromatographic run, a new air sample was preconcentrated with a sampling time of 50 min and a sampling flow of 80ml min^{-1}, which resulted in 4l of sampled air. Identifications of the VOCs were based on mass spectra and retention times of pure chemicals (Fluka and Aldrich, purity >93%) or by using reference mass spectra from the NBS library. The system was calibrated using different permeation sources, containing pure chemicals in individual vials as described in chapter 2.4. Reproducibility of VOC concentration measurements using the permeation sources was on the order of 10-15% for most compounds. The detection limit of the analytical system was between 1 and 5 ppt for all compounds.

2.4 Permeation/diffusion devices

Reference standards are of utmost importance for instrument calibration. Gaseous standard mixtures in aluminium cylinders are available but due to degradation of less stable biogenic compounds not recommended. Apel *et al.* (1999) described a loss of α-pinene of up to 45% in such cylinders. Non storing techniques like permeation or diffusion devices showed better results for the calibration of reactive biogenic VOCs. However, a loss of reactive compounds like sesquiterpenes was also observed by Schuh *et al.* (1997) with these devices. Larsen *et al.* (1997) indicated other possible uncertainties like absorptive losses to the walls or impurities in the standards which might lead to a change of the diffusion rate. Figure 14 shows the setup of the permeation/diffusion devices at the Research Centre Jülich. The setup was similar to the system described by Schuh *et al.* (1997) and by Komenda *et al.* (2003).

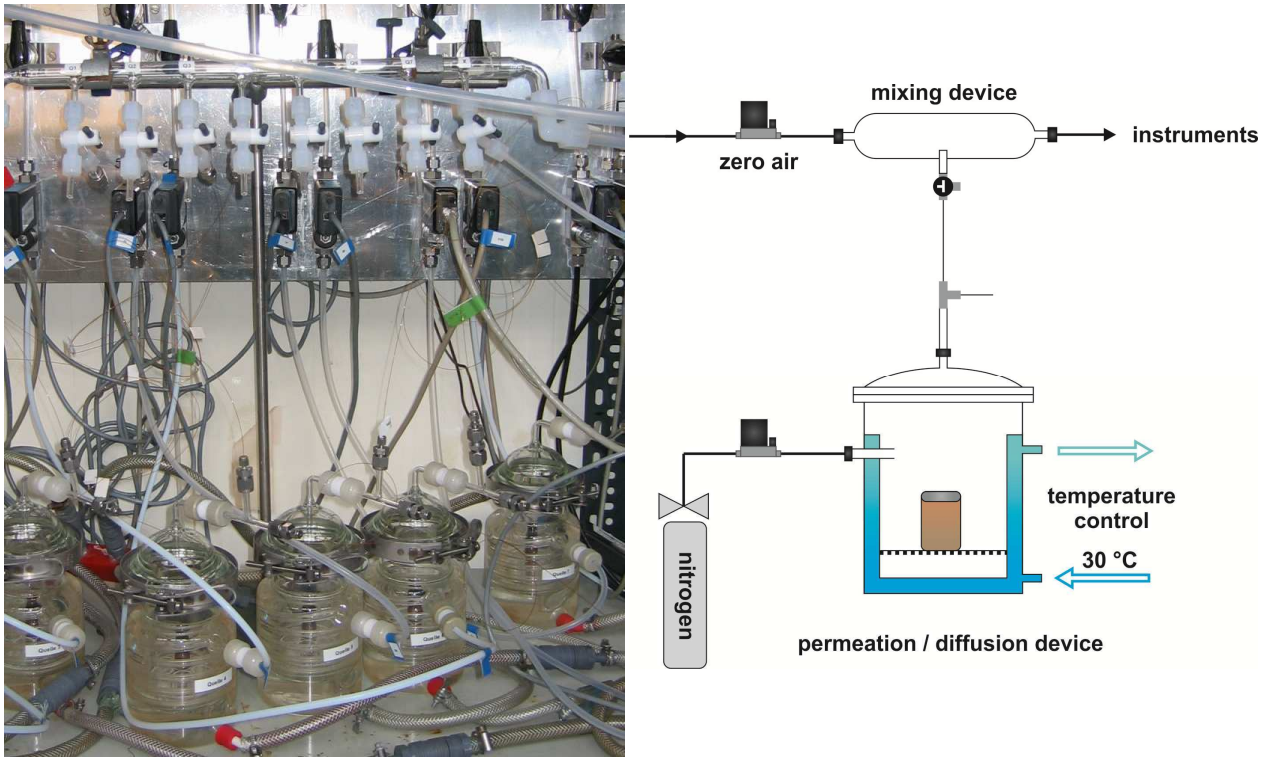

Figure 14: Setup of the permeation/diffusion devices.

The permeation source consists of a double walled glass vessel with a volume of approximately 500 ml which was kept at a constant temperature of 30°C with the help of an external thermostat (Julabo FP 50). The volatile organics were stored as liquid substances in small amber glass vials (volume: 4 ml) with a small punctured Teflon membrane. Through the membrane the compounds diffused into the glass vessel and were diluted by a constant nitrogen flow (flow rate: 500 ml min^{-1}) to mixing ratios at a level of parts per million (ppm). Thereby, size and number of the holes in the membrane adjusted the boil-off rate. On the outlet of the glass vessel there was a T-connector with two capillaries (FS-Pheny-SIL pre-column, CS Chromatographie Service Langerwehe, inner diameter 320 µm) of different lengths. By means of this capillary restrictor flow split, a small fraction of the volatile organic compound enriched nitrogen flow was further diluted with zero air. The VOC concentrations fed to the GC-MS were in the ppb range. The mixing ratios were determined via the inlet and the two outlet flows (on both capillaries), which were measured regularly. Due to the known capillary lengths ratio, the concentrations were calculated. All permeation devices were connected via a 3-way-valve to a mixing device. Single compounds or compound mixtures could be obtained through the mixing device. These were used as calibration standards. The VOC concentrations were calculated by settling mass loss of the permeation vial by weighing every 2-3 weeks and with the flow rates of the

dilution gases. Table 6 shows the liquid standards used for calibration of the instruments. Intercomparison experiments exhibited an uncertainty of the permeation devices of ±15% for most compounds in the lower ppb/upper ppt level (up to ± 30% for sesquiterpenes) (private communication J. Wildt). This is a crucial factor when considering possible sources of error, as the uncertainty of the permeation devices exceed the instrument uncertainties of PTR-MS and GC-MS.

Table 6: Liquid standards used for calibration. Use of other compounds is possible depending on the experiment.

PTR-MS	GC-MS
Isoprene	Isoprene
α-Pinene	α-Pinene
β-Caryophyllene	β-Caryophyllene
	Z-3-Hexenol
	MeSA
	Nopinone

2.5 Plant chamber and species

The enclosure experiments were carried out at the Jülich Plant Atmosphere Chamber (JPAC). The chamber consists of a continuously stirred tank reactor (CSTR) as described by Wildt *et al.* (1997). The CSTR is build of glass (Duran, borosilicate glass, Schott Engineering) which is transparent for the spectral range of light that is important for plant physiology (PAR: 400-700 nm), representing a chemical inert surface. It is supplied with several connections to introduce temperature- and light intensity sensors and to connect the tubings for gas-phase analysis and air supply. The volume of the used CSTR was 1100 l. The upper part of the plant, containing leaves and stem was placed in the chamber. The bottom of the plant chamber was closed using a Teflon sheet with a hole at the midpoint for the stem. A plastic material (Optosil©, Bayer Dental) was used to seal the gaps. Figure 15 shows the setup. Inside the CSTR the air was continuously stirred by a Teflon fan to assure a homogenous mixing of the gas volume. The plant chamber was constantly flushed with cleaned ambient air. It was purified from ozone, NO and NO_2 by an adsorptive device (Zander, KEA 70). Hydrocarbon concentrations were minimized to below the

detection limit of the measuring instruments by a palladium catalyst (Type H54 44, 0.5% Pd Hüls AG, Marl) at a temperature of 450°C. The air flow through the chamber was typically set to 50-140 l min^{-1}, which resulted in air retention times of approximately 7-20 min.

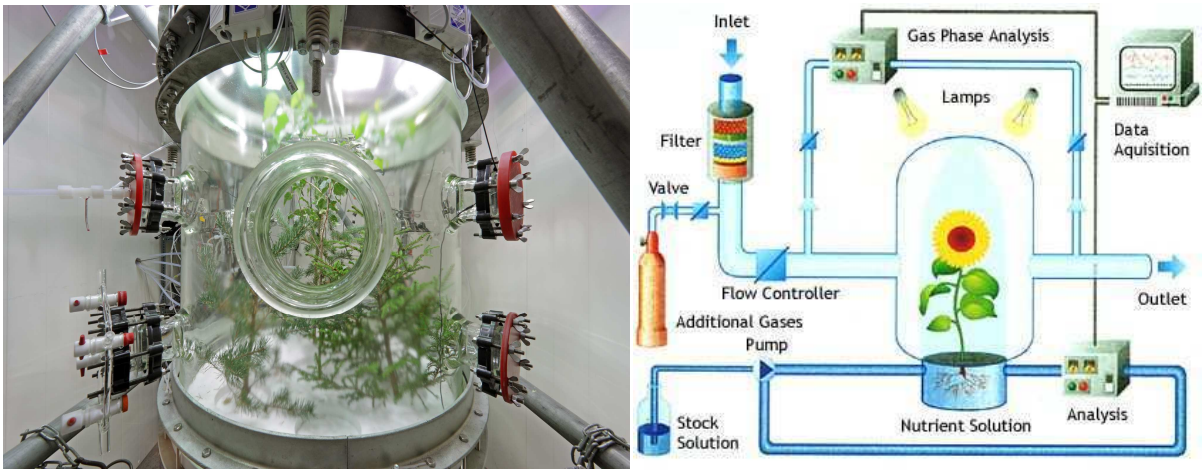

Figure 15: Setup of the Jülich Plant Atmosphere Chamber (JPAC).[10]

CO_2 from a cylinder was added at the chamber inlet to keep the CO_2 concentration at about 350 ppm. Furthermore, other gases could be added to the cleaned ambient air, dependent on the experiment. Ten discharge lamps (Osram HQI 400 W/D), with a photosynthetic photon flux density at mid-canopy height of 400 μmol m^{-2} s^{-1}, were used as light source. To avoid radiative overheating of the chamber, infrared (IR) filters (OptoChem type IR3), which reflect wavelengths between 750 and 1050 nm, were used (Heiden *et al.* 1999). Temperatures and light intensities could be varied independently.

For the plant chamber experiments three different plant species were used. *Populus x canescens, Pinus sylvestris* and *Quercus ilex* were installed into the plant chamber in two different experiments. All species are known to be major VOC emitting plants (see Table 2). *Pinus sylvestris* and *Quercus ilex* are major emitting plants for monoterpenes, whereas *Populus x canescens* is known to mainly emit isoprene. The emissions of the different species were analyzed by the total NMOC analyzer, PTR-MS and GC-MS measurements.

[10] http://www.fz-juelich.de/portal/DE/Forschung/EnergieUmwelt/KlimaBiooekonomie/Pflanzenforschung/_node.html

2.6 Infrared gas analyzer

CO_2 mixing ratios from the outlet of the plant chamber were measured with a differential, non-dispersive infrared (NDIR) gas analyzer (model Li 7000, Li-COR). The general setup of the infrared gas analyzer can be compared to the detector of the total NMOC analyzer (see Figure 8). A gas with a known CO_2 concentration was purged through a gas sampling cell (reference cell) and a gas with an unknown concentration was passed through a second cell (sample cell). Infrared radiation with a wavelength of 4.26 µm was transmitted through and measured in both cells. The CO_2 concentration of the unknown gas was determined by the difference in absorption of the infrared radiation within both cells. A vacuum sealed tungsten filament was used as an infrared source. A lead selenide solid state device regulated to -5°C served as detector. To avoid interferences from ambient CO_2 and H_2O the source and the detector were sealed and purged by a purifier bottle which contained soda lime and magnesium perchlorate.

2.7 Data analysis and statistics

Several statistical procedures were used to evaluate the measured data. The following statistical techniques were applied:

2.7.1 Average and standard deviation

Formula 2.7.1 was used to determine the arithmetic average of a group of symmetrical distributed data points. The deviation of random samples from their arithmetic mean was calculated with formula 2.7.2, the standard deviation. The variables in both formulas are n: number of data points, $\bar{x}$: arithmetic mean, x_i: single value and s: standard deviation. In general, all measurements were executed multiple times with at least three repetitions. If the average of these multiple repetitions is presented it is indicated in the figure caption.

$$\bar{x} = \frac{\sum x_i}{n} \qquad 2.7.1$$

$$s = \sqrt{\frac{n \cdot \sum x_i^2 - (\sum x_i)^2}{n \cdot (n-1)}} \qquad 2.7.2$$

2.7.2 Linear regression

A linear regression line can be drawn through a group of data pairs (x_i, y_i) with n data points. Formula 2.7.3 shows the equation for a linear regression line, with $\bar{x}$ and $\bar{y}$ representing the respective averages of all x and y values, m the slope and b the y-intercept for the linear regression. Formula 2.7.4 and 2.7.5 show the equation for the calculation of the slope (2.7.4) and the y-intercept (2.7.5) with n: number of data points, x_i: value of data point i at x-axis and y_i: value of data point i at y-axis.

$$\bar{y} = m\bar{x} + b \qquad 2.7.3$$

$$m = \frac{n \sum x_i y_i - (\sum x_i) \cdot (\sum y_i)}{n \sum x_i^2 - (\sum x_i)^2} \qquad 2.7.4$$

$$b = \frac{\sum y_i - m \sum x_i}{n} \qquad 2.7.5$$

The linear relationship between two datasets (x_i, y_i) can be determined with the Pearson product moment correlation coefficient r (2.7.6). The best linear correlation is given by resulting coefficients of +1 and -1. A correlation is likely, with a coefficient ranging between -1 and +1, but there is no correlation if coefficient results in 0. The coefficient of determination R^2 is used frequently, where the best correlation is given with a coefficient equalling 1.

$$r = \frac{n(\sum x_i \cdot y_i) - (\sum x_i) \cdot (\sum y_i)}{\sqrt{(n \sum x_i^2 - (\sum x_i)^2) \cdot (n \sum y_i^2 - (\sum y_i)^2)}} \qquad 2.7.6$$

2.7.3 Errors and error propagation

Measured values are always affected by an error. Errors that can occur are coarse, systematic and random errors. Appropriate approximations and uncertainty intervals for the measured values must be determined and specified by the measurement

result. Errors of individual measuring devices are specified by the manufacturer or can be estimated. If the desired end result can only be determined by a calculation, the different faulted sizes have to be considered. Are all variables independent, the Gaussian error propagation can be applied (2.7.7).

$$\Delta G = \sqrt{\left(\frac{\partial G}{\partial x} \cdot \Delta x\right)^2 + \left(\frac{\partial G}{\partial y} \cdot \Delta y\right)^2 + \left(\frac{\partial G}{\partial z} \cdot \Delta z\right)^2 + \ ...} \qquad 2.7.7$$

Gaussian error propagation: ΔG: error of the calculated value, $\frac{\partial G}{\partial x}$: partial derivative of the function G of x (the same applies for y, z,...), Δx: error of the variable x (the same applies for y, z,...)

2.7.4 Calculation of carbon mixing ratios and carbon amounts in ng

The carbon mixing ratios can be calculated from the CO_2 ratio and the volume sampled (2.7.8). Due to different CO_2 mixing ratios during calibration, a linear calibration line is obtained. With the help of this calibration line the carbon mixing ratio of an unknown carbon mixture can be determined (2.7.9).

$$Mixing\ ratio_{Cal} = c_{Standardgas} \cdot \left(\frac{FCO_2}{FHe + FCO_2}\right) \qquad 2.7.8$$

Carbon mixing ratio (calibration) in ppb: $c_{Standardgas}$: concentration of the CO_2 calibration gas [ppb], FCO_2: flow CO_2 [ml min^{-1}], FHe: flow helium [ml min^{-1}]

$$Mixing\ ratio = \frac{\left((area_{NMOCSample} - area_{CO2Sample}) - b\right)}{m \cdot F_{dilution}} \qquad 2.7.9$$

Carbon mixing ratio in ppb: $area_{NMOCSample}$: area of the total NMOC sampled [ppm s], $area_{CO2Sample}$: area of the CO_2 sampled (CO_2 background)[ppm s], b: y-intercept from calibration line [ppm s], m: slope of the calibration line [ppm s ppb^{-1}], $F_{dilution}$: dilution factor (originates from different sampling voluminas)

The amount of carbon in ng is calculated similar to the carbon mixing ratio. However, the molar mass of carbon, the mole volume of an ideal gas and a temperature correction have to be taken into account. Fomula 2.7.10 shows the calculation for the calibration loop und formula 2.7.11 the one for a sample.

$$ng\ C_{Cal} = \left(\frac{c_{Standardgas} \cdot \left(\frac{FCO_2}{(FHe+FCO_2)} \right) \cdot V_{Loop} \cdot m_C}{\frac{V_i}{T_n} \cdot (T_n + T_{Ref})} \right) \quad 2.7.10$$

Absolute carbon amount (calibration) in ng: $c_{Standardgas}$: concentration of the CO_2 calibration gas [ppb], FCO_2: flow CO_2 [ml min^{-1}], FHe: flow helium [ml min^{-1}], V_{loop}: volume of the calibration loop [ml], m_c: molar mass of carbon [g mol^{-1}], V_i: mole volume of an ideal gas [22.4l mol^{-1}, 0°C, 1bar], T_n: temperature [273K], T_{Ref}: reference temperature NMOC analyzer [°C]

$$ng\ C = \frac{\left((area_{NMOCSample} - area_{CO2Sample}) - b \right)}{m} \quad 2.7.11$$

Absolute carbon amount in ng: $area_{NMOCSample}$: area of the total NMOC sampled [ppm s], $area_{CO2Sample}$: area of the CO_2 sampled (CO_2 background)[ppm s], b: y-intercept from calibration line [ppm s], m: slope of the calibration line [ppm s ng^{-1}]

2.7.5 Reproducibility

The reproducibility is only influenced by random errors. Therefore, it can be calculated by the arithmetic average and the standard deviation of a series of measurements at the same conditions:

$$E = \frac{s}{\bar{x}} \cdot 100 \quad 2.7.12$$

Reproducibility E in percent: s: standard deviation, $\bar{x}$: arithmetic mean

2.7.6 Detection limit

The detection limit can be calculated according to formula 2.7.13. It is defined as the lowest concentration of a sample that can still be detected.

$$LOD = \overline{x_B} + 3s_B \qquad 2.7.13$$

Limit of detection (LOD): $\overline{x_B}$: arithmetic mean of the $area_{NMOCSample}$ and $area_{CO2Sample}$ subtraction result, s_B: standard deviation of the same one

3. Instrument optimization

3.1 CO_2 preconcentration unit

3.1.1 Breakthrough volume

The breakthrough volume (BTV) is defined as the volume of carrier gas that will purge an analyte through an adsorbent at a specific temperature. It can be tested with a gas standard, which can be passed through the sorbent. If the concentration ratio of the effluent gas, compared to the incoming gas, gains a pre-defined value (from 1% to 50%, according to different definitions) the breakthrough volume is reached (Bertoni and Tappa 1997). Because only small amounts of CO_2 were sampled the pre-defined value for the concentration ratio was specified to 1%. The breakthrough volume of the CO_2 preconcentration unit was tested with a different setup of the unit. One hand operated 3-way-2-position valve (3-way ball valve, 1/4", Swagelok, B-42XF2) was positioned preliminary to the first electrical 3-way-2-position valve in gas flow direction. The second electrical valve of the CO_2 preconcentration unit remained connected to the original setup. The manually operated valve was connected to the helium carrier gas and to the CO_2 standard gas. The method involved 1 min carrier gas flow, bypassing the preconcentration unit and switching to the CO_2 gas standard manually after 1 min. The CO_2 standard gas was bypassing the unit for another 2 min, to ensure that the system was flushed with CO_2. After 2 min the electrical 3-way-2-position valves were switching from the bypass to the preconcentration unit. The CO_2 was sampled on the unit and the CO_2 signal at the detector droped back to zero (see Figure 16). The time was measured until the CO_2 signal increased again. After approximately 335 s the CO_2 signal reached a ratio of 1% of the incoming gas concentration compared to the effluent gas concentration. This resulted in a breakthrough volume of 558 ml at a set flow rate of 100 ml min^{-1} and a sampling temperature of 30°C. Dindorf (2006) determined a breakthrough volume of 644 ml by injecting 1 ml of the CO_2 gas standard (347 ppm CO_2 in synthetic air, Messer Griesheim) into the instrument via the calibration loop and observing the retention time of the chromatographic CO_2 peak.

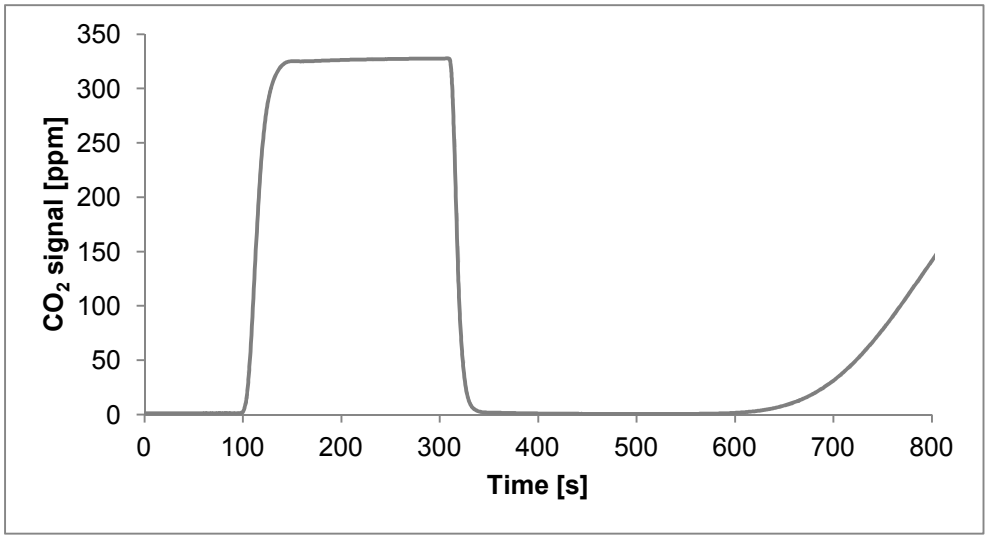

Figure 16: Course of the breakthrough volume determination. The first 60 s show the zero signal from helium bypassing the CO_2 preconcentration unit. After 60 s it is manually switched to the CO_2 standard gas which is still bypassing the unit. After 3 min the preconcentration unit is switched into the CO_2 in synthetic air gas stream by the electrical 3-way-2-position valves. The uptake of the CO_2 can be identified by the decrease of the signal to zero.

The difference in the two values could be due to the dead volume of the instrument, which was not taken into account when considering the retention time. Also the manual switching of the operating valve could cause differing values. Probably the most important factor identified was the use of different carrier gases, synthetic air or helium, as the correct flow estimations are based on the determination of thermal conductivity. To ensure that the breakthrough volume was not reached during the measurement, the CO_2 preconcentration unit was only switched to the instrument for a certain time, to sample the CO_2 resulting from the VOC oxidation. As the breakthrough volume was dependent on the temperature, it could be enhanced by cooler unit temperatures. But since the preconcentration unit was only cooled with a ventilator, it was not possible to reach temperatures lower than the ambient one. At first measurements were set to a carrier gas flow of 100 ml min^{-1}. Later measurement flows were adjusted to 50 ml min^{-1}. Dindorf (2006) showed that flow rates of ≤ 100 ml min^{-1} resulted in a proportional relationship between the breakthrough volume and the flow rate. For experiments with a flow rate of 50 ml min^{-1} a twice as high breakthrough volume was assumed.

3.1.2 Sampling efficiency

Next to the breakthrough volume, the sampling efficiency is an important property. Therefore, the CO_2 preconcentration unit was tested for its sampling efficiency with the calibration method. The method comprised of the injection of different CO_2 ratios mixed in a separate loop of a defined volume with the help of a CO_2 standard gas and a dilution gas (helium 6.0). Further details about the calibration were given in chapter 2.1.6. Calibration runs including the CO_2 preconcentration unit were compared to calibration runs bypassing it. Both experiments showed linearity between the injected carbon amount and the detector response (Figure 17). The results of the measurements including the CO_2 preconcentration unit always resulted in slightly but conspiciously higher values. Presumably not all CO_2 was released from the unit or CO_2 remained in small amounts in the system due to adsorption effects or dead volumes.

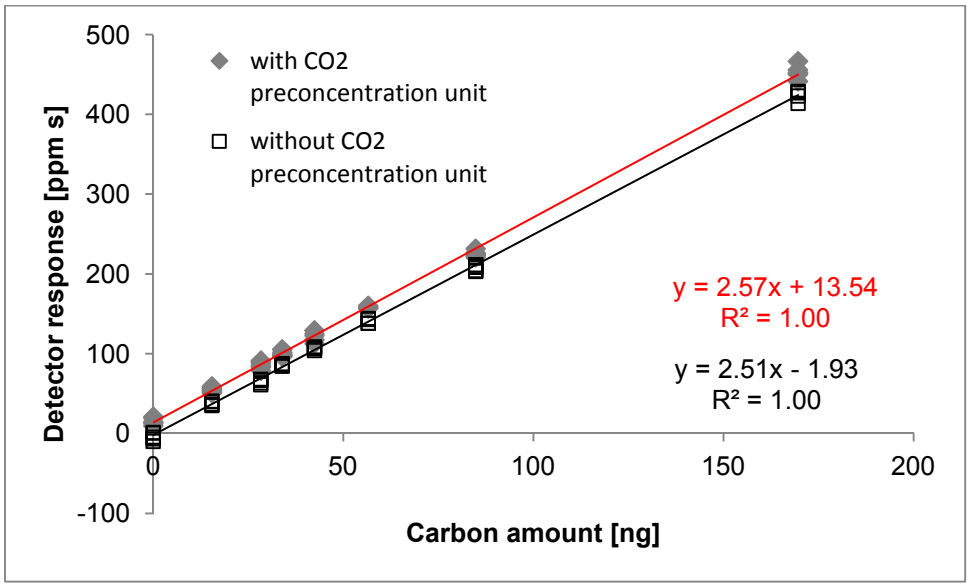

Figure 17: Signal development of different CO_2 ratios (CO_2 standard gas diluted in different volumes of helium (6.0) (see Table 4) including the CO_2 preconcentration unit (grey diamonds and red linear regression line) and without the CO_2 preconcentration unit (empty squares and black linear regression line). A shift to to higher values was observed when using the unit.

Measuring only the carrier gas without adding any CO_2 also resulted in a signal which was referred to as the helium blank. It was subtracted from every value obtained when including the CO_2 preconcentration unit, as long as no other blank value was

measured. Figure 18 shows that a good agreement between both experiments was received.

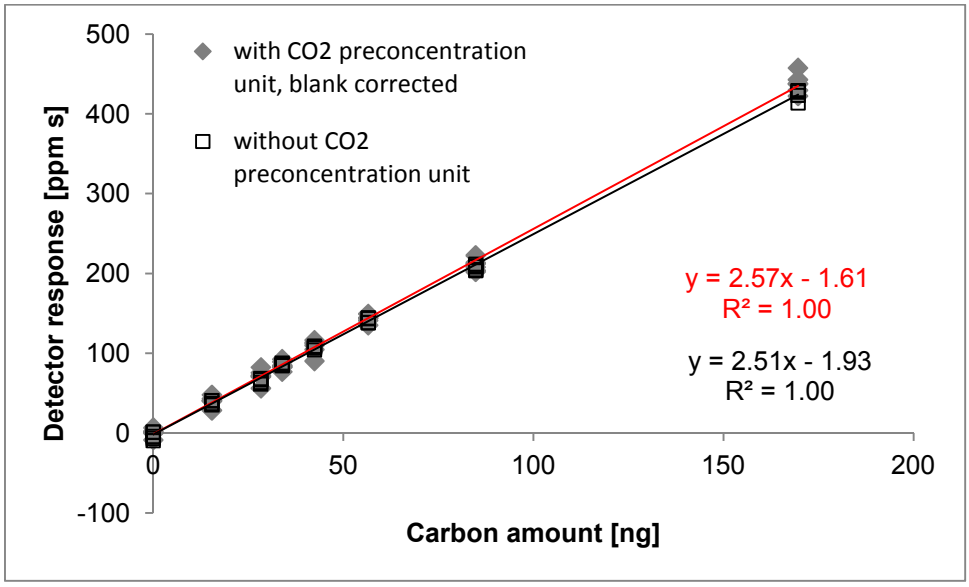

Figure 18: Comparison between the blank corrected values of measurements including the CO_2 preconcentration unit (grey diamonds) and the values without the CO_2 preconcentration unit (empty squares) of different CO_2 ratio measurements.

These results showed that a blank measurement was always necessary. For calibration measurements (see Figure 17) the blank value was in the order of 12 ng carbon. For sample measurements where more carbon was introduced into the instrument and consequently into the CO_2 preconcentration unit the blank reached values of approximately up to 25 ng carbon. Nevertheless, the experiments showed that the preconcentration unit was efficiently sampling the CO_2 and releasing it again when heated for desorption, but the blank value had to be determined and considered.

3.2 Oxidation unit

3.2.1 CuO catalyst

As mentioned in chapter 2.1.4 the original NMOC analyzer was equipped with an oxidation tube (length 360 mm, external diameter 28 mm) filled with 250 g of CuO as a catalyst. In the course of the experiments it soon became clear, that the catalytic material might not be suitable for the application of the instrument. Difficulties with the recovery rate as described by Dindorf (2006) might have been due to the fact that the oxidation efficiency was insufficient. Measurements with single compounds, like isoprene, Z-3-hexanol, α-pinene and β-caryophyllene, showed varying results. For isoprene and Z-3-hexanol a linear relationship between compound concentration (from the permeation/diffusion device) and detector response was observed. The measurements with α-pinene and β-caryophyllene did not result in linearity but in a saturation trend. However, a clear conclusion about the oxidation efficiency could not be taken, because the mixing ratios measured with the analyzer could not be determined and compared to the calculated values of the permeation/diffusion devices due to high CO_2 background signals, which were not measured separately. Nevertheless it was one of the most plausible explanations. Although Dindorf (2006) observed oxidation efficiencies of nearly 100% for CO and CH_4, higher molecular carbon structures like mono- and sesquiterpenes seemed to be not completely oxidized to CO_2. Other possibilities like a breakthrough of α-pinene or β-caryophyllene through the solid adsorbent material was highly unlikely. Since all settings remained the same for each measurement, other reasons could be largely excluded. Therefore, an oxidation test with β-caryophyllene was performed. The caryophyllene concentration was kept constant during this experiment, but oxidation unit temperatures and the addition of oxygen was varied. Figure 19 shows the results from the oxidation test.

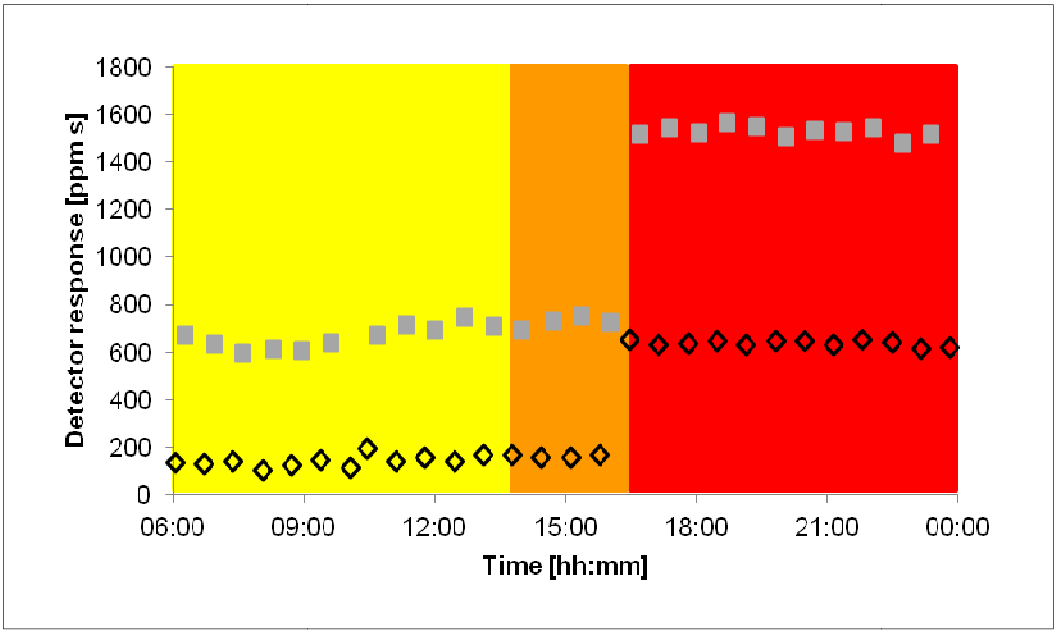

Figure 19: Peak integral values for an oxidation test with β-caryophyllene. The black diamonds represent the single CO_2 blank signal of the carrier gas (he 6.0) including the oxidation unit (note: not the CO_2 collected on the NMOC solid adsorbent unit) and the grey squares the CO_2 signal from single β-caryophyllene measurements; yellow background: temperature oxidation unit, 800°C; oxygen addition: 10%; orange background: temperature oxidation unit: 1000°C, oxygen addition: 10%; red background: temperature oxidation unit: 1000°C, oxygen addition: 15%

Temperature variation of the oxidation unit from 800°C to 1000°C at constant oxygen addition did not result in significant differences. But an increase of the oxygen addition showed a large effect on the detector response. The peak values even doubled. Also the CO_2 background value, which was basically derived only from the carrier/oxidation gas mixture, almost tripled. This can only be understood by assuming a release of CO_2 from the CuO catalyst material due to oxidation processes from carbon compound contamination of the catalyst material when adding more oxygen into the catalyst. A simple procedure was used to check the CO_2 release from the catalyst. The CO_2 preconcentration unit was bypassed and the oxidation unit flushed continuously with the carrier gas. Oxygen addition was repeatedly switched on and off every ten minutes. Figure 20 shows the results of the experiment.

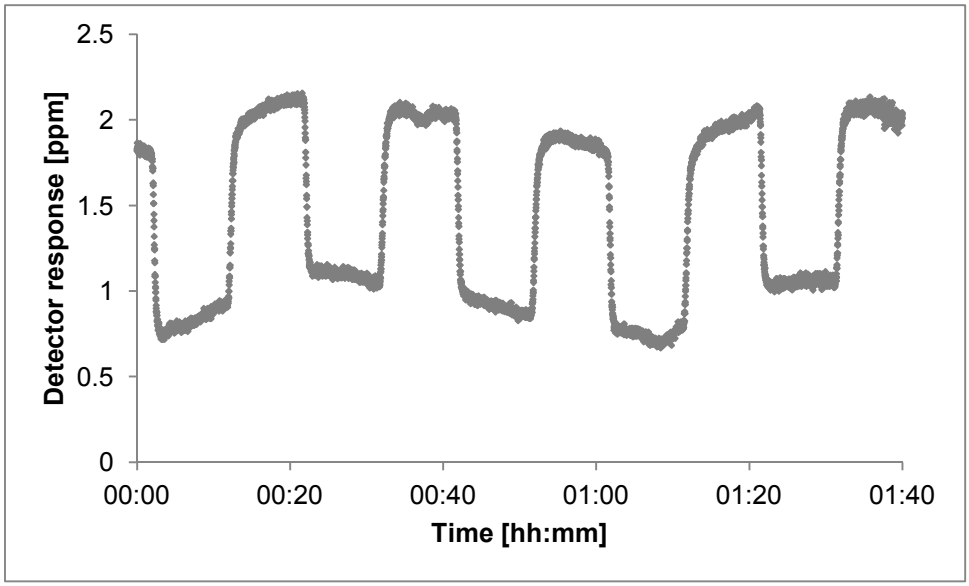

Figure 20: CO_2 signal arriving at the IRGA when continuously flushing the oxidation unit with helium. The oxygen addition is switched on and off every ten minutes.

One can clearly see an increase of the CO_2 mixing ratio of approximately 1 ppm when 10% oxygen was added to the carrier gas flow. The diagram also shows a slight drift of the detector response with time. The results clearly showed that the CuO catalyst cannot be used for the applications of the total NMOC analyzer. A size reduction of the oxidation unit still resulted in carbon blank values of approximately 115 ng carbon. Next to the problematic nature of the high carbon blank values due to oxygen addition, the apparently insufficient oxidation efficiency to oxidize higher molecular carbon structures resulted in the conclusion that the CuO catalyst was inappropriate.

3.2.2 Pd catalyst

Still with the original oxidation unit setup (glass tube length 360 mm, external diameter 28 mm placed in a vertical tube furnace) a further catalytic material was tested. It was an Al_2O_3 carrier material coated with palladium (Type H54 44, 0.5% Pd Hüls AG, Marl). The glass tube, containing the new catalytic material, was constantly flushed with zero air at a temperature of 400°C to ensure that no carbon was left on the surface of the material. After installing the new oxidation tube into the oxidation unit, it was flushed with helium at a flow rate of 100 ml min^{-1} for at least 48 h. But the first test with the oxidation unit again showed an approximately 0.5 ppm higher CO_2 mixing ratio signal arriving at the detector, when switching the oxidation unit into and

out of the helium carrier gas flow every five minutes. Repeating this experiment but adding 10% oxygen to the carrier gas flow resulted in almost the same discrepancy, which indicated that there was still CO_2 stored within the catalytic material but no carbon in form of other compounds as contamination on the catalyst. Due to the fact that during the experiment the CO_2, which was released from the oxidation unit, was slightly decreasing, it was assumed that the material needed more cleaning by flushing with helium. For this reason, the catalyst was flushed again with helium for approximately one week to reach a stable baseline. This problem was further investigated by injecting different amounts of CO_2 via the calibration loop (see chapter 2.1.6) into the oxidation unit (note: during a normal calibration the oxidation unit was bypassed). The resulting peaks all resulted in the same value regardless of the carbon amount injected into the system. Bypassing the oxidation unit showed a clear linear calibration line (see Figure 12). Including the oxidation unit into the system resulted in a kind of uptake and storage of the CO_2 when flushing with higher mixing ratios of CO_2, and a release of the stored CO_2 when flushing with low CO_2 mixing ratios or only carrier gas. This property of the catalytic material led to the conclusion that it could not be used when measuring VOCs as they should be converted into CO_2 in the oxidation unit. Not knowing how much of the generated CO_2 from VOCs or from adsorption of ambient CO_2 on the NMOC solid adsorbent unit was affiliated or released depending on the saturation level of the catalytic material even at temperatures of 400°C, led to the conclusion that this oxidation unit was impractical. These experiments led to the decision to change the oxidation unit setup and reduce the size of the oxidation tube and associated with this the surrounding setup of the heating unit.

3.2.3 Pt catalyst

The new oxidation unit setup with the new catalytic material was made available by the “Stickoxid Chemie” group from IEK-8 of the Research Centre in Jülich. The catalyst consisted of spherical Al_2O_3 carrier material that was coated with platinum. After the installation of the new oxidation unit, it was flushed with helium for 48h and kept at a temperature of 400°C. A first test was carried out to see if there was any CO_2 uptake or release from the material. The whole system was flushed with the CO_2 standard gas (352 ppm in synthetic air, Air Liquide) for a short time excluding the

purifier cartridges. One CO_2 course was recorded without the oxidation unit and the second one including it. Both were inserted into one diagram and compared to each other. Figure 21 shows the comparison. Before and after switching to the CO_2 standard gas, the system was flushed with helium.

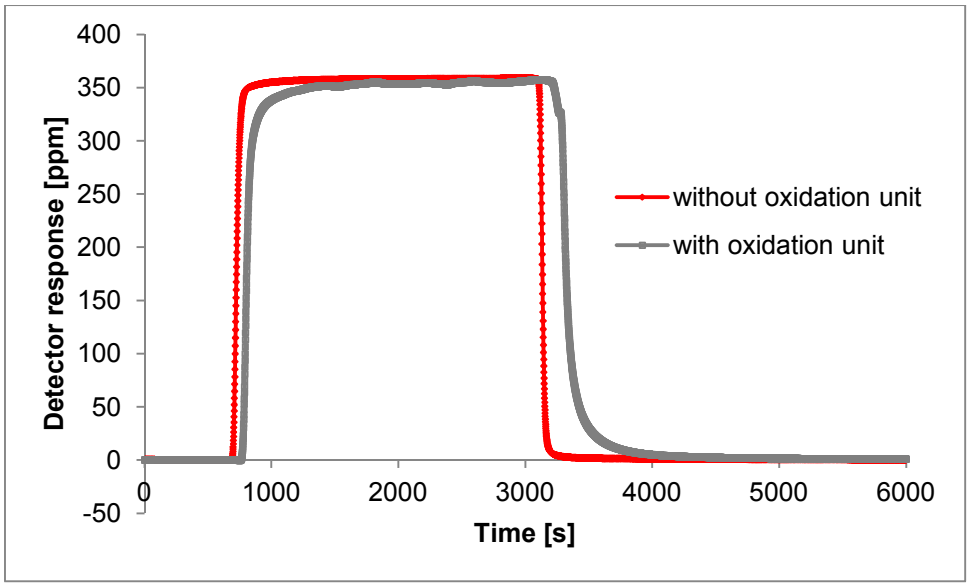

Figure 21: CO_2 uptake und release test with the Pt catalyst material. The red line represents the CO_2 signal of the standard gas flushed through the system without the oxidation unit and the grey line including the oxidation unit.

Despite the fact that the two graphs are not completely superimposed, the comparison can give a first indication that this material also took up CO_2 and slowly released it as indicated by the delays of the signals obtained with the oxidation unit. Further tests were needed to characterize the catalytic material. A measurement series with zero air containing ambient CO_2 mixing ratios was performed. Due to the fact that the NMOC solid adsorbent unit also sampled CO_2 (see chapter 3.3.1), these CO_2 quantities corresponded to a regular measurement. Different instrument settings were performed. Table 7 gives an overview of the applied program files.

Table 7: Applied program files and the units in- and excluded during the measurement.

File	NMOC unit	oxidation unit	CO_2 preconcentration unit
$HeCO_2$	×	×	✓
$TestCO_2$	3000 ml zero air with ambient CO_2 concentration	×	✓
$SysCO_2$	×	✓	✓
TestSam	3000 ml zero air with ambient CO_2 concentration	✓	✓

× not included in the carrier gas stream
✓ included in the carrier gas stream

The first program file represented the measurement values of the CO_2 amount collected on the CO_2 preconcentration unit in the helium carrier gas. The NMOC solid adsorbent unit and the oxidation unit were not included into the system and the gas flow. This program file was called $HeCO_2$. The second file $TestCO_2$ illustrated the measurement values when sampling zero air containing CO_2 on the NMOC solid adsorbent unit. The carbon amount which was injected into the instrument due to CO_2 sampling on the adsorbent material was bypassing the oxidation unit and was preconcentrated on the CO_2 preconcentration unit. The analysis of this CO_2 amount represented the CO_2 blank value ($area_{CO2Sample}$) of the system. In both measurement sequences the oxidation unit was bypassed and cut off any gas flow during that time. The third program file $SysCO_2$ displayed the measurement values for the CO_2 amount within the carrier gas flow when flushing the oxidation unit but excluding any air sampling on the NMOC solid adsorbent unit. Therefore, this file represented the results for the amount of CO_2 coming from the oxidation unit. They were directly compared to the values from the $HeCO_2$ program file measurements. At best, they should both result in the same value. The fourth and last program file illustrated again the measurement values from sampling CO_2 from zero air on the NMOC solid adsorbent unit. This file was called TestSam. The NMOC solid adsorbent unit and the oxidation unit were included in the analyzer system in this program sequence. With this measurement file the values for the total carbon amount of the NMOCs (including also the sampled CO_2) ($area_{NMOCSample}$) were obtained. Further details on the iteration of the different program files can be found in appendix D. Due to the fact that the sampled air did not contain any VOCs, the results from the TestSam program file can

be compared to the ones from the $TestCO_2$ file measurements. In case there was no CO_2 uptake or release from the catalytic material, the data from $HeCO_2$ and $SysCO_2$ and the data from $TestCO_2$ and TestSam should result in the same values respectively. Figure 22 shows the results of the above measurement series.

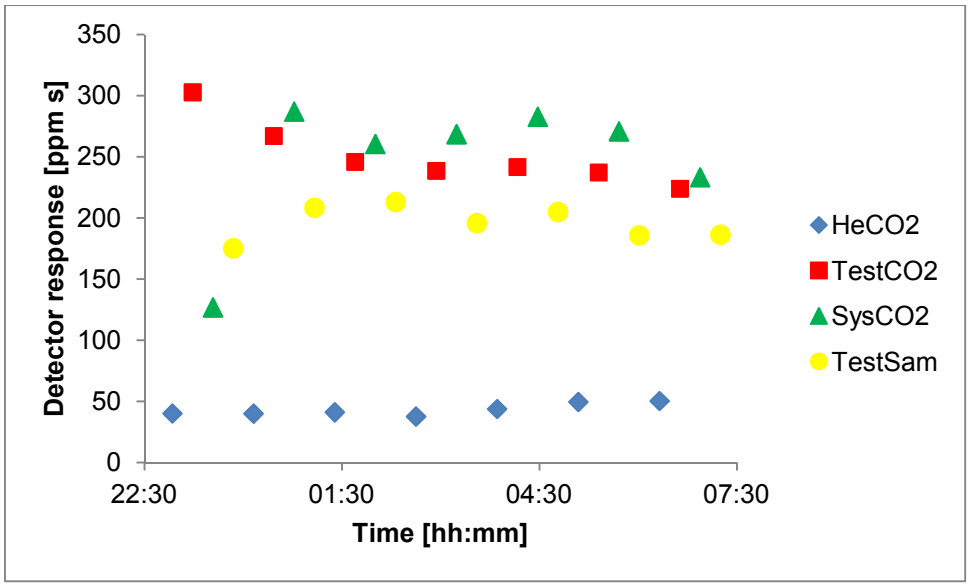

Figure 22: Development of the detector response under different instrument settings. Measurements were carried out with zero air containing CO_2 in ambient mixing ratios. The blue diamonds represent the values for $HeCO_2$, the red squares the results for $TestCO_2$, the green triangles illustrate the values of $SysCO_2$ and the yellow circuits display the results from the TestSam measurements (see also Table 7 and Appendix D). The sequence of the measurement series was as followed: $HeCO_2$, $TestCO_2$, $SysCO_2$, TestSam.

At a glance, one can see immediately that the figure does not show the expected results. Furthermore, it indicates instantly that the catalytic material must have had an effect on the CO_2 amount available in the carrier gas flow. The $HeCO_2$ data resulted in stable values, which was expected as these measurements only involved the CO_2 preconcentration unit and the carrier gas helium. The values were as anticipated by earlier measurements. The $TestCO_2$ measurement results varied slightly particularly at the first values, which might be due to memory effects on the NMOC solid adsorbent unit as this was not in use for a few days. However, the values were more or less stable. The $SysCO_2$ results showed a large deviation from the expected trend. Except for the first value, all other values from the $SysCO_2$ measurements resulted in the highest data points. The first value can be explained by the fact that the oxidation unit was continuously flushed with helium before the experiment, and did not have any contact with CO_2 for a longer period. Only a small amount of CO_2 is released

from the catalytic material. However, after one measurement series sequence and the oxidation unit coming in contact with CO_2, the values increase significant. This can only be understood if we assume that the CO_2 which was introduced to the oxidation unit in the first measurement series was released in the subsequent measurements. The assumption that CO_2 is stored and released within the catalytic material would also confirm the values of the TestSam series which showed lower results than the corresponding TestCO_2 series. The only explanation for this behavior was an uptake of the CO_2 by the catalytic material. The circumstance that the SysCO_2 values were the highest can be understood by the sequence of the program files. As the oxidation unit was excluded in the two subsequent files and closed off from any gas flow, the affiliated CO_2 accumulated in the oxidation unit and was released to the carrier gas flow upon flushing the oxidation unit during the SysCO_2 measurement series. According to these understandings the oxidation unit build-up was changed. A different setup of the valves connecting the oxidation unit to the instrument was implemented. Instead of two 3-way-2-position valves that created a bypass and closed off the oxidation tube from the carrier gas flow, a 6-way-2-position valve (oxidation valve) was mounted, that enabled a constant flushing of the oxidation unit with helium. Even when the catalyst was not connected to the carrier gas flow of the instrument during a measurement, the converted dilution flow controller (see Figure 7) provided the catalyst with a constant helium flow. With this modification the same measurement series was carried out again. The results are shown in Figure 23. In the diagram stable signal values for HeCO_2, TestCO_2 and SysCO_2 can be observed. This was a progression compared to the experiment with the originally oxidation unit setup and Figure 22. The TestCO_2 values showed stable carbon signals from CO_2 sampled on the NMOC solid adsorbent unit. The HeCO_2 and SysCO_2 measurement series also resulted in steady values. Moreover, they exhibited the same CO_2 detector response which verified that under constant flushing of the oxidation unit, there was no excessive CO_2 stored on the catalytic material and released during the measurement. Not so promising were the resulting values from the TestSam measurements. They showed a decrease with time. This could only be interpreted by the assumption that the catalytic material adsorbed the CO_2 which was introduced into the oxidation unit. The adsorbed CO_2 was flushed out with the continuous helium flow when the oxidation unit was not connected to the carrier gas flow. Consequently, this CO_2 is lost and cannot be measured. Moreover, the catalytic

material seemed to be cleaned from CO_2 more and more after each measurement series which allowed an even higher CO_2 uptake in the following TestSam measurements. This led to the conclusion that this catalytic material was also unusable for the application of the instrument, because the determination of the exact total carbon amount from a TestSam measurement was crucial for the final determination of the total NMOC mixing ratio.

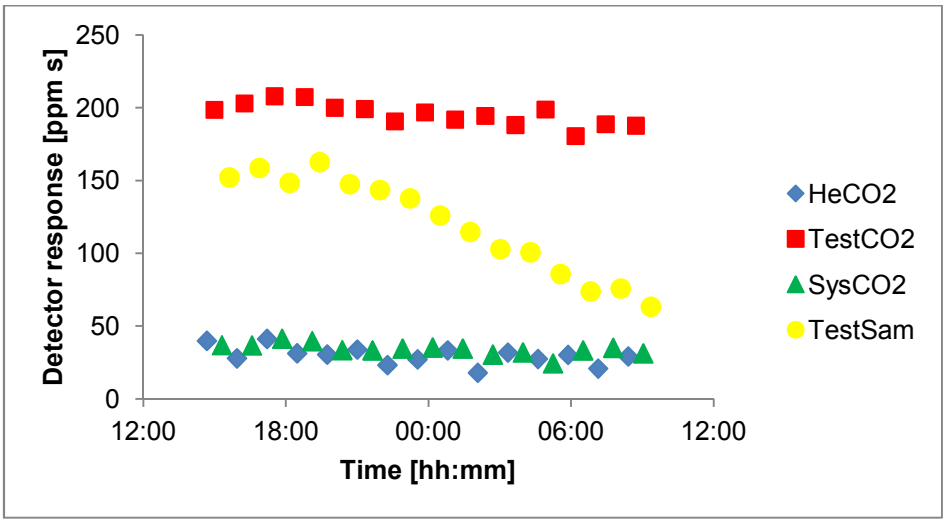

Figure 23: Development of the detector response under different instrument settings. The oxidation unit was continuously flushed with helium. The blue diamonds represent the values for $HeCO_2$, the red squares the results for $TestCO_2$, the green triangles display the values of $SysCO_2$ and the yellow circuits illustrate the results from the TestSam measurements (see also Table 7 and Appendix D). The sequence of the measurement series was as followed: $HeCO_2$, $TestCO_2$, $SysCO_2$, TestSam.

The observation of the two catalytic materials in this chapter and in chapter 3.2.2 showed that there was a great problem with catalysts based on porous carrier materials with a high surface. Both materials exhibited these properties and besides temperatures of 400°C, CO_2 was still adsorbed and released. Also the size reduction of the whole oxidation unit did not lead to better results. However, the new setup of the oxidation unit represented a significant improvement, both in terms of size reductions and in the continuous flushing of the catalytic material. Oxidation efficiency tests were not carried out with these catalysts as the mentioned problems were too severe.

3.2.4 Pt-Rh catalyst

Due to the fact that porous catalytic materials proved to be the inappropriate choice for the application of the total NMOC analyzer, a new solution had to be found. At choice was a platinum-rhodium wire (Pt/Rh-mix 50/50, diameter: 0.3 mm, Evonik Degussa GmbH, Essen, Germany). Approximately 5 m of the wire was spiralled into the oxidation tube. It filled only half of the glass tube but more wire was not available at this time. The temperature for the oxidation unit was set to 500°C. Wire has a small surface compared to the other two materials tested in chapter 3.2.2 and 3.2.3. An uptake of CO_2 was not expected with this catalytic material. Nevertheless, the same experiment as in chapter 3.2.3 was deployed. Again the instrument was flushed with CO_2 standard gas, once with and once without the oxidation unit. Figure 24 shows the corresponding graphs.

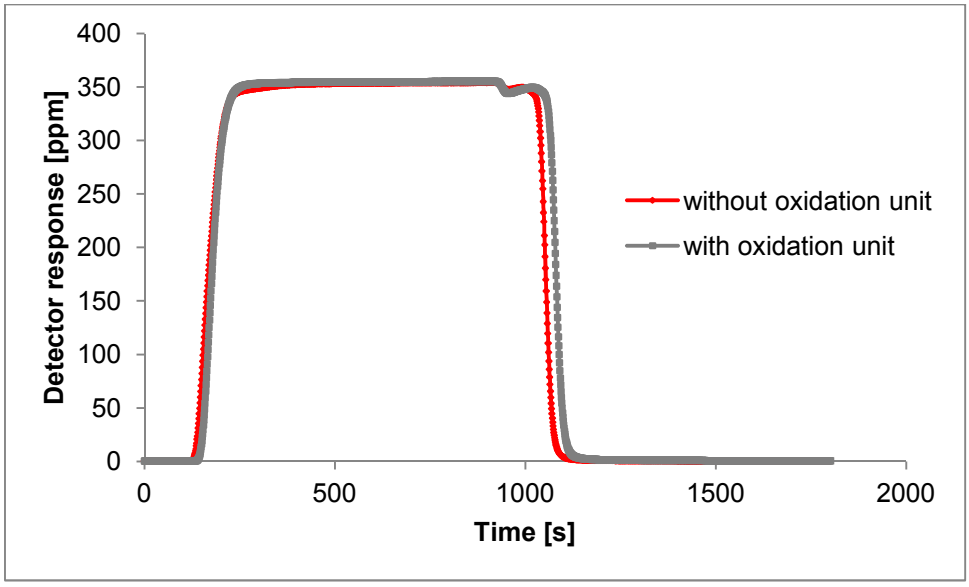

Figure 24: CO_2 uptake and release test with the Pt-Rd wire catalyst. The red line represents the CO_2 signal of the standard gas flushed through the system without the oxidation unit and the grey line including the oxidation unit.

They were superimposed. The slight delay can be explained by manually switching of the valves. A CO_2 uptake or storage was excluded. Another undesirable property, despite from the one shown with the Pd- and the Pt-catalyst, was the CO_2 signal increase due to oxygen addition as shown with the CuO catalyst. For this reason an oxidation unit test like the one mentioned in chapter 3.2.1 was applied. During permanent oxygen addition (10%) the oxidation unit was switched into and out of the

carrier gas flow every ten minutes. The data did not show any visible change. Furthermore, the measurement series from chapter 3.2.2 and 3.2.3 was repeated. In addition to the previous mentioned four program files $HeCO_2$, $TestCO_2$, $SysCO_2$ and TestSam a fifth program file (KatCO2) was added. With this file the CO_2 amount which was emerging from the oxidation unit upon oxygen addition to the helium carrier gas flow (90%/10%) was measured. The program file sequence was similar to the $SysCO_2$ file except for the oxygen addition. Table 8 gives an overview of the applied program files. The results of the measurement series are shown in Figure 25.

Table 8: Applied program files and the units in- and excluded during the measurement.

File	NMOC unit	oxidation unit	Oxygen addition (10%)	CO_2 preconcentration unit
$HeCO_2$	×	×	×	✓
$TestCO_2$	3000 ml zero air with ambient CO_2 concentration	×	✓	✓
$SysCO_2$	×	✓	×	✓
$KatCO_2$	×	✓	✓	✓
TestSam	3000 ml zero air with ambient CO_2 concentration	✓	✓	✓

× not included in the carrier gas stream
✓ included in the carrier gas stream

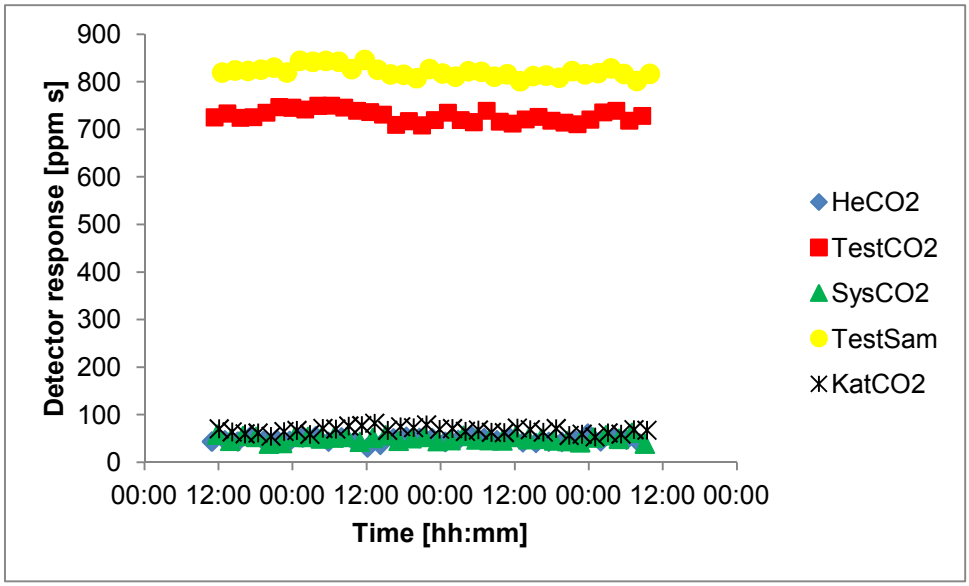

Figure 25: Development of the detector response under different instrument settings. Measurements were carried out with zero air containing CO_2 in ambient mixing ratios. The oxidation unit was continuously flushed with helium. The blue diamonds represent the values for $HeCO_2$, the red squares the results for $TestCO_2$, the green triangles display the values of $SysCO_2$, the yellow circuits illustrate the results from the TestSam measurements and the black crosses point out the new value $KatCO_2$. The sequence of the measurement series was as followed: $HeCO_2$, $TestCO_2$, $SysCO_2$, $KatCO_2$, TestSam (see also Table 8 and Appendix D).

The $HeCO_2$ and $SysCO_2$ values showed a good agreement. Also the $KatCO_2$ measurements resulted in a stable signal which was slightly enhanced compared to the other two carrier gas measurements. This indicated that the Pt-Rh-wire also released small amounts of CO_2 but it was negligible compared to the CuO catalyst. The $TestCO_2$ and TestSam measurements also resulted in stable values. However, the values for TestSam exceeded the ones from $TestCO_2$ with a deviation of approximately 30-40 ng carbon. What caused this deviation is not clear. It might be a result of VOC compounds left in the zero air or due to memory effects from the NMOC solid adsorbent unit. Anyway, the Pt-Rh-wire seemed to be the right choice as a catalyst after the previous test. The only but probably most important property left to clarify was the oxidation efficiency. First tests with isoprene showed good recovery rates for the comparison of the NMOC analyzer results with the mixing ratios from the permeation/diffusion device. Other compounds did not result in as good recovery rates. Whether the poor results for the recovery rates of other compounds like α-pinene or nopinone were caused by the catalyst was not clarified. More details on this issue can be found in chapter 3.3.

3.3 NMOC solid adsorbent unit

3.3.1 CO_2 background

Carbon compounds occurring in air in high concentrations like CO_2, CO and CH_4 might influence the measurement of the total NMOC significantly. Dindorf (2006) showed that the sampled amount of these compounds on the chosen solid adsorbent material was relatively low (see Table 9).

Table 9: Sampling efficiency of the compounds CO_2, CO and CH_4 in % taken from Dindorf (2006).

Compound	Sampling efficiency in %
Carbon dioxid ($CO_{2)}$	0.008
Carbon monoxide (CO)	0.115
Methane ($CH_{4)}$	0.076

This data demonstrated that CO_2, CO and CH_4 were only sampled in very small amounts on the NMOC solid adsorbent unit. Generally the observed low sampling efficiencies are a result from the special properties of the applied graphitised carbon black adsorbent Carbograph 1 and 5 (Brancaleoni et al. 1999). However, even these low amounts can cause severe background signals especially from CO_2 which is present in ambient air with mixing ratios of approximately 390 ppm (Wolff 2011) as compared to the ppb levels of VOC. Because the instrument was reconstructed and different flow rates applied for the carrier gas the sampling efficiency for CO_2 was redetermined. With the current setup, sampling efficiency rates were higher than the ones obtained with the previous setup. With varying CO_2 mixing ratios the recovery rates of CO_2 reached roughly 0.015 – 0.042% for a total sampling volume of 5250 ml (3000 ml ambient air plus 2250 ml flushing with helium). Figure 26 shows the results of an experiment where repeated ambient zero air measurements with different CO_2 mixing ratios was implemented.

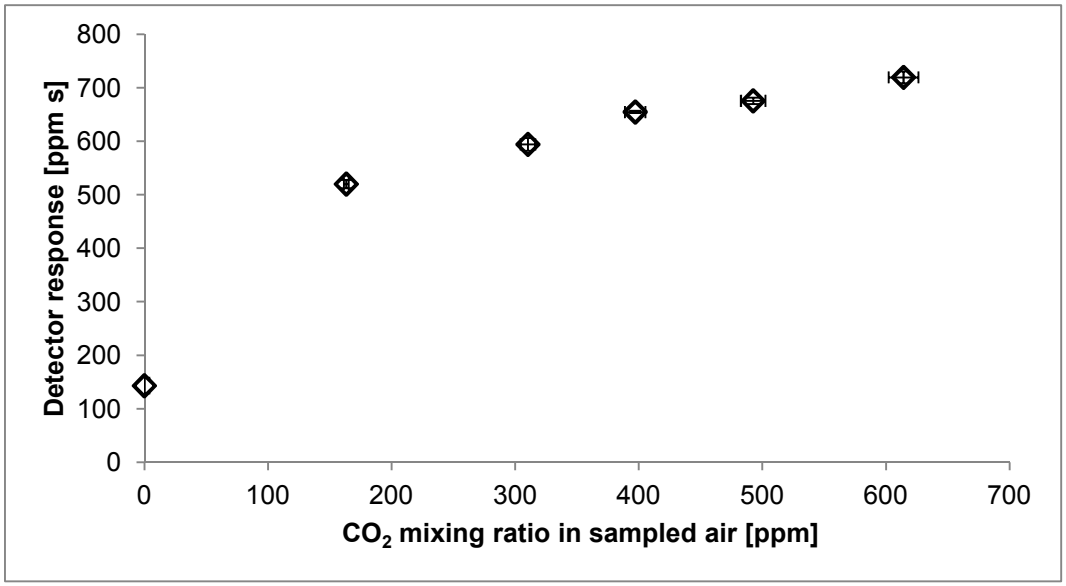

Figure 26: Detector response of repeated zero air measurements containing different CO_2 mixing ratios. The black diamonds represent the mean average (n>3) of the measured values from the total NMOC analyzer with the corresponding average CO_2 mixing ratios including standard deviation.

Excluding the value for zero CO_2 (only helium was sampled), the diamonds show a linear course. 0.015 – 0.042% sampling efficiency corresponded to carbon mixing ratios of approximately 69 - 95 ppb which is a high background signal for ambient NMOC measurements. Nevertheless, through measuring the background signal corresponding to every NMOC value, the CO_2 background signal can be subtracted. The diagram also shows a signal for a measurement where only helium was measured. This result indicated that not only CO_2 was sampled from ambient air but also released or produced from the adsorbent material. The following chapters show the attempt to minimize CO_2 sampling efficiencies on the solid adsorbent unit by variation of the sampling volume, the sampling temperature, the flush volume and the desorption temperature.

3.3.1.1 Sampling volume

The sampling volume is an important factor for VOC analysis. Due to the properties of the solid adsorbent material the settings for the sampling volume have to be considered. CO_2 adsorption, water condensation, and breakthroughs of compounds with a low carbon structure have to be minimized. Water condensation can be avoided by choosing a temperature above room temperature. Therefore, the sampling temperature was set to 35°C for the experiment. A closer observation of the

sampling temperature concerning the CO_2 adsorption and NMOC sampling efficiency can be found in the chapters 3.3.1.2 and 3.3.3.2. Different sampling volumes were tested concerning the CO_2 adsorption by varying the sampling time. The sampling flow was set to 300 ml min^{-1}. A helium flush volume of 2250 ml (3 min flushing time with a flow rate of 750 ml min^{-1}) was applied.

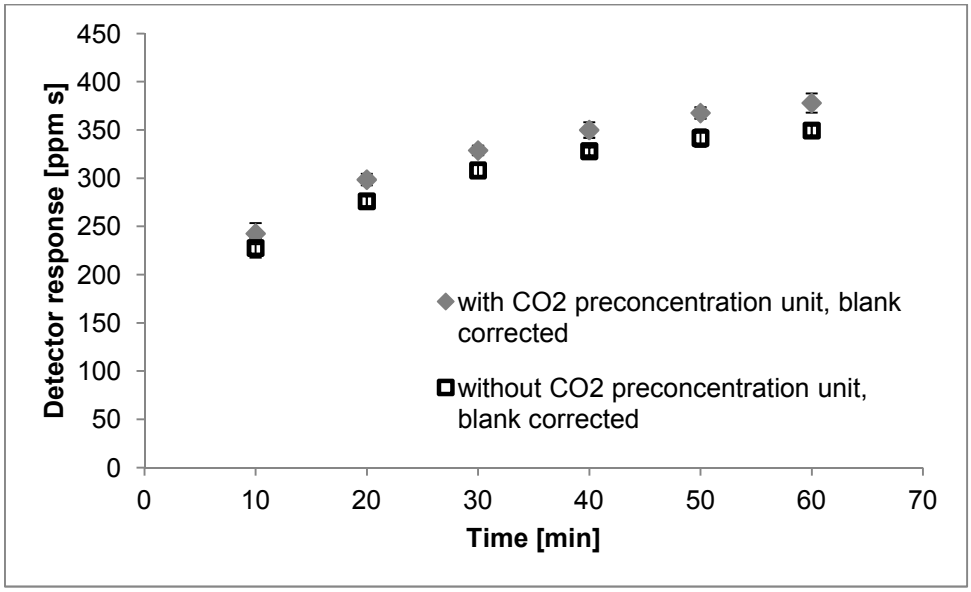

Figure 27: Increasing CO_2 background signal (mean average from n>3 measurements including standard deviation) from CO_2 adsorption on the NMOC solid adsorbent material with increasing sampling time and by association increasing sampling volume. The black squares represent the values obtained without the CO_2 preconcentration step and the grey diamonds show the results for the measurement including the CO_2 preconcentration unit. Both results are blank corrected.

Figure 27 shows the results for the sampling of zero air containing 670 (+/- 70) ppm CO_2. For sampling times of 10 min the smallest CO_2 background signal was observed. The CO_2 adsorption was increasing and slowly reaching a breakthrough with increasing sampling time/volume. The discrepancy between the measurements with and without the CO_2 preconcentration unit can be explained by a peak broadening of the signal without the CO_2 preconcentration unit and a probable loss of small amounts of CO_2 sampled on and released from the NMOC adsorbent unit.

Another important factor of the sampling volume is the breakthrough of VOC compounds. Table 10 shows an overview of various compounds and their safe sampling volume (Brancaleoni et al. 1999, Dindorf 2006). A safe sampling volume is the volume which can be sampled on the solid adsorbent cartridge for a special compound without a breakthrough.

Table 10: Safe sampling volumes to avoid breakthrough of various compounds for the two adsorbent materials used in the NMOC solid adsorbent unit (Brancaleoni et al. 1999, Dindorf 2006).

Compound	Carbograph 1 in ml	Carbograph 5 in ml
Propane	< 100	200
Propene	< 100	200
Isobutane	< 100	> 5000
n-butane	< 100	> 5000
1-butene	< 100	> 5000
Isopentane	100	> 10000
n-pentane	200	> 10000
1-pentene	< 100	> 10000
n-hexane	> 5000	> 10000
1-hexane	> 5000	> 10000
n-heptane	> 5000	> 10000
Benzene	2000	> 10000

The combination of the two solid adsorbent materials allowed the safe sampling of VOC compounds with a carbon structure C>3 with the applied sampling volume of 3000 ml (10 min sampling time with a flow rate of 300 ml min^{-1}) and a helium flush volume of 2250 ml. This resulted in a total volume of 5250 ml. C_4 and higher structured VOC compounds should be sampled quantitatively and CO_2 background signals were minimized due to the short sampling time.

3.3.1.2 Sampling temperature

The CO_2 background signal is an important factor for the correct determination of the NMOCs. As shown in the previous chapter it plays a major role for these kinds of measurements. CO_2 background sources can be found in various units of the instrument. One of these units is the NMOC solid adsorbent unit as it also collects small amounts of CO_2 present in ambient air. Even if this CO_2 is only collected in very small quantities, compared to the abundance of CO_2 and NMOCs in the atmosphere, high blank values are reached through to this adsorption. They were in the same order of magnitude or even higher as the expected carbon mixing ratios from NMOC compounds. Even through preconcentration steps, the NMOC carbon amounts did not reach higher values. The sampling temperature plays a major role in adsorption processes. Especially to minimize or avoid water condensation, the temperature has to be set high enough. By choosing temperatures around or above 30°C only little

water should be accumulated. As the test experiments were executed with dry zero air containing ambient mixing ratios of CO_2, the moisture did not play any role in this experiment setup. However, temperatures should not be set lower in case of ambient air or plant chamber experiments where moisture is present. As the breaktrough volume is dependet on the temperature, an increase of the adsorption temperature can reduce the amount of sampled CO_2 on the NMOC solid adsorption unit which would be desirable. However, this also increases the risk of loosing NMOCs. Figure 28 shows the results of a test experiment where different adsorption temperatures were applied.

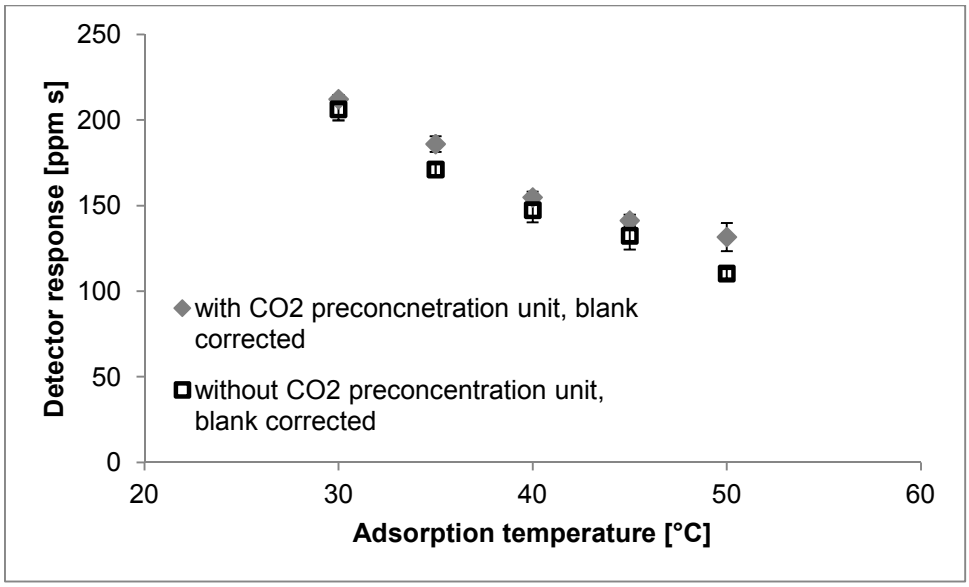

Figure 28: Decrease of the CO_2 background signal (n>3 including standard deviation) with increasing sampling temperature. The black squares represent the values obtained without the CO_2 preconcentration step and the grey diamonds show the results for the measurement including the CO_2 preconcentration unit. Both results are blank corrected.

The figure shows the same course for both measurement series. They were not superimposed which might be due to the fact that the measurement series were carried out a few weeks apart, with slightly varying CO_2 mixing ratios in the measured zero air. Sampling time and volume was set to 300 ml min^{-1} for 10 min resulting in a total volume of 3000 ml. The CO_2 mixing ratio in the zero air amounted to 385 (+/- 25) ppm. The measurement values showed the expected course. With higher sampling temperatures the sampling of CO_2 was reduced. However, there is a narrow ridge in finding the right balance in the choice of increasing the sampling temperature with less CO_2 background and the risk of losing NMOC compounds due

to breakthrough. Further tests concerning the breakthrough of NMOC compounds had to be carried out to consider a choice of the sampling temperature (see chapter 3.3.2.2). However, the sampling temperature of 35°C applied by Dindorf (2006) was maintained for most experiments.

3.3.1.3 Flush volume

The excessive ambient air which was left in the tubing and the dead volume of the sample inlet and the NMOC solid adsorbent unit after air sampling had to be flushed out by a helium flow to avoid background signals from CO_2 from ambient air and from other carbon based compounds. This helium flow was called the flush volume. As shown in previous chapters, CO_2 was sampled on the solid adsorbent material. Through the flush volume the sampled CO_2 can be reduced due to a breakthrough of the CO_2. Different test runs with the flush volumes were already carried out and discussed by Dindorf (2006) concerning the sampling amount of CO_2 on the solid adsorbent material. Since sampling amounts of CO_2 on the solid adsorbent unit were different from the previous measurements, the flush volume was observed again for this setup of the NMOC analyzer. Zero air samples with a set CO_2 mixing ratio of 430 (+/-40) ppm were sampled on the solid adsorbent unit and different flush volumes were applied. Flush volumes were set to 1875 ml, 2250 ml, 4000 ml and 9000 ml. This corresponded to 2.5 min, 3 min, 6 min and 12 min flushing time with a flow rate of 750 ml min^{-1}. As the sample flow controller (see Figure 7, (8)) was calibrated for N_2 and the settings were optimized for ambient air sampling with 300 ml min^{-1}, a sample flow set of 500 ml min^{-1} was applied for the flush volume with helium. As the thermal conductivity of helium differs from the one of ambient air (or N_2), the set flow rate of 500 ml min^{-1} corresponded to a helium flow of approximately 750 ml min^{-1}. The flows were measured at regular intervals.

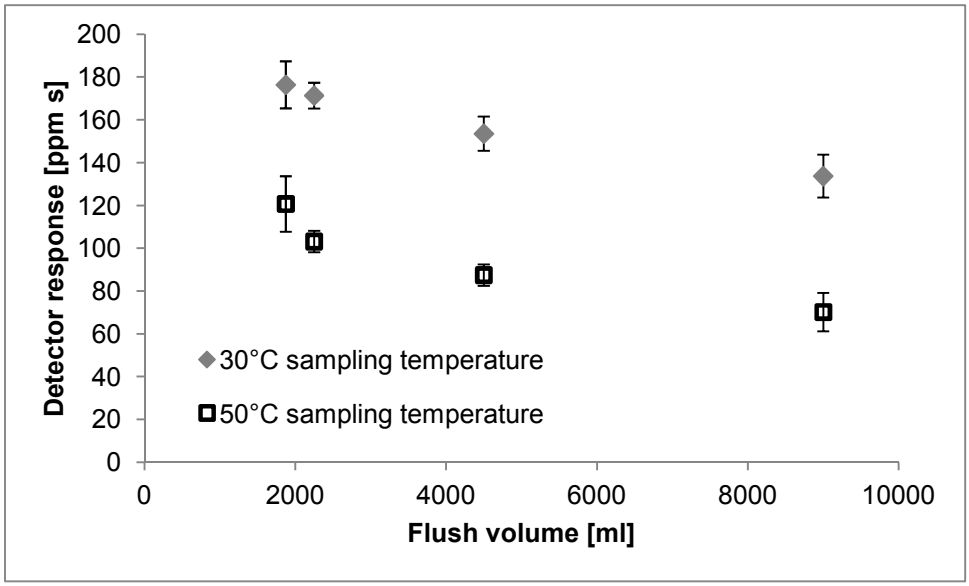

Figure 29: Decreasing CO_2 blank values with increasing flush volume. The grey diamonds represent the average values (n>3 including standard deviation) of a flush volume experiment with a sampling temperature of 30°C. The black squares are the mean results (n>3 including standard deviation) with a sampling temperature of 50°C. Both measurements were carried out excluding the oxidation unit and the CO_2 preconcentration unit. All mean values are blank corrected.

Figure 29 shows the dependence of the CO_2 signal compared to the helium flush volume applied after 10 min air sampling time with 300 ml min^{-1} with two different sampling temperatures (30°C and 50°C). For both measurement series the oxidation unit and the CO_2 preconcentration unit was bypassed. The values were corrected with the carbon blank signal coming from the NMOC solid adsorbent unit when no air was sampled. A clear discrepancy between the two temperature settings was observed as already shown earlier (chapter 3.3.1.2). Also a reduction of the CO_2 blank signal with increasing flush volume was found. Figure 30 shows the same relationship, but this time referring to the total volume which includes the 3000 ml sampling volume plus the applied flush volume. The carbon mixing ratios resulted in CO_2 blank values of 70 - 25 ppb for a sampling temperature of 30°C and between 45 - 10 ppb for a temperature of 50°C.

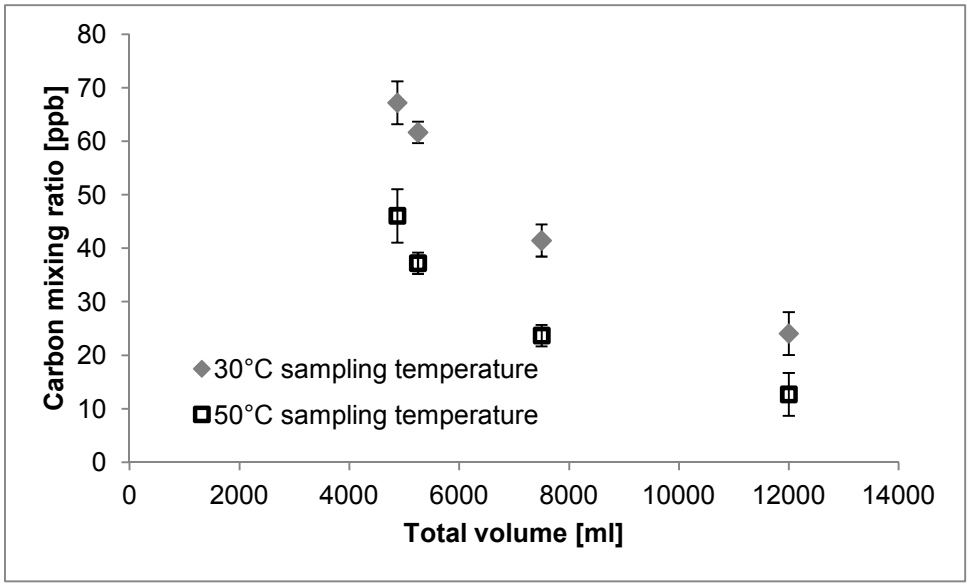

Figure 30: Decrease of the carbon signal (n>3 including standard deviation) with increase of the flush volume considering the total volume (sample volume = 3000 ml plus flush volume).

Both figures (29 + 30) demonstrate a CO_2 background signal reduction with increasing flush volume. Nevertheless, an increased flush volume also means an increased total volume which endangers a breakthrough of other compounds on the solid adsorbent unit. A flush volume of 2250 ml (= 3 min) was applied in order to avoid a possible breakthrough. Again, it is a difficult consideration between the CO_2 background signal and the NMOC adsorption amount.

3.3.1.4 Desorption temperature

As indicated in Chapter 3.3.1 (Figure 26) a CO_2 blank value was also depending on the NMOC solid adsorbent unit due to heating. Blank values were obtained from sampling with helium for 10 min with 300 ml min^{-1} including the flush volume or only from flushing the solid adsorbent unit with the helium flush volume without previous air sampling. As the oxidation unit and the CO_2 preconcentration unit were excluded from the helium gas flow during the measurement, no CO_2 was produced or released from these units. Memory effects from the NMOC solid adsorbent unit might be one reason for CO_2 blank values but still after several runs with only helium, carbon signals were detected. A small decrease in the signal was observed which means that there might be some kind of memory effect caused by the solid adsorbent unit but this could certainly not explain the high CO_2 blank values. To allow fast heating of the NMOC adsorbent unit, a new transformer was connected to the heating coil

which was surrounding the adsorbent tube. The previous setup allowed desorption temperatures of 250°C which were reached relatively slowly. The new setup allowed faster heating, up to 300°C. As the recovery rate of the previous setup only resulted in 48% (Dindorf 2006) a better recovery rate was expected to be obtained by a faster temperature increase or by applying a higher desorption temperature.

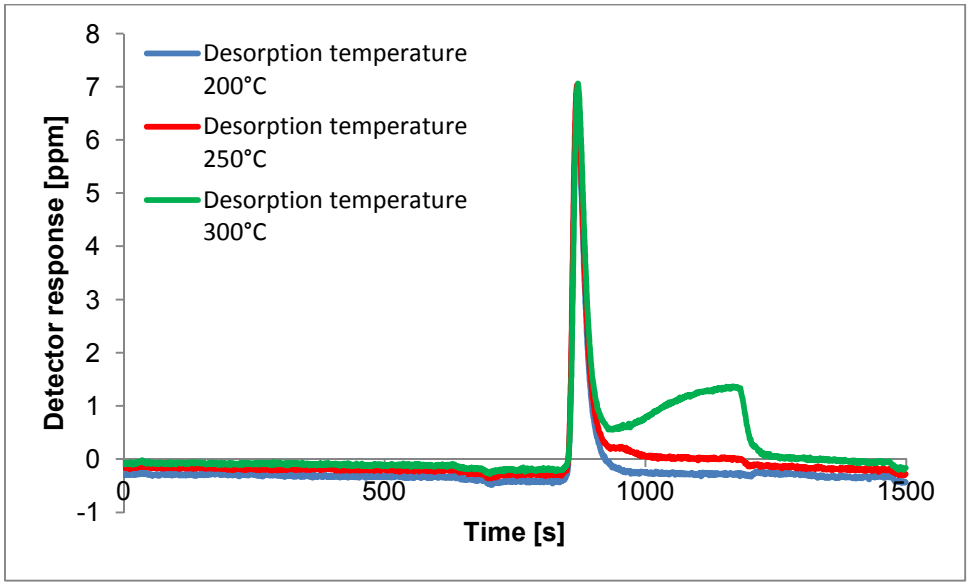

Figure 31: Different CO_2 background signals from zero air sampling containing CO_2 in ambient mixing ratios. The blue line shows the course with a desorption temperature of 200°C, the red one the CO_2 signal for the run with a desorption temperature of 250°C and the green line shows the result for 300°C desorption temperature.

Different desorption temperatures (200°C, 250°C and 300°C) were applied resulting in increasing CO_2 background signals for higher temperatures. Figure 31 shows a result from a test run with zero air containing 375 (+/-30) ppm CO_2 sampled on the solid adsorbent unit with different desorption temperatures. Figure 32 summarizes single CO_2 signals for the different desorption temperatures in course of the experiments. In Figure 31 a clear superimposition of the CO_2 peak which originates from CO_2 sampling on the solid adsorbent unit is shown. However, a further signal was observed. Except for the graph at 200°C desorption temperature, the signal did not return to the baseline as long as the heating of the desorption unit continued. At a desorption temperature of 300°C, a clear increase of the CO_2 signal was observed. Figure 32 shows the signal curves from Figure 31 separated, along with the corresponding temperature courses.

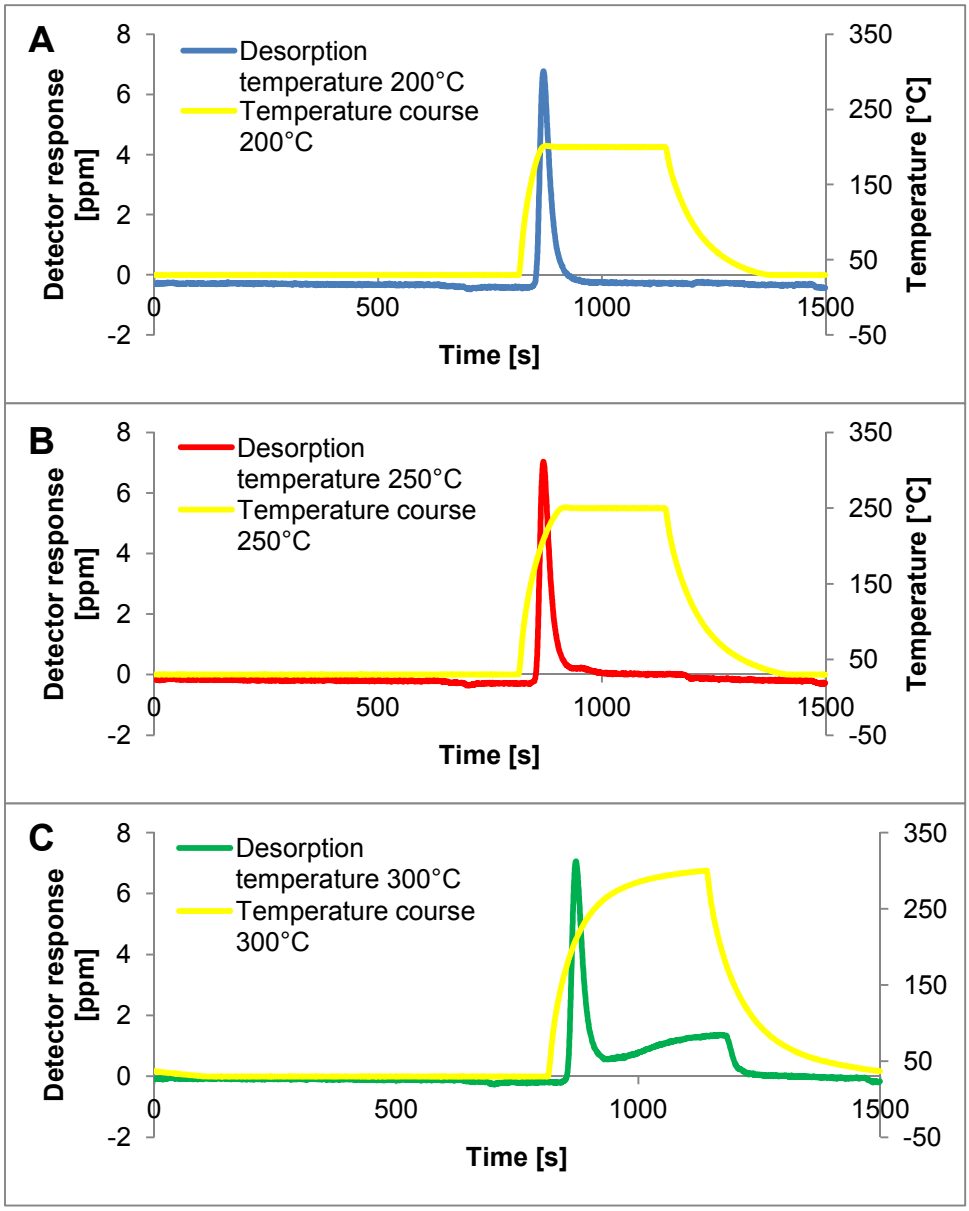

Figure 32: CO_2 background signals (primary y-axis) from an ambient zero air measurement with different desorption temperatures (A = 200°C, B = 250°C, C = 300°C). The colours are corresponding to Figure 31. Yellow represents the temperature course of the measurement run (secondary y-axis).

Desorption temperatures of 200 and 250°C were reached quite fast but the desorption temperature of 300°C was reached only at the end of the heating period. By reaching a desorption temperature of 300°C, an increase of the baseline signal was observed. It seemed that due to the high temperatures the adsorbent material released CO_2. This might be due to oxidation reactions of the material itself with leftover oxygen from sampled air. With a desorption temperature of 250°C only a small CO_2 background signal was originating from the adsorbent material. With 200°C there was no signal increase visible. To minimize CO_2 background signals, temperatures of 200°C or a maximum of 250°C should be applied. Further tests

concerning the desorption behavior of different NMOCs at these temperatures had to be applied (see chapter 3.3.2.3).

3.3.2 Sampling efficiency

The most important question was, to understand the behavior of the NMOCs on the solid adsorbent unit. Dindorf (2006) reported a recovery rate of 48% at the most with a NMOC standard mixture. Non sufficient oxidation or problems with the NMOC adsorbent unit might explain such a loss. Given this poor recovery rate, a closer look at the NMOC adsorbent unit was necessary. This test involved sampling and thermal desorption of the NMOCs and a subsequent analysis of the desorbed sample by PTR-MS. A different setup had to be applied. Basically, the NMOC solid adsorbent unit was connected to a PTR-MS and to a second infrared gas analyzer (IRGA). The substances that were tested were isoprene, nopinone and α-pinene. Isoprene was chosen because it is one of the substances, which is emitted most frequently by the biosphere, and due to its reactivity and carbon structure it is really important for air chemistry. Besides, it is one of the compounds which should not show a breakthrough under the prevailing sampling conditions (3000 ml sampling volume, 2250 ml flush volume and 35°C sampling temperature). Smaller carbon structure compounds might have a breakthrough due to the sampling and flush volume of approximately 5 l. Isoprene was also used to examine the breaktrough behavior with respect to the sampling temperature. Also a potential separation of the sampled CO_2 from the NMOC fraction was tested with isoprene. Nopinone was used to have a closer look at the behavior of an oxygenated VOC on the solid adsorbent unit. With this single compound, the choice of the desorption temperature was verified. α-pinene represented one of the most frequently emitted substance groups of the biosphere – the monoterpenes. Every single compound was diluted with zero air containing ambient CO_2 mixing ratios within the empty plant chamber. Figure 33 shows the schematic setup of the experiment.

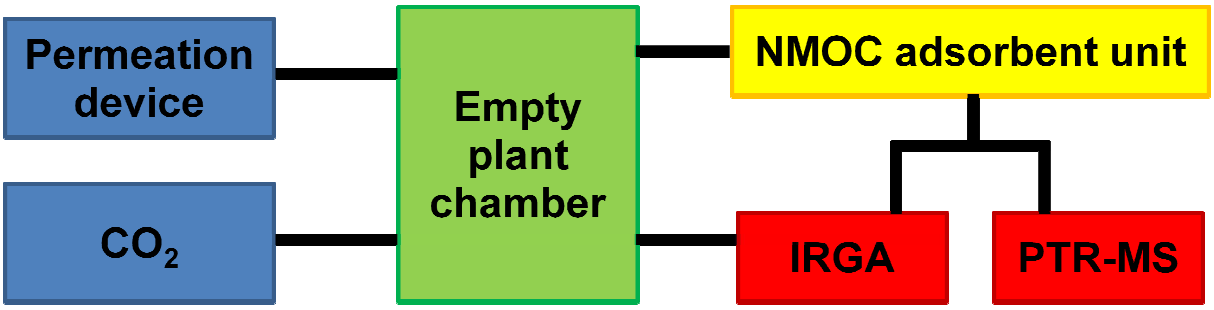

Figure 33: Schematic setup for the compound measurements with the NMOC solid adsorbent unit.

One channel of the infrared gas analyzer was connected to the NMOC adsorbent unit to detect the released CO_2 and the other one to the plant chamber to measure the ambient CO_2 mixing ratios. For most experiments the flush and carrier gas was helium. One experiment had to be carried out with synthetic air. PTR-MS data determination was realized with the different compounds from the permeation/diffusion devices, but most measurements were carried out rather qualitative than quantitative. If quantitative values were necessary, the mixing ratios from the permeation/diffusion device were measured with the PTR-MS before and after the experiment including a measurement of zero air for the background signal. The two different channels of the infrared gas analyzer were calibrated with a CO_2 gas standard (352 ppm in synthetic air) and with helium as a zero reference value. The following chapters show the results for the tests with the single VOC compounds.

3.3.2.1 Separation of CO_2 from NMOC fraction during desorption

As discussed in chapter 3.3.1 the sampled CO_2 on the NMOC solid adsorbent unit plays a major role in terms of background signal, and corresponding with this the detection limit. It was important to examine if the sampled CO_2 could be separated from the NMOC compounds during desorption which would lead to a much lower background signal. The NMOC solid adsorbent unit was set up as shown in chapter 3.3.2 Figure 33. Isoprene was used to represent the NMOC fraction in this experiment. Figure 34 shows the results for the first desorption experiment with sampled isoprene and sampled CO_2. Sampling time was set to 10 min with a flow rate of 300 ml min^{-1} at 35°C. The applied flush volume was 2250 ml corresponding to 3 min flushing with 750 ml min^{-1} helium. The desorption temperature was 200°C for approximately 5 min 30 s which means that no CO_2 background was produced from the solid adsorbent material itself. The desorption process starts straight after

switching the sample valve when the NMOC solid adsorbent unit is in the backflush mode. As both instruments had to receive a sufficient gas flow the desorption flow was set to 100 ml min^{-1}. 50 ml min^{-1} was the flow rate for each instrument.

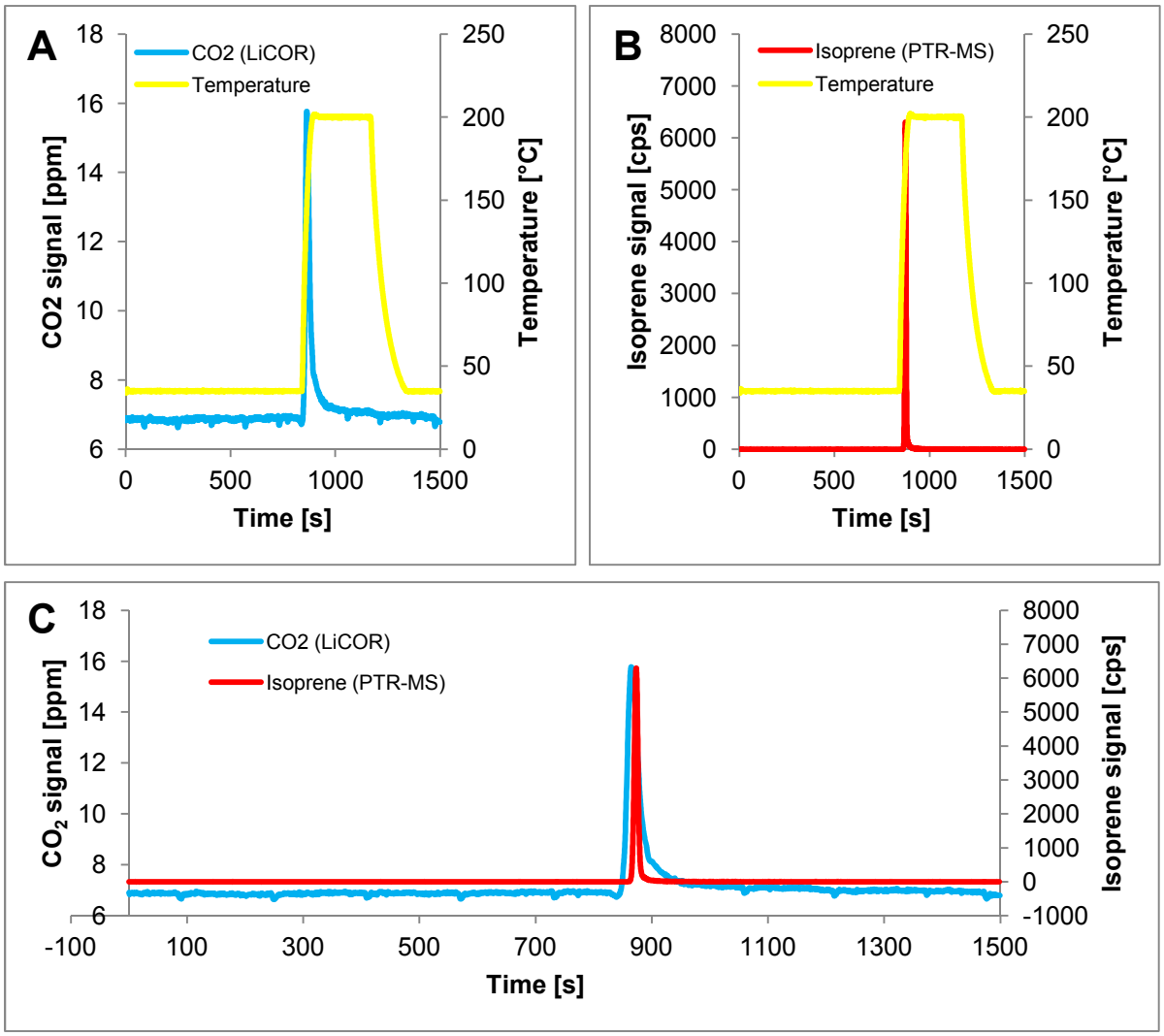

Figure 34: A: Desorption course of sampled CO_2 (blue line) from the NMOC solid adsorbent unit and the corresponding temperature course (yellow line). B: Course of the isoprene signal (red line) during desorption with the temperature course. C: CO_2 signal (primary y-axis) together with the isoprene signal (secondary y-axis).

Figure 34A shows the results for the CO_2 signal on the primary y-axis including the temperature course (secondary y-axis). A relatively sharp peak was obtained shortly after starting the desorption process. Figure 34B shows the isoprene signal from the PTR-MS measurement (primary y-axis) together with the desorption temperature (secondary y-axis). It seemed that both compounds were desorbed at the same time. In Figure 34C one can clearly see that the two resulting peaks are superimposed. No separation was possible. Another attempt for the separation of the sampled CO_2 and

the NMOC fraction was to apply a temperature program to the NMOC solid adsorbent unit. Therefore, the solid adsorbent unit was heated up in slow steps. After setting the NMOC solid adsorbent unit into backflush mode the temperature was first kept at the sampling temperature of 35°C for 2 min. The next steps involved three temperature increases to 50°C, 75°C and 100°C. Each temperature was kept for 2 min. Within the last temperature step the NMOC adsorbent unit was heated up to 200°C. Figure 35 shows the results of the experiment.

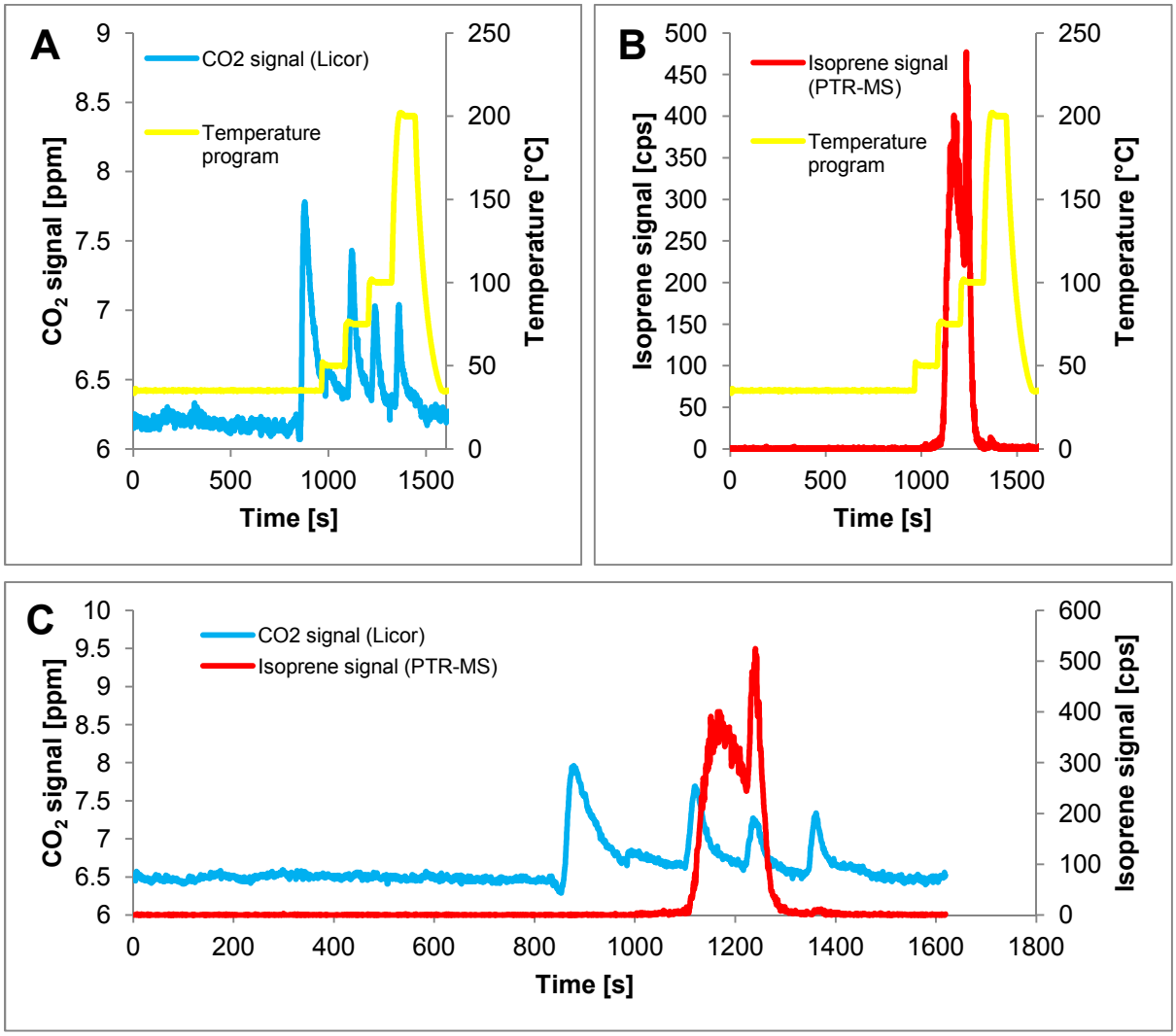

Figure 35: A: CO_2 signal after desorption in relation to the temperature. B: Isoprene signal in relation to the temperature. C: Comparison of the CO_2 and the isoprene signal (primary y-axis: CO_2 signal; secondary y-axis: isoprene signal).

Figure 35A and B again show the behavior of the single signals compared to the temperature course. The CO_2 signal was split into several peaks. The first peak was released in backflush mode without any temperature increase, indicating to be

derived from a dead volume. The remaining CO_2 was released upon heating. The temperature program also had an effect on the desorption of isoprene (see Figure 35B). It was still desorbed in one peak but a broadening occured. Both signals were combined in one diagram to see if any CO_2 separation was possible (Figure 35C). The first CO_2 peak which was released due to the backflush flow can be clearly separated from the isoprene signal. The remaining CO_2 could not be segregated. Different temperature programs were applied to the NMOC solid adsorbent unit for the desorption process but they all resulted in the same outcome. Only a small amount of the CO_2 could be separated by backflushing the solid adsorbent unit at sampling temperature before heating up for the desorption. Therefore, a 5 min time period was included in the measurement sequence to backflush the NMOC adsorbent unit previous to the desorption step. Tests showed that isoprene was not released from the solid adsorbent material during the 5 min backflush. During these 5 min the oxidation unit and the CO_2 preconcentration unit were bypassed. As soon as the temperature started to increase, both units had to be switched into the carrier gas flow again. Another test was carried out where the temperature of the adsorbent unit was increased to 50°C during the backflush period, but it resulted in a substantial isoprene loss. A significant reduction of the CO_2 peak was not observed which justified the substantial amount of lost isoprene or potential other compounds. After each measurement with isoprene a blank measurement where only helium was sampled on the solid adsorbent material was executed. A memory effect for isoprene was not found (PTR-MS). However, measurements with and without isoprene resulted in slightly different values for the CO_2 background peak at the infrared gas analyzer indicating an interference at the detector. Lide (2005) reported about interferences which occurred from alkynes. However this was unlikely for the measurements with isoprene. Nevertheless a possible interference from the VOC compound or a reaction product has to be considered.

3.3.2.2 NMOC adsorption temperature

As already discussed in chapter 3.3.1.2 the sampling temperature is limiting the sampling volume caused by breakthrough of the different compounds. Due to its low carbon structure (C_5) isoprene is a compound with a potential breakthrough at the applied sampling volumes and temperatures. Therefore, sampling temperature tests

were carried out with this compound. The setup of the instruments was as explained in Figure 33, but without the infrared gas analyzer. Sampling temperatures from 25°C to 50°C in 5°C steps were applied. The ambient zero air containing CO_2 and isoprene in a known concentration were sampled for 10 min with 300 ml min^{-1} and a helium flush volume of 2250 ml. Desorption time was 5 min at a desorption temperature of 200°C. In between the different temperature measurements helium was sampled at the same sampling temperatures. The desorbed isoprene amounts were measured with PTR-MS. The resulting peaks were integrated and the values of the integrals were compared to each other. Table 11 shows the results for the integration values for three consecutive measurement runs at the applied temperatures. There was no visible memory effect for isoprene on the NMOC solid adsorbent unit.

Table 11: Integrated values for isoprene peaks at different sampling temperatures from PTR-MS measurements.

Sampling temperature:	25°C	30°C	35°C	40°C	45°C	50°C
Integral 1 in counts	92516	92981	92829	91811	88554	43298
Integral 2 in counts	92505	93045	93219	91951	88088	42513
Integral 3 in counts	92672	91539	92393	92719	90105	45383

The values in the Table represent the integrals of a single isoprene peak which is released from the NMOC solid adsorbent unit due to thermal desorption. The integrals for sampling temperatures up to 35°C resulted in similar values. A safe sampling temperature of 35°C was defined. For a temperature of 40°C a slight trend to decreasing integrated values was found. At 45°C and definitely at 50°C a breakthrough was observed. Integral values for 50°C were halved compared to the values for temperatures between 25°C and 40°C. To ensure that no breakthrough occurs for carbon compounds with a C_5 – structure or above a sampling temperature of 35°C was applied for all measurements. As the detector response of the PTR-MS is varying when using helium instead of ambient air as a carrier gas, the integrated values for the isoprene measurements could not be used to verify the recovery rate of the compound from the solid adsorbent unit. A different experiment had to be applied to validate this question.

3.3.2.3 NMOC desorption temperature

The desorption temperature is a critical factor for sampled NMOC compounds to be completely released from the adsorbent material again. The previous chapter showed that isoprene seemed to be easily desorbed, as the compound peak resulted in a sharp signal at the PTR-MS. Next to isoprene a great variety of other NMOC compounds is emitted by plants with a versatility of structures and different chemical behavior due to a variation of functional groups within the molecules. An example for one of these compounds with a more complex structure is nopinone. It belongs to the group of oxygenated VOCs. With the installation of the new oxidation unit and the reduced carrier gas flow the original desorption time of 4 min was delayed to 8 min. Due to the limitation of the breakthrough volume of the CO_2 preconcentration unit a longer desorption time could not be realized. The setup of this experiment is shown in Figure 33. However, the NMOC adsorbent unit was only connected to the PTR-MS.

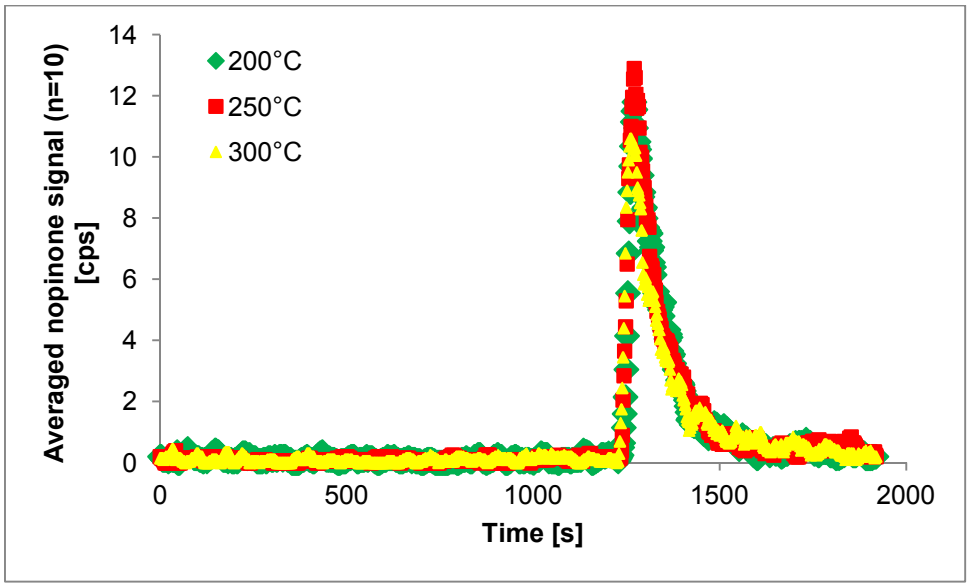

Figure 36: Signal development for nopinone desorbed at different temperatures (200°C, 250°C, 300°C). Each nopinone value was averaged over 10 individual values (n=10).

A desorption flow of 50 ml min^{-1} was applied. Sampling of nopinone was realized with a flow of 300 ml min^{-1} for 10 min at a temperature of 35°C. A flush volume of 2250 ml helium was applied. In backflush mode the NMOC unit was flushed at sampling temperature for 5 min with the applied desorption flow. The desorption temperature was varied for each measurement. Figure 36 shows the results from this application. To receive a more precise peak signal from the PTR-MS measurement, averaged

values (n=10) were plotted on the y-axis. As shown in Figure 36 the three peaks are superimposed. The temperature variance did not make any difference for the desorption of nopinone. However, the peak signals resulting from the desorption of nopinone from the NMOC solid adsorbent unit were broadened. This is clearly shown in Figure 36 and 37. Additionally in Figure 37 the peak signals were plotted individual for each temperature combined with the corresponding logarithmic plot (secondary y-axis: red squares). It gives a more detailed view of the desorption process of nopinone. After a fast rising nopinone signal, a very slow decrease was observed. However, with this experiment it was not possible to determine if nopinone was fully desorbed from the NMOC solid adsorbent unit as the same problem in the determination of the recovery rate occurred as already explained in chapter 3.3.2.2. for isoprene. As the PTR-MS response is different with helium, the value for the recovery rate could not be calculated. The conclusion from this measurement was that a desorption temperature of 200°C was apparently sufficient for the desorption of NMOC compounds from the solid adsorbent unit. For higher temperatures the nopinone signal resulted in similar peaks. Furthermore, the desorption temperature is important for the CO_2 background as observed in chapter 3.3.1.4. A desorption temperature of 300°C was excluded. The difference in the CO_2 background signal for 200°C and 250°C was small. Therefore a temperature of 250°C was chosen to support the desorption of other unknown compounds.

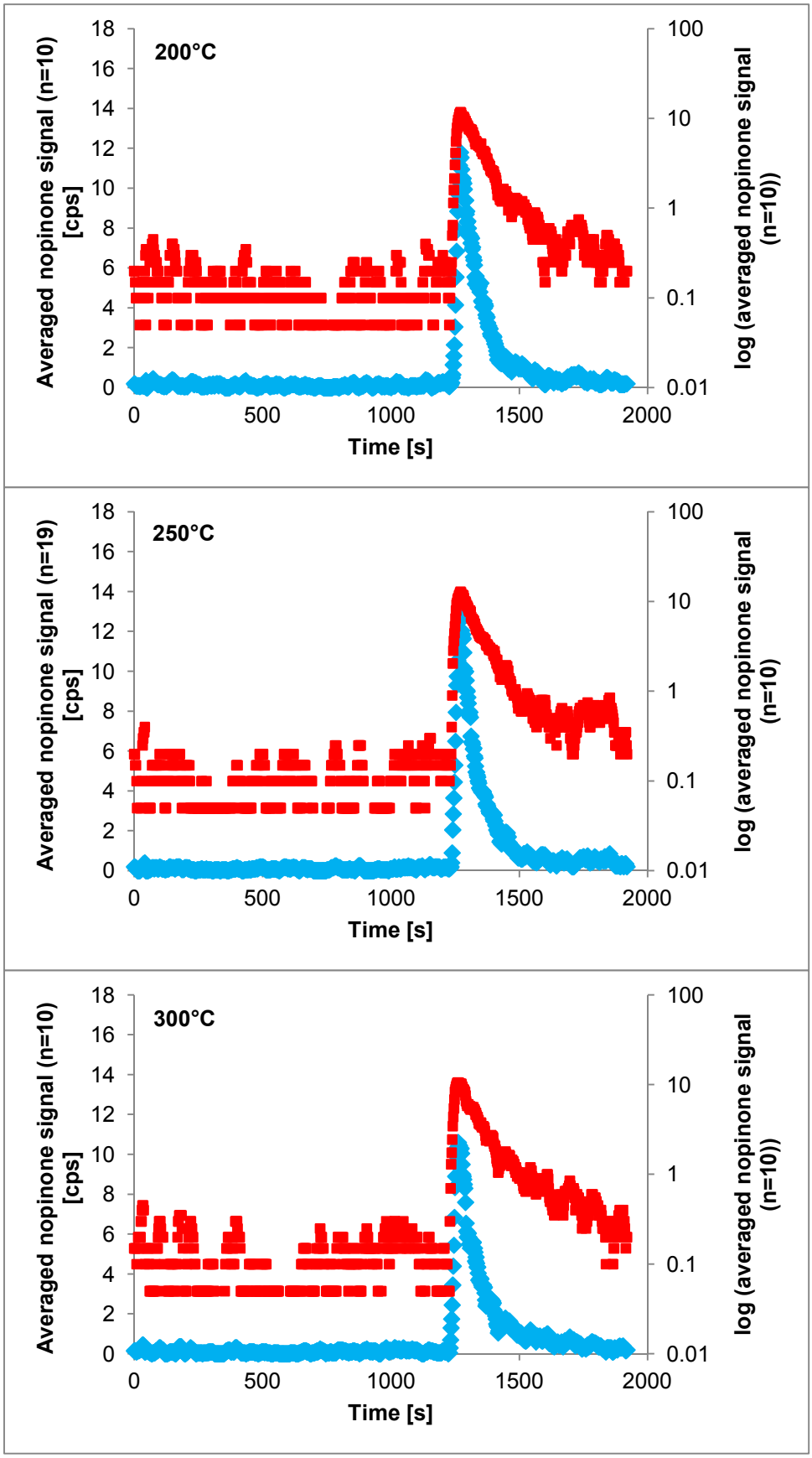

Figure 37: Single nopinone desorption courses (primary y-axis: blue diamonds) for different temperatures (200°C, 250°C, 300°C) shown together with the respective desorption peaks as logarithmic plots (secondary y-axis: red squares) for a more detailed view of the desorption course.

3.3.2.4 Recovery rates of single NMOC compounds

The results from the previous chapters supported only qualitative statements. To receive quantitative results the experimental setup was changed. As the response of the PTR-MS instrument is different when utilizing helium gas instead of ambient air the experiment was repeated with synthetic air as carrier gas. This setup however, carried the risk of VOC compounds getting oxidized during the desorption process. This would lead to a loss of the compounds for the detection with the PTR-MS. However, the experiment was carried out to observe which recovery rate could be obtained for the mentioned compounds – isoprene, α-pinene and nopinone. Again, the setup from Figure 33 was applied but only the PTR-MS instrument was connected to the NMOC solid adsorbent unit. The sampling volume was 200 ml min^{-1}. The temperature was set to 35°C during sampling. As helium was replaced by synthetic air for this experiment, a flush volume of 530 ml min^{-1} was applied. After switching the sample valve, the solid adsorbent material was backflushed for 5 min with a flow of 50 ml min^{-1} synthetic air. Thermal desorption was realized at 250°C for 8 min. Figure 38 shows the resulting peaks after thermal desorption. All compounds were measured separately but plotted together in one diagram.

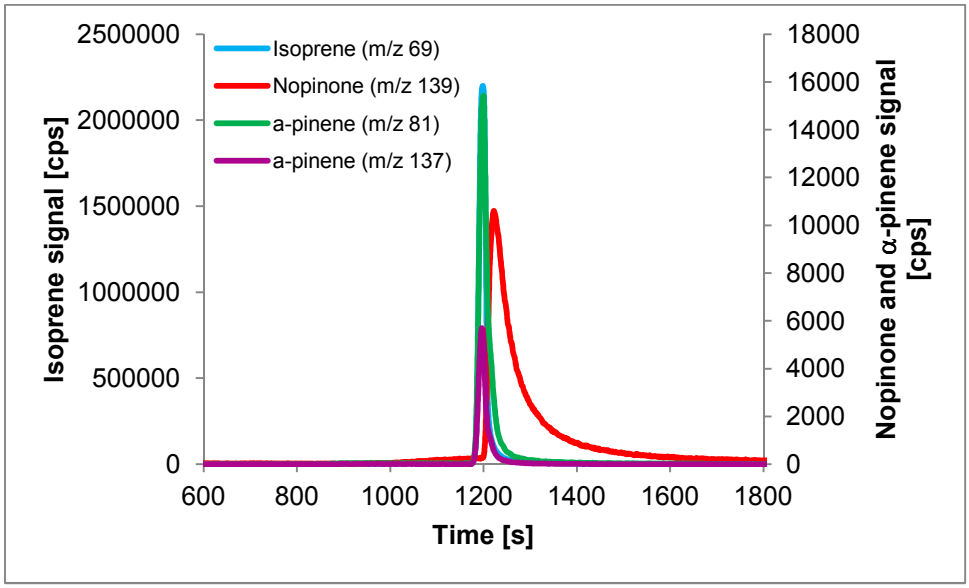

Figure 38: Compound signals after thermal desorption. As the signal intensity was different for the chosen compounds the isoprene signal was plotted on the primary y-axis and the other compounds (nopinone and α-pinene) on the secondary y-axis.

The resulting peaks for isoprene and α-pinene are superimposed. Both compounds were desorbed at the same time and resulted in sharp peaks. Nopinone as an oxygenated compound was released delayed, resulting in a very broad peak indicating that the oxygenated compound was not desorbed as easy as non-oxygenated VOCs. In particular, the peak-broadening showed that such compounds might not get desorbed quantitatively from the solid adsorbent material. To receive quantitative results the single compounds were directly measured with the PTR-MS before and after the experiments with the NMOC adsorbent unit. Thus, the signal intensities for the mixing ratios of the compounds were known. The peaks obtained from the NMOC adsorbent unit were integrated and the integration value compared to the measured intensities of the single compound measurements with the PTR-MS. Table 12 shows the results from these measurements.

Table 12: Recovery rates from the NMOC adsorbent unit for single compound measurements.

	Isoprene (m/z 69)	α-Pinene (m/z 81)	α-Pinene (m/z 137)	Nopinone (m/z 139)
PTR-MS substance signal	4968 counts	44 counts	12 counts	64 counts
Peak integral from NMOC unit	6635 counts	22 counts	7 counts	37 counts
Recovery rate	134%	50%	58%	58%

The table shows the mean values (n>3) of the results. The recovery rate for isoprene with more than 100% cannot be explained as the PTR-MS substance signal was measured from the same air which was sampled on the solid adsorbent unit. Errors from the sampling flow and the permeation/diffusion device might have caused a large error for the measurement. This should not however, result in a discrepancy of more than 30%. The recovery rates for nopinone and α-pinene are in the order of 50-60%. These low recovery rates might result from oxidation processes during the thermal desorption as oxygen was present in the carrier gas. The low recovery rate for nopinone could also be associated with insufficient desorption. However, as isoprene seemed to be fully recovered, oxidation processes for α-pinene and nopinone might be largely excluded. Generally, it has to be noted that we found

different recovery rates for different compounds. With this result a quantitative analysis for a measurement of an unknown composition with unknown NMOC compounds including their unknown recovery rates is not possible.

3.4 Characterization of the analytical system

A measurement technique is characterized by its responses and limits. In the previous chapters the important main components were analysed. Based on these studies and experiments the whole instrument can be characterized regarding the detection limit and the reproducibility of measurements.

3.4.1 Limit of detection

Usually the detection limit is defined as three times the standard deviation of the detector noise level. As this instrument was constantly flushed with helium there was no direct detector noise level which could be determined. For the definition of the detection limit the minimum single result that can be distinguished from a suitable blank value was used. The blank value was calculated from the $area_{CO2Sample}$ value subtracted by the $area_{NMOCSample}$ when measuring zero air which was containing CO_2 in ambient concentration. From multiple measurements a mean value and the standard deviation were determined. The detection limit can be calculated according to formula 2.7.13. The zero air measurement resulted in a detection limit of 48 ng or 29 ppb carbon when sampling 3000 ml volume.

3.4.2 Reproducibility

In general the reproducibility can be calculated according to formula 2.7.12. For the calibration with the CO_2 standard gas, a precision of ± 3.5% for a carrier gas flow of 100 ml min^{-1} and of ± 2.6% for a carrier gas flow of 50 ml min^{-1} was determined. For this calculation the slopes of the different linear calibration fits from different calibration days were taken into account. To specify a value for the reproducibility of the entire instrument represented a larger problem. Repeated measurements of single compound concentrations (n>3) of α-pinene, nopinone and isoprene (from permeation/diffusion device) showed a precision of ± 0.75-3.5%. Because the

permeation sources can generally be specified only with a reproducibility of 100 ± 5%, the values obtained are within this limit.

3.5 Discussion

The previous chapters presented the test results of the single units of the total NMOC analyzer. The important parts of the construction were explained in detail. However, a lot of difficulties were identified. Some of them were improved or at least reduced, but modification was not always possible. The functional principles of the analyzer are based on elemental analysis. The preconcentrated NMOC compounds which were mostly separated from the stable carbon compounds CO_2, CO and CH_4 through the preconcentration step on a solid adsorbent unit were oxidized in an oxidation unit and the resulting CO_2 was measured. From the measured CO_2 mixing ratios the total carbon amount from NMOC compounds could be obtained. The detection of the CO_2 analysis was realized by the application of an infrared gas analyzer. The detection limit of the detector in the default "flow through" setup is in the range of 200 ppb.[11] Even though the utilized gas analyzer was less sensitive than a FID detector which is used in commercially available total carbon analyzers or in setups from previous publications (Maris *et al.* 2003, Roberts *et al.* 1998), the resulting detection limit from the NMOC analyzer was much lower than the default "flow through" setup detection limit. It is in the dimension of 48 ng or 29 ppb carbon at sampling volumes of 3000 ml. This enhancement of the sensitivity was due to the utilization of the CO_2 preconcentration unit. With a carrier gas flow of 50 ml min^{-1} the detector response reached values of > 16 ppm CO_2 for CO_2 injections of ~ 180 ng carbon. In contrast to this system, application of a FID detector (Maris *et al.* 2003, Roberts *et al.* 1998) needs two NMOC conversion steps. Firstly the compounds have to be oxidized to CO_2 to receive an equal carbon response from the versatility of NMOC compounds. Secondly the resulting CO_2 has to be reduced to CH_4 as the FID detector is insensitive to CO_2. Compared to the utilization of a FID detector the present analyzer was only depending on one NMOC conversion step. Since each conversion step involves the risk of a decreased recovery rate, the setup as used within this work may be of advantage.

[11] ftp://ftp.licor.com/perm/env/LI-6262/Manual/LI-6262_Manual.pdf

The CO_2 preconcentration step was enabled by the application of a modified silica material. This unit allowed the sampling of the CO_2 obtained from the oxidation step. It was one of the limiting factors of the instrument as the CO_2 breakthrough causes the limitation for the NMOC desorption period from the NMOC adsorbent unit. As the breakthrough corresponds with the gas flow and the temperature, a higher breakthrough volume could be obtained by applying a cooler temperature to the unit. However, the current setup only allowed cooling to room temperature, because only a ventilator was available for the cooling purpose. Therefore, the unit was set to a consistent temperature of 30°C and breakthrough volumes were tested for this adjustment. The CO_2 preconcentration period was determined to not exceed 4 min at a carrier gas flow rate of 100 ml min^{-1} or 8 min for 50 ml min^{-1}. To avoid the sampling of CO_2 which arose from sources other than the oxidized NMOC compounds, a bypass was created. By the utilization of two 3-way-2-position valves mounted on each end of the CO_2 preconcentration unit, the gas flow could be directed past the unit. Compared to the previous setup this allowed experiments where the CO_2 amounts could be detected directly at the infrared gas analyzer without the preconcentration step. Especially for the reduction of the CO_2 background signal it was an important improvement. Nevertheless, a small CO_2 blank value was always emitted by the unit and had to be considered for some measurements. However, for total NMOC analysis the CO_2 background signal from the CO_2 preconcentration unit could be neglected since this background occurred for the total CO_2 background signal ($area_{CO2Sample}$) from the NMOC solid adsorbent unit and the total NMOC sample measurement ($area_{NMOCSample}$) equally.

The oxidation unit was also one of the most important elements of the analyzer. The oxidation of the NMOC compounds to CO_2 has to be ensured and the CO_2 background signal should be kept as low as possible. Various catalytic materials were tested. Different issues occurred for the individual catalysts. The CuO catalyst from the previous setup was emitting a high CO_2 background signal when adding oxygen to the catalyst to obtain enhanced oxidation efficiencies. However, the oxidation efficiency with the CuO catalyst seemed to decrease with an increased carbon structure. While isoprene and Z-3-hexanol measurements resulted in a linear fit when applying different mixing ratios to the instrument, α-pinene and β-caryophyllene did not. A saturation trend was observed for higher mixing ratios. Apparently higher carbon structures were not oxidized completely to CO_2. However, it

was difficult to give an accurate statement concerning the oxidation efficiencies as the compounds were not injected directly into the oxidation unit, but were sampled on the NMOC solid adsorbent unit first. Errors could also occur from there. As oxidation efficiency and CO_2 background signal were not satisfying, different catalytic materials were tested. The second catalytic material was an aluminium based palladium catalyst. It is commonly used for zero air setups from ambient air and is known to minimize the NMOC mixing ratios from ambient air down below the detection limit of the measuring instruments. This catalytic material revealed a new problem. Measurements with defined CO_2 injections showed that with high CO_2 mixing ratios the material was adsorbing CO_2 and releasing it again at low CO_2 mixing ratios. As it was ambiguous how much CO_2, which is arising from oxidation, is adsorbed or released from the catalyst, the material could not be used for the purpose of the oxidation unit. A size reduction was the first attempt to solve this problem as the previous oxidation unit held a far too large volume for the application. With the smaller unit a different catalytic material was necessary because of the pellet size of previously used palladium catalyst. A platinum catalyst which is also based on aluminium oxide was applied. Although the catalyst unit was significantly reduced, the same effects occurred. The uptake and release of the CO_2 must be correlated with the high surface area of the catalytic material. Even though the volume was reduced and the temperature kept constantly at 500°C, the latter effect was observed. By utilization of a 6-way-2-position valve the oxidation unit was flushed continuously with helium. This led to the result that CO_2 was affiliated during the measurements and released again when flushing the catalytic material subsequently. Thus, no reliable statement about the CO_2 could be made. The conclusion from these experiments is that catalysts with high surface areas are not suitable for the application of the NMOC analyzer. To overcome the problems arising from catalysts with high surfaces, a Pt-Rh wire was tested. Compared to the CuO wire catalyst, the CO_2 emission from the Pt-Rh wire was negligible. Oxidation efficiencies were tested with single VOC compounds. The results are presented in chapter 4. For the application of the NMOC analyzer the best results were obtained with this catalyst.

The sampling step of the NMOC analyzer comprised the sampling of the non-methane organic carbon compounds and the combined separation of CO_2, CO and CH_4. Looking more closely however, the CO_2 amount which was sampled on the solid adsorbent material resulted in a background signal of up to 100 ppb carbon.

These background values exceeded ambient NMOC mixing ratios by far. Therefore, for each NMOC value a corresponding CO_2 blank had to be determined. Several attempts were carried out on how to reduce the amount of sampled CO_2 like variation in the sampling temperature, the sampling volume or the flush volume. Various experiments were executed concerning the reduction of the CO_2 background signal originating from sampled ambient CO_2. However, due to the properties of the solid adsorbent material most of these steps would also lead to a loss of NMOC compounds. On the other hand, the widely emitted compound methanol and other low molecular weight organics (C_n<4) cannot be sampled quantitatively on the applied adsorbent materials anyway. A compromise had to be found to reduce the background signal, but still efficiently sample the NMOC compounds. As the NMOC adsorbent material is based on carbon, there is also a risk to create a CO_2 background signal from the applied graphitized carbon black material. At high desorption temperatures reaching 300°C a clear signal caused by the NMOC adsorbent material was observed. Therefore, desorption temperatures were not set higher than 250°C to keep the CO_2 blank value low. Several tests were performed with the attempt to separate the sampled CO_2 amount from the NMOC fraction during desorption. The experiments showed that a separation of the main CO_2 peak from isoprene was not possible. However a small CO_2 peak which might result from a dead volume within the NMOC solid adsorbent unit setup could be separated by a backflush period at sampling temperature.

Probably the most important factor was the recovery rate of NMOC compounds from the solid adsorbent unit. With the previous setup only 48% of the sampled compounds were finally recovered. Various reasons could be responsible. Concerning the behavior of different NMOC compounds on the solid adsorbent material different experiments were applied. For all these experiments the NMOC solid adsorbent unit was directly connected to a PTR-MS. First the sampling temperature was varied and a compound with a low breakthrough volume (isoprene) was chosen. This was to examine at which sampling temperature a breakthrough occurred at a set sampling volume of 5250 ml (3000 ml sample volume + 2250 flush volume). A safe sampling temperature of 35°C was found for compounds C_n≥5 for the applied volume. The desorption temperature is also an important factor for the recovery rate of the NMOC compounds as they are manifold and with different chemical behaviors. Due to the characteristics of the solid adsorbent materials which

are hydrophobic and interact non-specifically with all groups of adsorbates (Brancaleoni *et al.* 1999), all compounds should be desorbed equally. To verify the desorption temperature an oxygenated organic compound (nopinone) was chosen which has a different chemical behavior than commonly tested NMOCs like isoprene or monoterpenes. A very broad peak was observed with a time-delayed desorption in comparison to the other two tested compounds isoprene and α-pinene.

However, different desorption temperatures did not cause a visible change in the desorption behavior of nopinone. Thus, the chemical structure is important for the desorption of the NMOC compounds from the solid adsorbent unit. Recovery rate experiments showed that probably every single volatile organic carbon compound has a different recovery rate and as a result a measurement of an unknown NMOC composition cannot be determined with the current analyzer setup. Further experiments with this focus must be considered. As the calibration of the instrument was based on a detector calibration with different amounts of CO_2 mixing ratios, good results for the calibration lines were shown. A precision of ± 2.6% was obtained with the CO_2 ratios from the calibration measurements. The detection limit was determined with 48 ng or 29 ppb carbon for 3000 ml sampling volume. Despite high CO_2 background values a relatively low detection limit was obtained due to the good reproducibility of the instrument and due to the fact that for every NMOC value the corresponding CO_2 blank value was measured. However, this resulted in a poor time resolution.

4. An application: Measurement of biogenic volatile organic compound emission

The instrument was tested with single VOC species and used to follow VOC emissions in two plant chamber experiments with several plants. The plant chamber measurements were accompanied by PTR-MS and GC-MS measurements. All experiments were accomplished under laboratory conditions at the Research Centre Jülich. The instruments were calibrated regularly especially before and after the plant chamber experiments. For the plant chamber experiment an 11 hour day and 11 hour night cycle with one hour dawning time each in between was adjusted. Between 5 and 6 o'clock in the morning as well as 5 and 6 o'clock in the evening the lights in the plant chamber housing were successively switched on or off. The temperature was kept constant within the plant chamber housing whether day or night period. During the day period the temperature was slightly increased (~ 4°C) due to the light sources. The temperature settings were changed during the experiments to observe the temperature dependent change of the NMOC emissions. Samples were collected continuously for 24 h. The NMOC compounds were preconcentrated on 100 mg Carbograph 1 and 200 mg Carbograph 5. As discussed in chapter 3 the more or less ideal sampling procedure was realized by a sampling volume of 3000 ml (sampling flow of 300 ml min^{-1} for 10 min), a flush volume with helium of 2250 ml (flush flow of 750 ml min^{-1} for 3 min), a backflush volume of 250 ml (helium carrier gas flow of 50 ml min^{-1} for 5 min) bypassing the oxidation and the CO_2 preconcentration unit, a sampling temperature of 35°C, a desorption temperature of 250°C and a desorption period of 8 min. As a catalyst a Pt-Rh wire at a temperature of 500°C was applied. 10% pure oxygen was added to the carrier gas flow to ensure sufficient oxidation efficiency. The oxidation unit was flushed with helium (50 ml min^{-1}) at all times. The CO_2 preconcentration unit was switched into the system during the desorption and oxidation process of the NMOC compounds. The subsequent thermal desorption of the CO_2 sampled on the preconcentration unit was performed at a temperature of 200°C for 6 min. With each NMOC sample (TestSam=$area_{NMOCSample}$) a corresponding CO_2 background signal (TestCO2=$area_{CO2Sample}$) had to be measured. Also the amount of carbon in the carrier gas flow (excluding the oxidation unit)($HeCO_2$), the amount of carbon in the carrier gas system (including the oxidation unit)($SysCO_2$) and the signal of the oxidation unit when adding 10% oxygen to the

carrier gas flow but not injecting any VOCs into the system was determined. In this way all the individual units and their CO_2 background signal were monitored. Thus, the time resolution was deteriorated. One NMOC sample measurement and the corresponding CO_2 blank run needed 35 min each. Together with the monitoring CO_2 background files $HeCO_2$ (17 min), $SysCO_2$ (17 min) and $KatCO_2$ (22 min) (see also table 8) a measurement cycle for one NMOC mixing ratio took 2 h and 6 min. The zero air from the plant chamber inlet was measured separately at the beginning and at the end of the experiment. The corresponding CO_2 blank value was subtracted from the NMOC sample value, as the CO_2 background signals were varying depending on the ambient CO_2 mixing ratio in the plant chamber. One method sequence was measured in the following series: $HeCO_2$, $TestCO_2$, $SysCO_2$, $KatCO_2$ and TestSam (see Appendix D). The measurements were completed by monitoring the CO_2 exchange with an infrared gas analyzer. This was also important for the CO_2 background signal development of the NMOC analyzer due to changing ambient CO_2 mixing ratios which were caused by plant activities. From the plant chamber to the analyzer the NMOC samples were piped through 1/2" PFA tubing which was heated to 50°C by an external heating cord surrounded by insulation material.

4.1 Single compound measurements

For a single compound based characterization several VOC species derived from permeation devices (see chapter 2.4) were mixed with zero air in the empty plant chamber. The CO_2 concentration was adjusted to ambient concentrations. In this way the CO_2 background signal was comparable to ambient air measurements. Besides these measurements the oxidation efficiency of the Pt-Rh wire was determined. Moreover, the results could be compared to the values for the recovery rates of the NMOC solid adsorbent unit. For this reason isoprene, α-pinene and nopinone mixing ratios were determined. Four to five different mixing ratios were measured several times with the total NMOC analyzer and compared to the calculated mixing ratios from the permeation/diffusion device. The same sequence as described in the latter paragraph was applied. The following chapter shows the results for the single compound measurements.

4.1.1 Isoprene

Isoprene is the most abundant non-methane volatile organic emitted by the biosphere. It is also one of the compounds, which is sampled reliably on the solid adsorbent material at the applied sampling method which was shown in chapter 3.3.2.2. Figure 39 shows the result for the isoprene measurement.

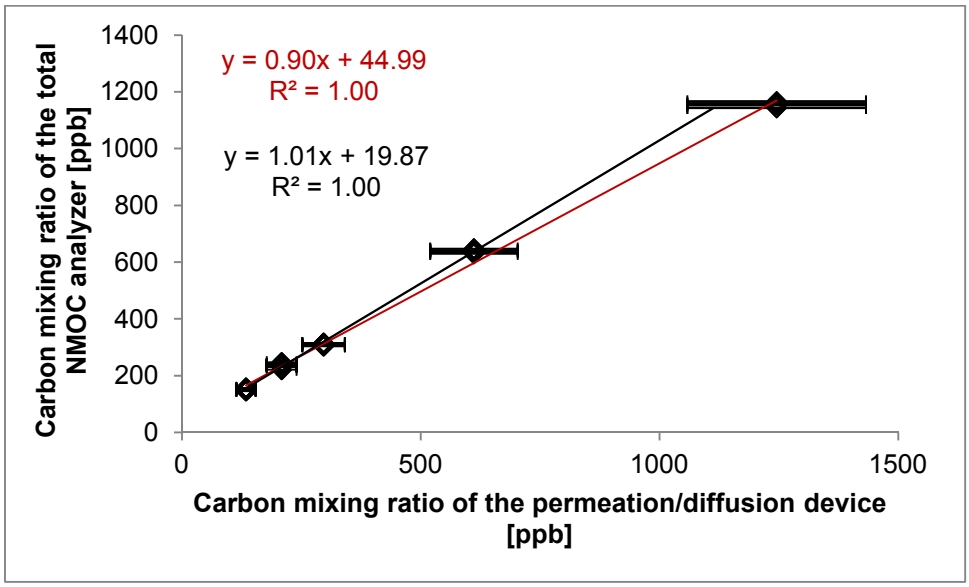

Figure 39: Correlation between the carbon mixing ratio values from isoprene obtained with the total NMOC analyzer (y-axis) and the calculated values from the permeation/diffusion devices (x-axis) (with an uncertainty of ±15%). The red line shows the linear regression including all isoprene mixing ratios. The black fit does not include the highest mixing ratio.

The correlation between the measured carbon mixing ratio and the calculated one from the permeation/diffusion device was observed. In the diagram the equations for the linear fits and the coefficients of determination are also specified. The data points correlate perfectly. Nevertheless, a discrepancy of 10% was found for the calculated mixing ratios and the measured ones when including all mixing ratios (red fit). A reason for the 10% discrepancy could be due to the fact that the oxidation efficiency of the Pt-Rh catalyst was not sufficient for as high carbon mixing ratios of 1 ppm or more. Excluding the highest mixing ratio, resulted in a perfect agreement of the values from the NMOC analyzer compared to the calculated ones from the permeation/diffusion device. These results clearly showed that the oxidation unit seemed to work efficiently for a carbon compound like isoprene. Up to a certain mixing ratio, isoprene was completely oxidized to CO_2. Besides, the discrepancy

between the values was in the range of the dominating uncertainty of the permeation/diffusion device which amounts ±15%. Moreover, the results further indicated that a subtraction of a high CO_2 background blank ranging up to a signal of 200 ppb carbon did not prevent a reasonable result. Despite the high CO_2 blank signals, an excellent reproducibility could be pointed out. It was in the range of 100 ± 0.75-2.5% for the different mixing ratios. These results clearly showed that isoprene was fully recovered from the NMOC solid adsorbent unit as indicated by the recovery experiment in chapter 3.3.2.4.

4.1.2 α-Pinene

The second compound which was tested with the total NMOC analyzer was α-pinene which represents the group of monoterpenes. The setup for the experiment was the same as for the one with isoprene. However, the vapor pressure of α-pinene is much lower than the one for isoprene. It did not provide sufficiently high mixing ratios of α-pinene within the plant chamber. Therefore, mixing ratio variations were obtained via the second capillary outlet from the permeation/diffusion device (see Figure 14) that was normally discarded, and by a second permeation/diffusion device with two α-pinene vials inside.

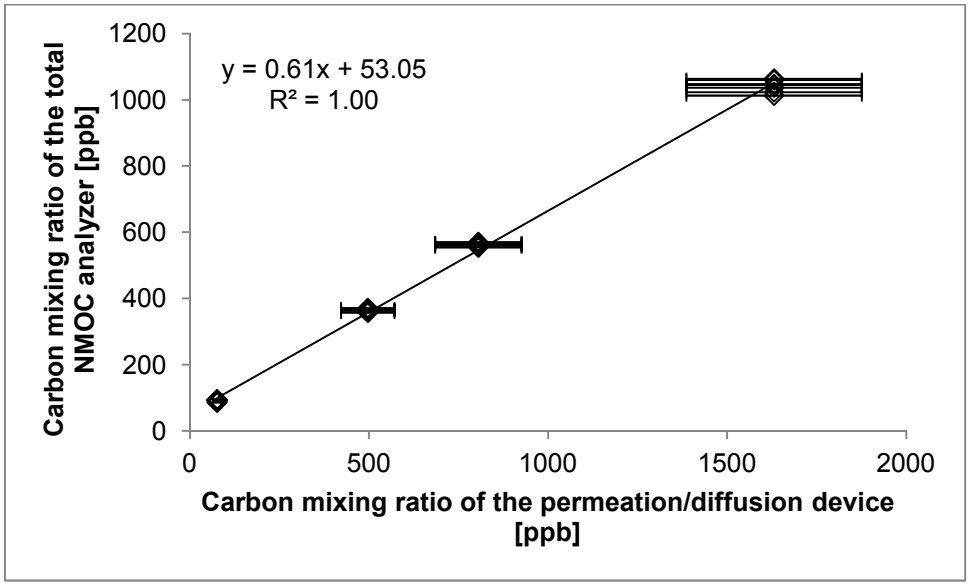

Figure 40: Correlation between the carbon mixing ratios from α-pinene obtained with the total NMOC analyzer (y-axis) and the calculated values (± 15%) from the permeation/diffusion devices (x-axis).

Four different mixing ratios were measured with the total NMOC analyzer and the measured results were correlated with the calculated mixing ratios from the permeation/diffusion device for α-pinene (Figure 40). A linear correlation with a perfect coefficient of determination (R^2=1) can be observed in the figure. This is again an unambiguous indication that the oxidation unit was efficiently oxidizing the injected α-pinene. In case of an insufficient oxidation process a saturation trend would be expected for higher mixing ratios. However, the slope of the linear fit indicated a recovery rate of approximately 60%. Compared to the recovery rate experiment from chapter 3.2.2.4 this would confirm the results for α-pinene. Only 58% α-pinene was recovered from the NMOC solid adsorbent unit with the PTR-MS. Nevertheless it has to be mentioned again that the recovery rate experiment of the NMOC solid adsorbent unit was performed with synthetic air and the risk of an oxidation reaction thereby must be considered. However Figure 40 shows again a very good reproducibility (100 ± 1-3.5%) between the individual measurements. CO_2 background signals during the measurements were again ranging at 200-250 ppb carbon. Nevertheless, the values were stable and a subtraction from the NMOC sample signal was reliable.

4.1.3 Nopinone

As monoterpenes react with ozone they are forming oxygenated compounds. The ozonolysis of β-pinene leads to nopinone (Cataldo et al. 2010). Therefore, nopinone was tested to represent the group of oxygenated volatile organic compounds. One characteristic of these oxygenated VOCs is their low vapor pressure which might induce the nucleation for the generation of secondary organic aerosol (SOA). The low vapor pressure might also have an influence on the adsorption of the compound on a solid adsorbent but a fortiori on the thermal desorption. Due to the low vapor pressure, a similar problem occurred as observed with α-pinene. The permeation/diffusion device did not provide high enough mixing ratios for further dilution within the plant chamber. To obtain different mixing ratios, again the regular capillary from the permeation/diffusion device was combined with the discarding capillary. Furthermore, a second permeation/diffusion device was equipped with three vials of nopinone. A correlation of the calculated and the measured values is shown in Figure 41.

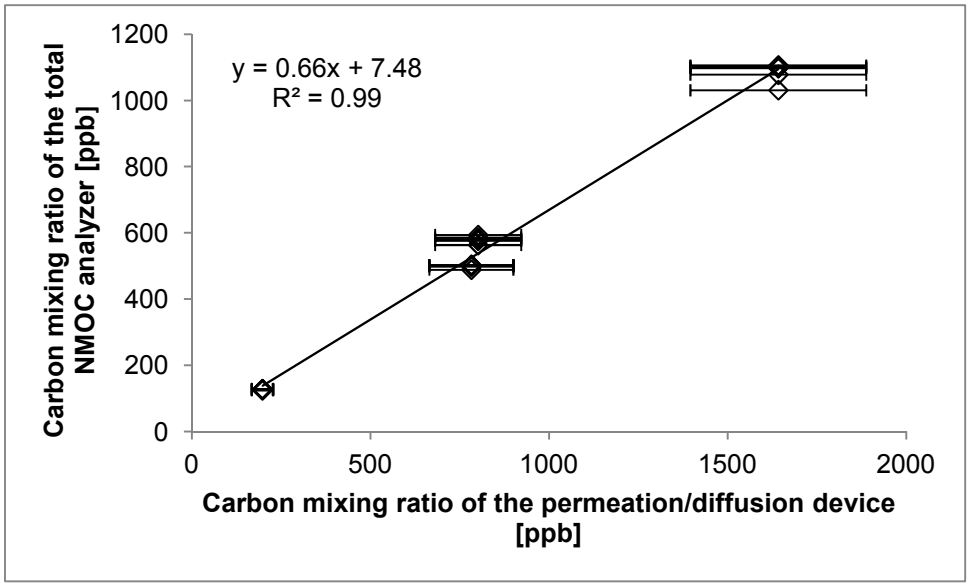

Figure 41: Correlation between the carbon mixing ratios from nopinone obtained with the total NMOC analyzer (y-axis) and the calculated value from the permeation/diffusion devices (x-axis) (with an uncertainty of ±15%).

Four different mixing ratios were measured. A good linear correlation was found. Again, it seems likely that the oxidation unit was functioning sufficiently for the lower mixing ratio values. However, there was more scattering of the measurement values obtained with the NMOC analyzer compared to the results for isoprene and α-pinene, in particular at the highest mixing ratio. The reasons for this might be an inefficient oxidation due to the high mixing ratio or the insufficient desorption of this compound from the NMOC solid adsorbent unit. Compared to the calculated values only 66% of the compound was recovered with the analyzer. This resulted again in a reasonable agreement with the recovery tests in chapter 3.2.2.4.

4.2 Plant chamber measurements

The plant chamber experiments were carried out for two weeks in October 2011. Two different experiments were set up. *Populus x canescens* and *Pinus sylvestris* were placed in the plant chamber for four days and *Quercus Ilex* for ten days. The chamber was continuously flushed with zero air. Air flows were typically set between 70-140 l min^{-1}. However, the zero air flow had to be adjusted individually for each experiment. Low air flows can lead to water condensation depending on the transpiration of the plant within the chamber. Therefore, the dew point on the chamber inlet was monitored and adjusted to approximately -10 to -15°C.

Background mixing ratios of VOCs, ozone and NO_x were lower than the detection limit of the measuring devices. CO_2 mixing ratios in the zero air flow were decreased compared to ambient mixing ratios. Therefore, CO_2 was added to the zero air prior to the inlet of the chamber to obtain ambient mixing ratios. Table 13 shows the measurement parameters, the measurement principles and the corresponding measuring devices.

Table 13: Measurement parameters for the plant chamber experiments.

measurement parameter	measurement principle	measuring device
total NMOC	elemental analysis	total NMOC analyzer
VOC	mass spectrometry	GC-MS
VOC	mass spectrometry	PTR-MS
CO_2	infrared analyzer	LiCOR 7000
H_2O	dew point monitor	Walz MTS MK1
Temperature	thermoelement	NiCrNi thermoelement
Ozone	ultraviolet analyzer	Thermo Environmental Model 49
PAR	radiometer, 400-700 nm	LiCOR Quantum

Measurements were started shortly after the incorporation, ignoring adaption needs for the plants.

4.2.1 Populus x canescens and Pinus sylvestris

The first experiment was carried out with a combination of two different plant species, i.e. *Populus x canescens* and *Pinus sylvestris.* They were incubated together into the plant chamber. The measurement period was three whole days and two half ones. Both species are known to emit NMOC compounds such as isoprene in case of *Populus x canescens* and monoterpenes in case of *Pinus sylvestris*. Figure 42 shows the VOC emissions of *Populus x canescens* and *Pinus sylvestris* measured with the total NMOC analyzer.

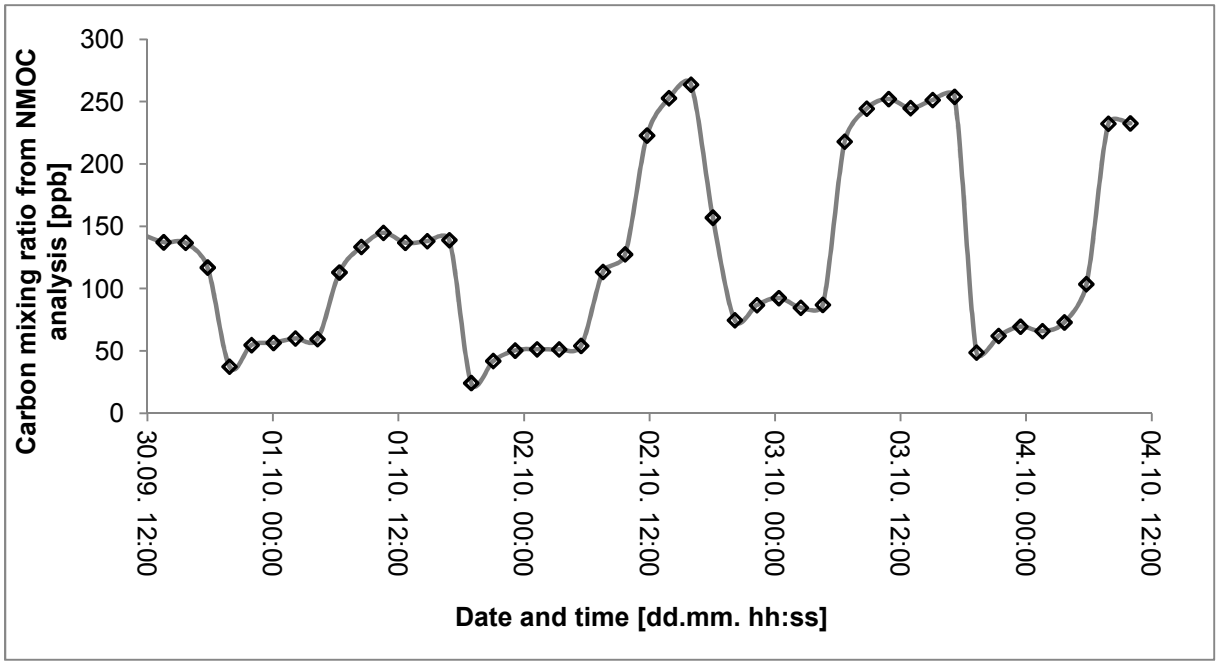

Figure 42: VOC emissions of *Populus x canescens* and *Pinus sylvestris* measured with the total NMOC analyzer. Carbon mixing ratios are shown in ppb.

A clear diurnal course can be observed which originates from the day-night cycles within the plant chamber. The temperature was set to 25°C between the 30th of September and the 02nd of October. For the following days the temperature in the chamber was 35°C. The temperature change can clearly be observed on the 02nd of October. Higher emission rates applied also on the following days with a temperature setting of 35°C. Carbon mixing ratios varied between 150 ppb at 25°C and up to 270 ppb for 35°C. Also during night time a VOC emission of approximately 50 to 70 ppb carbon was reached. This can be explained by contributions of the boreal coniferous trees with evaporation processes from storage pools. In general, it can be regarded that isoprenoid emissions (isoprene + monoterpenes) are released under strict temperature and light control (Kesselmeier and Staudt 1999). However, special cases are known, for example coniferous needles with monoterpenes stored in resin ducts. As a consequence the evaporation depends mostly on the saturation vapor pressure of the monoterpenes which is temperature dependent (Ghirardo *et al.* 2010, Grote and Niinemets 2008, Kesselmeier and Staudt 1999). Thus, as the temperature was high enough during night time a VOC emission could still be observed originating from *Pinus sylvestris.* However, also a light-dependent VOC emission was observed for some of the monoterpene species (Figure 45 + 46). VOC emissions (mainly isoprene) from *Populus x canescens* emerge from *de novo* biosynthesis which is

light- and temperature-dependent and accounts mainly for the diurnal course (Kesselmeier and Staudt 1999). However, it is puzzling that after reaching a lower carbon mixing ratio in the dark period the signals increased again. The low signal might have been caused by the termination of the *de novo* synthesis of VOC compounds and a delayed emission from the storage pools of *Pinus sylvestris* after stopping the *de novo* biosynthesis. Another explanation for this phenomenon might be found when taking a closer look at the CO_2 background signals which were measured in close relation to the CO_2 mixing ratio at the chamber outlet.

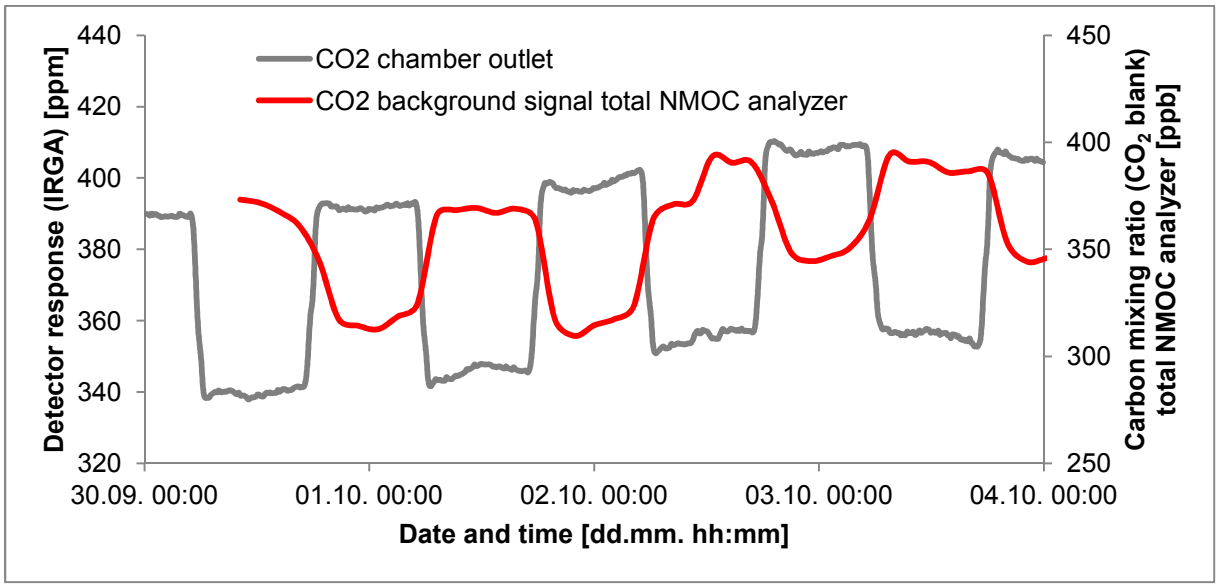

Figure 43: Comparison of the CO_2 mixing ratio at the chamber outlet (grey line) and the CO_2 background signal ($area_{CO2Sample}$ values) from total NMOC analysis (red line).

Figure 43 demonstrates the nocturnal course of the CO_2 signal at the chamber outlet. This is the expected behavior as the plants assimilate CO_2 during the day for biosynthesis and emit CO_2 during the night. However an opposing behavior of the CO_2 background signal was found. If the CO_2 background signal would be influenced only by the ambient CO_2 mixing ratio both signals should exhibit a similar course. Therefore, other factors affecting the CO_2 background signal of the total NMOC analyzer have to be discussed. As mentioned before the CO_2 signal of an IRGA at 4.26 µm might interfere with water vapor and alkynes, though water vapor was principally excluded by the use of a drying cartridge. The diurnal CO_2 background signal is puzzling and cannot be explained exactly. It seems likely that this interference was caused by water vapor initiated by plant transpiration following a diurnal course in close relation to temperature. This explanation would be in

accordance with the missing interference in experiments with single compounds in dry zero air resulting in lower CO_2 background signals without a diurnal course. However, further tests would be required to confirm this statement for the total NMOC analyzer and constant measurements of the water vapor with the detector would be necessary. Anyway, this behavior leads to an underestimation of the total NMOC signal during day time and an overestimation during night time which makes a quantitative statement about the total NMOC amount difficult. This might also explain the dropping of the first value under night condition, as a high CO_2 background value is subtracted from a low VOC signal because of the poor time resolution of the NMOC analyzer.

VOC emissions during the plant chamber experiments were measured by PTR-MS and GC-MS. Both instruments were calibrated with VOC species from the permeation/diffusion devices before and after the plant chamber experiments.

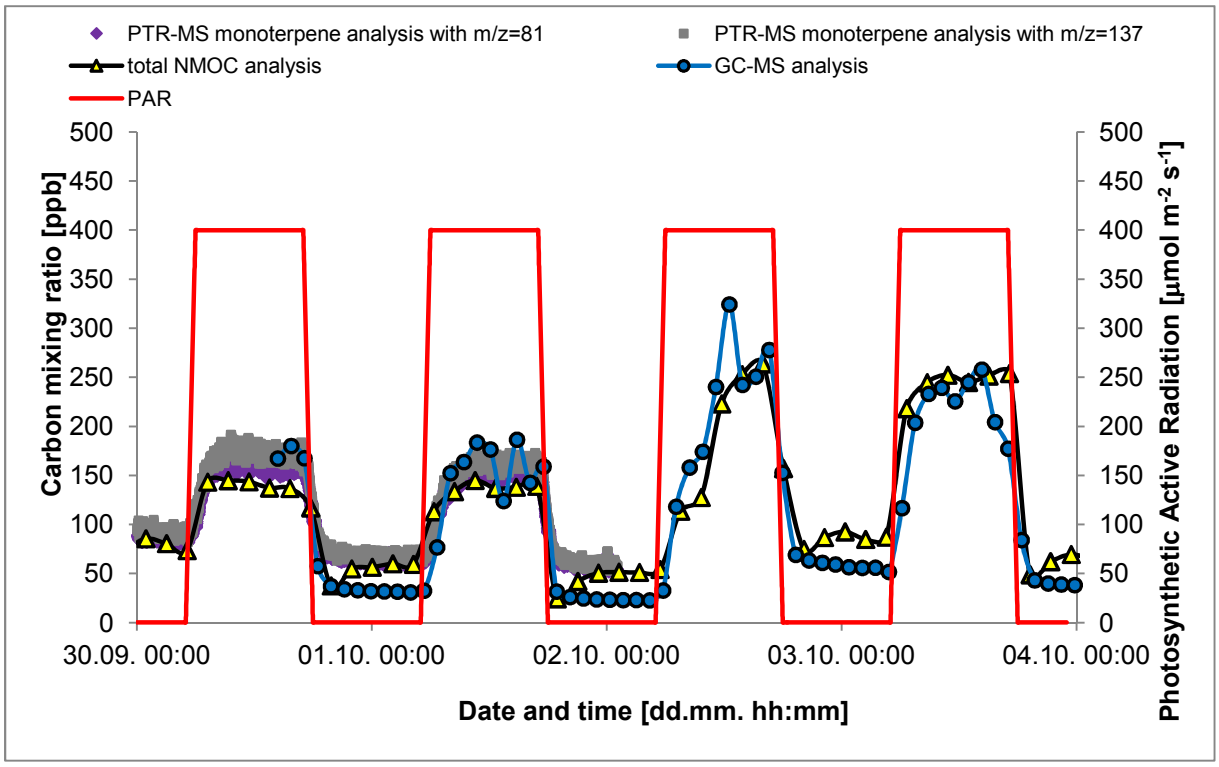

Figure 44: Diurnal fluctuations of carbon mixing ratios as observed with *Populus x canescens* and *Pinus sylvestris* at 25°C on the first two measurement days and after a temperature increase to 35°C on the third day which was kept till the end of this experiment. The carbon mixing ratios obtained are shown on the primary y-axis. The photosynthetic active radiation is plotted on the secondary y-axis.

Figure 44 shows an overview of the measurement results from the different instruments. Also indicated in the figure is the photosynthetic active radiation (PAR)

during the experiment to clearly demonstrate the light-dependent VOC emission. A reasonable agreement between the different measurement methods was observed. During the first two measurement days the total NMOC carbon mixing ratios were lower compared to the results of the other two methods during the day period. This might be due to the probable interferences with water. On the other hand an underestimation might be explained by poor recovery rates for monoterpenes. During the night period the total NMOC analyzer values range in between the results obtained with the PTR-MS and the GC-MS. The GC-MS values were always lowered during night time in comparison to the other two instruments. This might again confirm the overestimation of the carbon mixing ratios during night time because of the CO_2 blank values.

To understand the discrepancies of the signals of the different instruments during day and night time a closer look on the emission compounds was necessary. Figure 45 shows the most abundant compounds measured with the GC-MS and Figure 46 shows the results of the PTR-MS measurements (only day one and two).

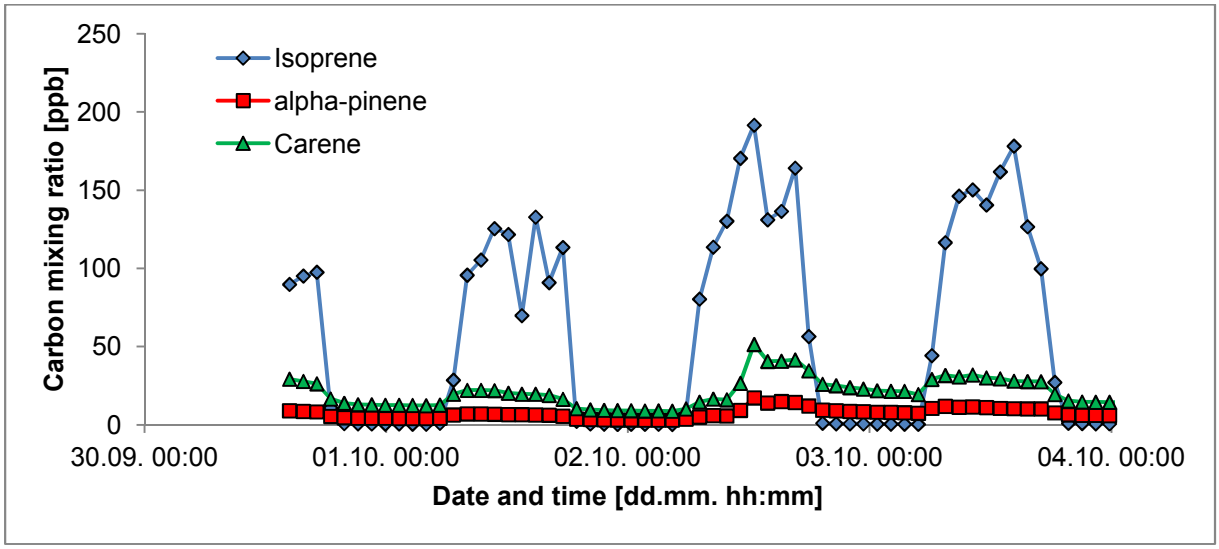

Figure 45: Carbon mixing ratios of the most abundant VOC compounds from the GC-MS measurements of the emission from *Populus x canescens* and *Pinus sylvestris.* The temperature at the plant chamber was set to 25°C on the first two measurement days. On the 02nd of October the temperature was increased to 35°C during the day.

Figure 45 clearly shows that isoprene is the dominating compound which was emitted by *Populus x canescens.* Monoterpenes were emitted by *Pinus sylvestris*. For carene an obvious diurnal course and a signal increase caused by a temperature rise from 25°C to 35°C was observed for day and night time emissions.

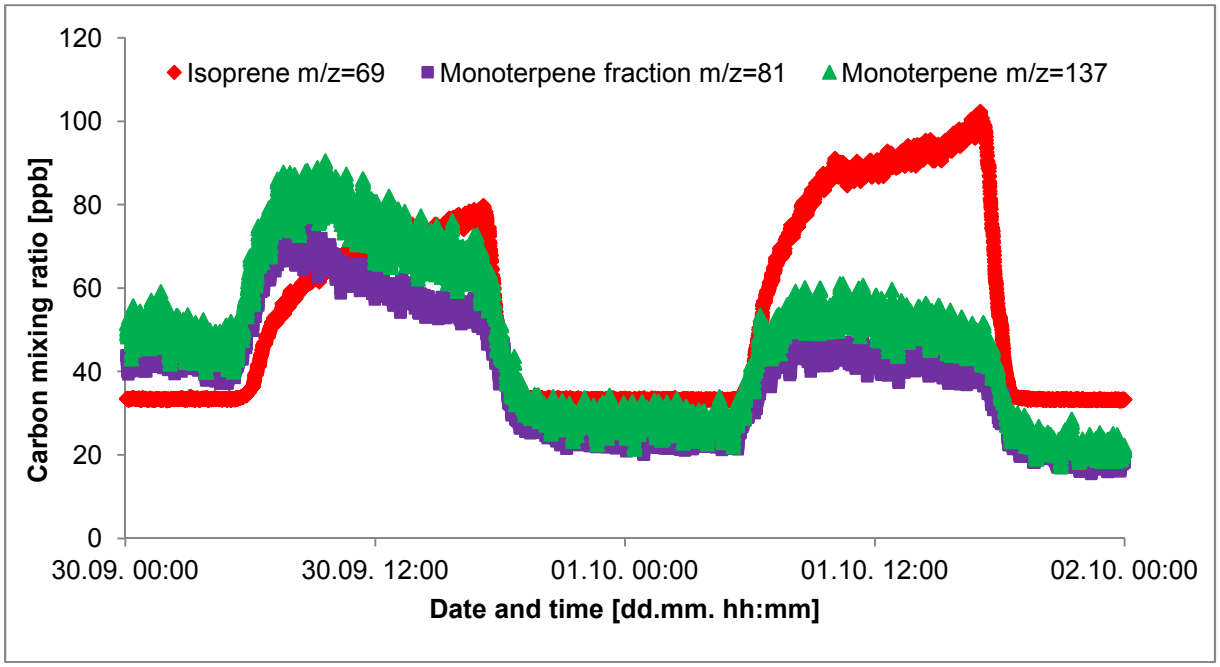

Figure 46: Carbon mixing ratios from the PTR-MS measurements of the emission from *Populus x canescens* and *Pinus sylvestris* at 25°C.

A closer look on the results from the PTR-MS measurements (Figure 46) showed that the monoterpene emission was decreasing on the first two measurement days. The main reason was probably the installation of the plants (especially *Pinus sylvestris*) into the plant chamber. Injuries and lost needles led to an increased monoterpene emission on the start of the experiment. This might also be the reason why the values obtained with the total NMOC analyzer during day time were lower than the results of the GC-MS and the PTR-MS. Also as the sum of monoterpene emission seems to exceed the isoprene emission, the poor recovery rates for monoterpenes might contribute to the lower values of the total NMOC analyzer. Strange however, was the isoprene measured with the PTR-MS during the night period (Figure 46). A clear diurnal course was found but the emission values did not decrease to zero but to 30-35 ppb carbon during night time which corresponds to 6-7 ppb isoprene concentration. What caused this discrepancy is uncertain but explains the enhanced carbon mixing ratios of the sum of VOCs from PTR-MS analysis during night time (see Figure 44). Conspicuous are also the lower isoprene mixing ratios measured with the PTR-MS in relation to the GC-MS data, demonstrating the general difficulties in comparing the different instruments. The last two measurement days (2nd and 3rd of October) showed a good agreement between the GC-MS and total NMOC measurement during the day (see Figure 44). The emissions were mainly dominated

by isoprene which should be fully recovered with the total NMOC analyzer. However an underestimation due to the high and probably interfering CO_2 blank values and the low recovery rates for monoterpenes from the NMOC adsorbent unit is still likely.

4.2.2 Quercus Ilex

The second plant chamber experiment was carried out with a *Quercus ilex.* It is known to be a monoterpene emitting plant species. One plant was incorporated into the chamber for ten days. The light period settings stayed as applied for the first experiment with *Pinus sylvestris* and *Populus x canescens.* However one lamp broke during the experiment which resulted in slightly lower photosynthetic active radiation values than at the beginning. The temperature was set to 25°C. During the ten days the temperature was increased to 30°C for two days and was decreased again. On two consecutive days experiments with ozone addition were carried out. 50 ppb and 75 ppb ozone were added once in the morning and once in the afternoon.

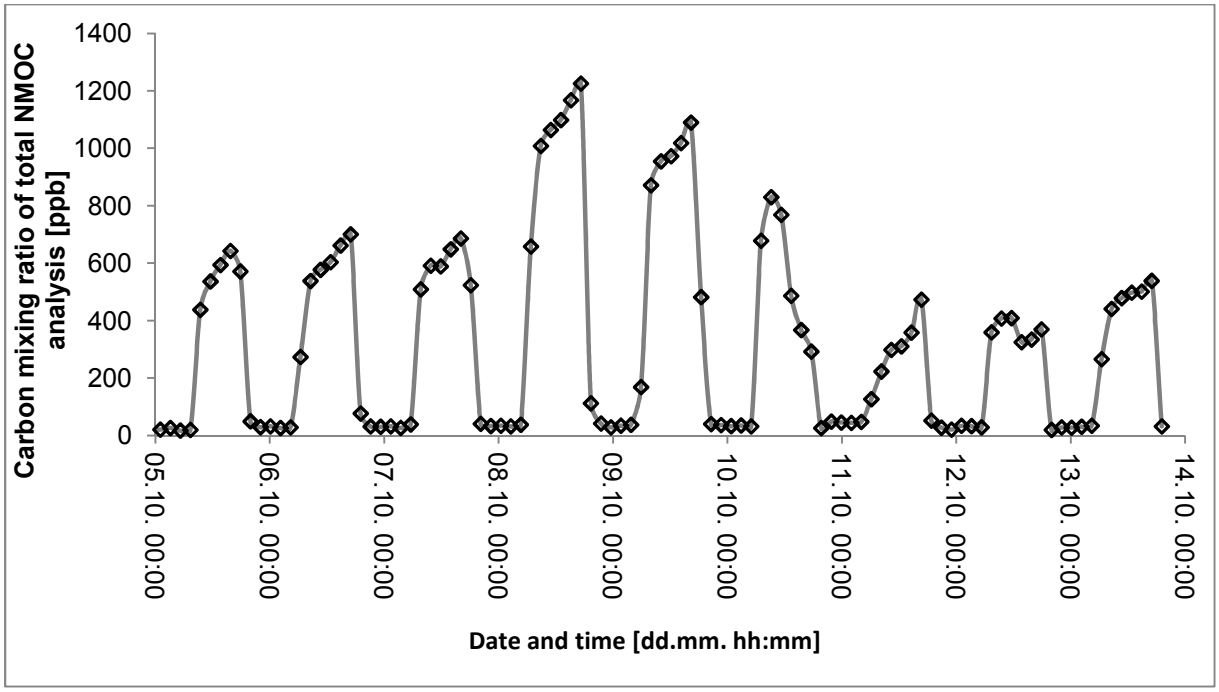

Figure 47: VOC emissions of *Quercus ilex* measured with the total NMOC analyzer. Carbon mixing ratios are shown in ppb. The temperature was set to 25°C on the first three measurement days. On the 8th and 9th of October the temperature was increased to 30°C and decreased to 25°C on the 10th of October. The ozone experiments were carried out in the morning of the 11th and on the afternoon of the 12th of October.

Figure 47 shows the carbon mixing ratios resulting from the total NMOC analyzer measurements. Compared to the preceding plant chamber experiment much higher carbon mixing ratios were obtained with *Quercus ilex*. The carbon mixing ratios were reaching values of up to 1300 ppb during the measurement period. A diurnal course with values near zero was observed which indicated a light-dependent emission. But also a temperature-dependent emission was demonstrated due to the higher emission rates during the day period when the temperature increase to 30°C was applied. VOC emissions during night time like in the first plant experiment with *Pinus sylvestris* did not occur. On the 11th and the 12th of October discrepancies in the diurnal course could be observed. During this time ozone was added into the chamber and caused a slight drop in the NMOC signal as some of the volatile organic compounds reacted with the ozone and resulted in compounds that could not be detected with the NMOC analyzer. If the analyzer would work best, there should be no effect from the ozone addition in the total NMOC signal since the instrument should be able to measure also the volatile organic compounds which originate from degradation reactions with ozone. The fact that compounds with a C_3 structure and below are not sampled efficiently on the solid adsorbent unit, and the risk of losing oxygenated compounds because of their low vapor pressure, might be an explanation for the decreased signals. Also a reaction of the plant due to the ozone addition and hence a change in the emission rates could be a reason for the decrease of the total NMOC signal.

Considering the data evaluation a closer look on the CO_2 background signal had to be taken again. Once more a diurnal course for the CO_2 background signal on the total NMOC analyzer was observed. Additionally, an obvious signal increase during ozone addition was found. Figure 48 shows the CO_2 background signal compared to the CO_2 mixing ratios at the chamber outlet.

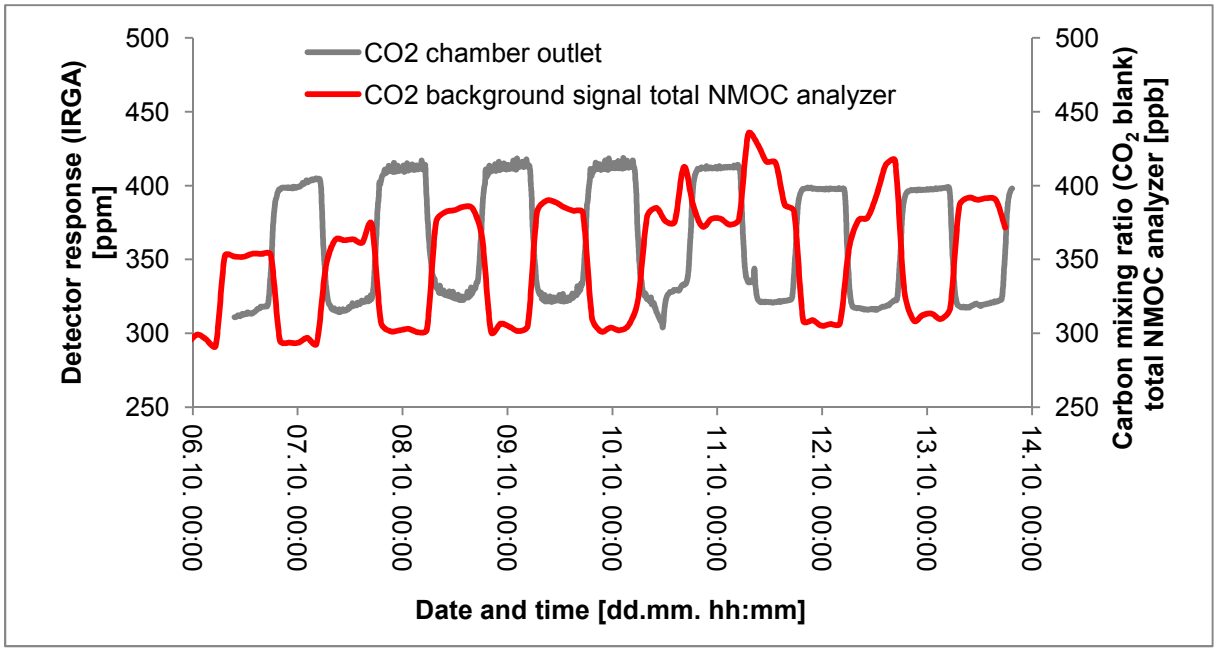

Figure 48: Comparison of the CO_2 mixing ratio at the chamber outlet (grey line) and the CO_2 background signal from total NMOC analysis (red line) for the *Quercus ilex* measurement at a temperature of 25°C. On the 8th and 9th of October the temperature is increased to 30°C and decreased again on the 10th of October. An attempt for an ozone addition was started already at the 10th but cancelled due to a leakage. Ozone addition was carried out in the morning of the 11th and in the afternoon of the 12th of October.

On the 11th in the morning and the 12th in the afternoon high CO_2 background signals were observed when ozone was added to the chamber. Also the temperature rise from 25°C to 30°C was visible in the blank values on the 8th and 9th of October. On the 10th the CO_2 background signal exhibited a sudden peak in the afternoon. This could be explained by an excessive ozone addition due to a leakage at the plant chamber during the attempt for an ozone experiment. Furthermore, on the two days (11th and 12th of October) with the executed ozone experiments the CO_2 background values also showed a clear peak which might be understood as a reaction of the plant to the sudden ozone values. However, as the corresponding CO_2 signal was always subtracted from the NMOC signal, an underestimation during the day and an overestimation during the night is likely for the total NMOC values. Due to the enhanced CO_2 background signals during ozone addition the underestimation of the total NMOC signal is probably even greater. Hence, a quantitative analysis was difficult with the CO_2 background signal taken into account. The comparison to the other methods, PTR-MS and GC-MS, is shown in Figure 49.

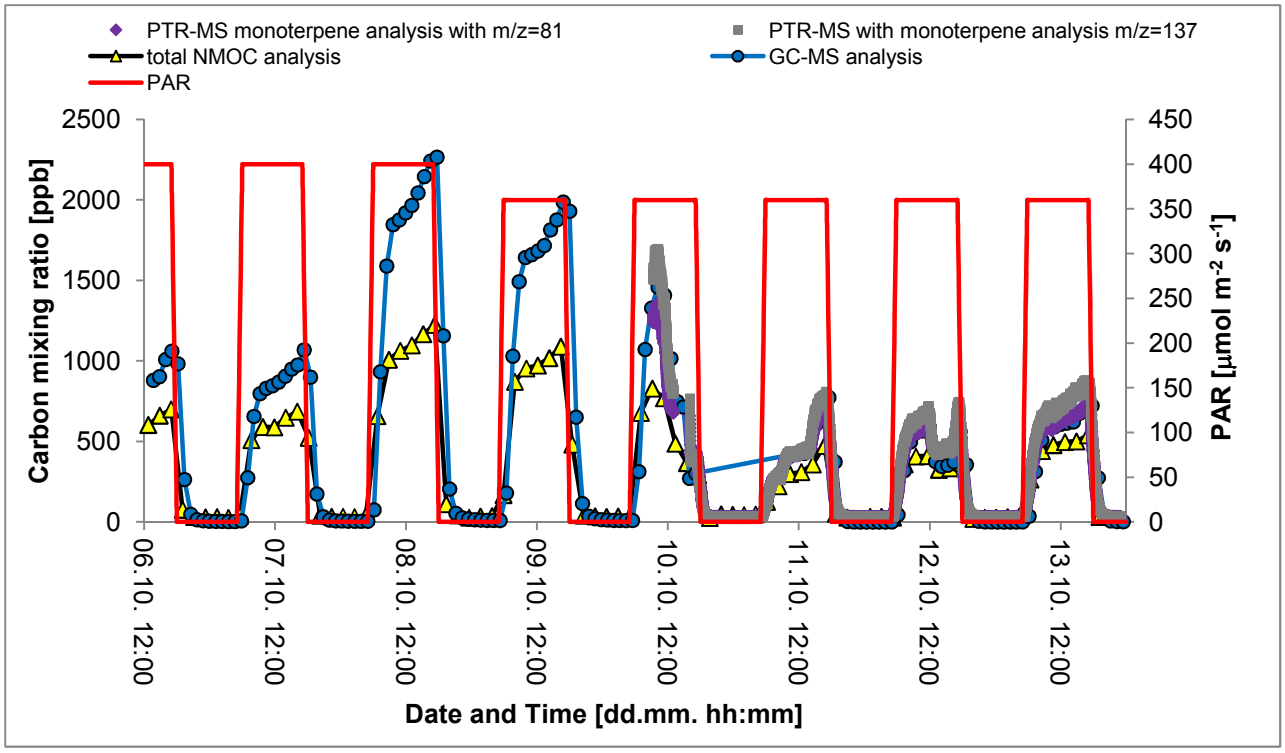

Figure 49: Overview of the carbon mixing ratios for the *Quercus ilex* measurements from the different instruments. The carbon mixing ratios obtained are shown on the primary y-axis. The photosynthetic active radiation is plotted on the secondary y-axis. The temperature was set to 25°C on the 6th and 7th of October and increased to 30°C on the 8th and 9th of October. On the 10th the temperature is decreased again to 25°C for the rest of the experiment.

The total NMOC data clearly followed the same course as found with the other instruments. However, discrepancies of up to 50% were observed for the total NMOC results compared to the GC-MS values especially on the 8th and 9th of October. During night time the results for the instruments are in close accordance. None of the instruments detected any significant VOC signal. PTR-MS data were only available on the last measurement days. Reasons for the discrepancy between the different methods could be the already mentioned difficulty with the interfering CO_2 background signal which leads to a signal underestimation during the day period. However, the main reason is probably the poor recovery rate for monoterpenes on the NMOC solid adsorbent unit. As *Quercus ilex* is primarily emitting monoterpenes such a high discrepancy would be possible. A closer look to the most abundant monoterpene emissions is shown in Figure 50.

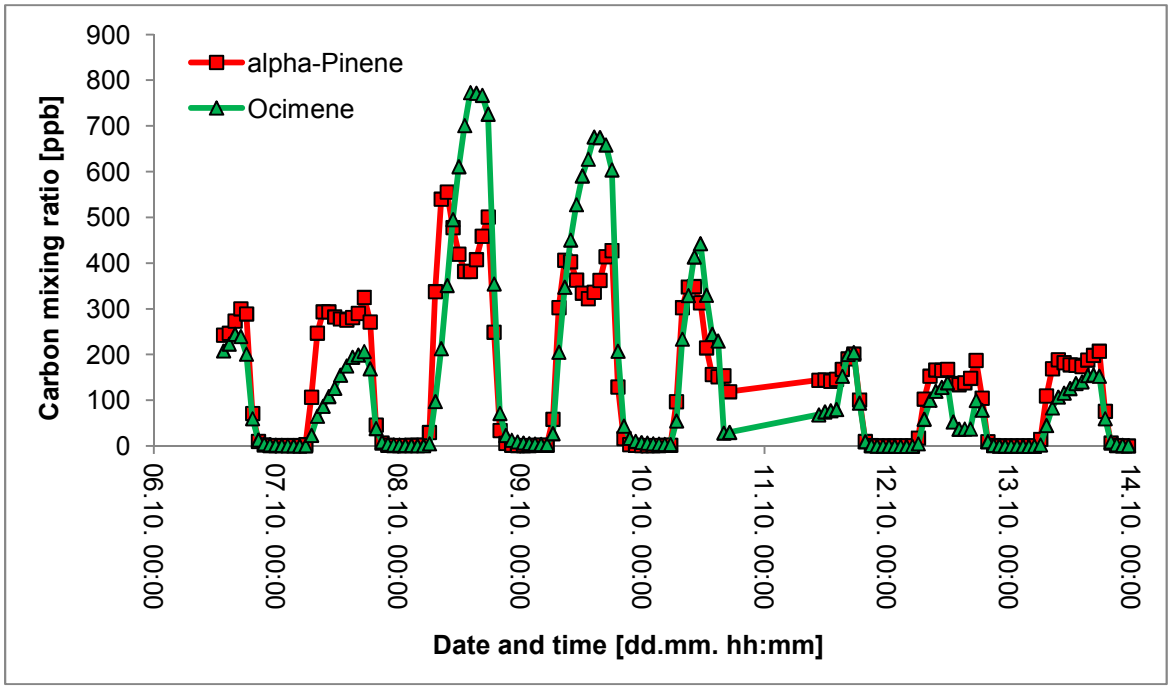

Figure 50: Carbon mixing ratios of the most abundant monoterpene compounds from the GC-MS measurements of the emission from *Quercus ilex.* The temperature at the plant chamber was set to 25°C on the 6th and the 7th of October. On the 8th and 9th of October the temperature was increased to 30°C and decreased to 25°C on the 10th of October till the end of the experiment. In the night from the 10th to the 11th the GC-MS was calibrated until the start of the ozone experiment in the morning of the 11th. Another ozone addition was carried out in the afternoon of the 12th.

Ocimene and α-pinene as measured by GC-MS were the most commonly emitted compounds. The recovery rate experiment carried out with α-pinene demonstrated a loss of approximately 40%. This supports the assumption that the major discrepancy is caused by the poor recovery rates for α-pinene. However, the recovery rate for Ocimene is unknown with the result that a clear statement about the sum of monoterpenes cannot be made.

Another reason for the discrepancy of 50% between the results of the two instruments might also be the really high monoterpene mixing ratios of more than 200 ppb which might lead to insufficient oxidation as it could be observed for the high isoprene mixing ratio of the single compound measurements (see Figure 39). With lower monoterpene mixing ratios the discrepancies subsided. Emission rates under the same temperature setting decreased during the measurement period. This decrease might be explained by higher VOC emissions triggered by environmental stress and injuries originating from the installation, thus declining in course of the experiment. On the 9th of October however, the decrease of the carbon mixing ratios

is assumed to originate from the reduction of the photosynthetic active radiation due to a broken lamp.

On the 11th and 12th of October an ozone experiment was carried out. An overview of the last three measurement days including the ozone experiments is shown in detail in Figure 51.

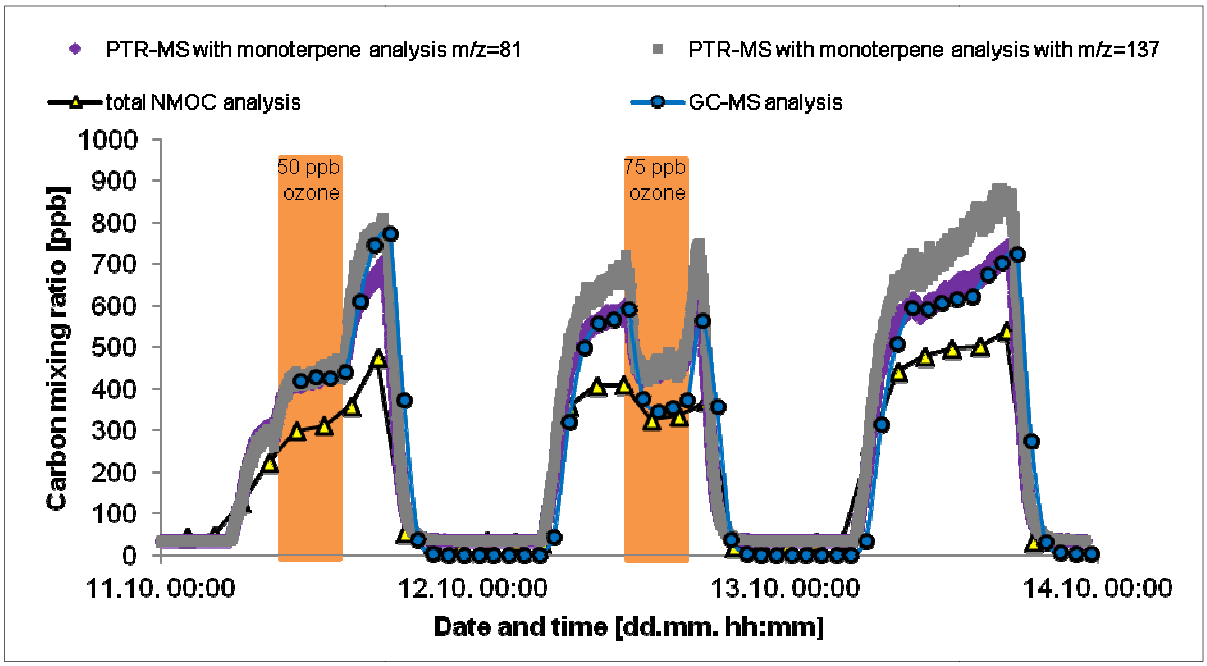

Figure 51: Section from Figure 49 of the last three measurement days showing the results of all measuring instruments and the periods of ozone addition into the chamber. The set temperature was 25°C.

In the morning of the 11th and in the afternoon of the 12th of October ozone was added into the chamber in concentrations of 50 ppb and 75 ppb (see Figure 51). In comparison with the other instruments the data obtained with the total NMOC analyzer are still lower but discrepancies only arise up to 40%. However, the discrepancies are in general lower than on the first measurement days (see Figure 49). Moreover, the total NMOC analyzer results closely follow the same trend as observed by the other two instruments. Especially during ozone addition the differences of the carbon mixing ratio between the total NMOC analyzer and the other two instruments were shrinking. The loss of VOCs was most visible by GC-MS and PTR-MS. Especially the ocimene signal showed a significant drop particularly in comparison with α-pinene (see Figure 50). The atmospheric lifetime of ocimene was

determined to range around 41 min under the influence of ozone.[12] This supports the assumption that the signal loss was due to degradation reactions caused by the ozone addition. The atmospheric lifetime of α-pinene in an ozone rich environment is 4.6 h (see Table 1), explaining the lower influence on the α-pinene signal. Hence, as the ozone addition period was always shorter than 4 h the decrease of the α-pinene signal could be also caused by a change of the emission rates as a reaction of the plant to the ozone addition.

The ozone addition also had an impact on the results of the total NMOC analyzer. Nevertheless, on the 12th of October the total NMOC analyzer and the GC-MS measurement nearly resulted in the same carbon mixing ratio values. This leads to the assumption that products from degradation processes can still be detected with the total NMOC analyzer. However the underestimation caused by the CO_2 background and the problem with the low recovery rates for monoterpenes still lead to lower carbon mixing ratios in comparison with other methods.

4.3 Discussion

The results from the experiments performed with single compounds and plants in a chamber demonstrated the difficulties with the analyzer setup. Main problems arose from the recovery rates of the different volatile organic compounds from the solid adsorbent material and from interferences on the infrared gas analyzer detector. The measurements of the single compounds showed a good agreement between the results of the recovery rate tests of the NMOC adsorbent unit in chapter 3.3.2.4 and the single compound measurements in chapter 4.1. Measurements of the single compounds resulted in better recovery rates which was expected as the experiments in chapter 3.3.2.4 were carried out with synthetic air and a degradation of the compounds during thermal desorption was likely. However, the plant chamber experiments and the plotting of the CO_2 background signal together with the CO_2 mixing ratio at the chamber outlet showed that there is also an underestimation of the total NMOC carbon mixing ratios due to high CO_2 background signals. Most likely the interference is caused by water vapor. This problem should be prevented by simultaneous measurements of water vapor on the detector in the future. However, influences from VOC compounds on the detector cannot be fully excluded.

[12] http://www.cas.manchester.ac.uk/restools/aerosolchamber/research/precursor/

Measuring the dry air at the chamber inlet as the CO_2 background signal would also be a possibility and mainly prevent the interferences from water vapor and also from VOC compounds, but the variation of the CO_2 mixing ratio on the outlet could not be taken into account. On the contrary, these variations probably result in lower effects than the interferences caused on the chamber outlet. However, environmental measurements outside the laboratory would be more difficult to realize.

The single compound measurements also showed that the oxidation unit seemed to efficiently oxidize the volatile organic compounds to CO_2. The different single compounds (isoprene, α-pinene and nopinone) all showed a linear correlation compared to the calculated values from the permeation/diffusion device. If the catalyst would not efficiently oxidize the compounds, a saturation trend for the higher mixing ratios should be observed. However, with high mixing ratios of more than 200 ppb the limit of the catalyst for the efficient oxidation might have been reached. This could also influence the recovery rates of the total NMOC analyzer when high mixing ratios occur. The oxidation efficiency has to be examined with single VOC compounds which have to be introduced into the analyzer excluding the sampling step on the solid NMOC adsorbent unit. Besides, it has to be ensured that there is no interference from water vapor originating from the oxidation reaction of the organic compounds arriving at the detector.

The plant chamber experiments showed that the total NMOC analyzer is principally capable of following diurnal courses in the same way the comparing instruments GC-MS and PTR-MS can. However, the values obtained with the total NMOC analyzer nearly always underestimate the carbon mixing ratios. For measurements with isoprene emitting plants the best agreement was achieved as isoprene was fully recovered in the applied experiments. The measurement of *Pinus sylvestris* and *Popolus x canescens* resulted in good agreements of the different methods. The total NMOC analyzer was able to follow the diurnal course and was also able to detect an emission of volatile organic compounds during the night arising from storage pools from *Pinus sylvestris*. Also the light- and temperature-dependet VOC emission of *Popolus x canescens* was shown. With a plant species like *Quercus ilex* which emits almost exclusively monoterpenes a much lower agreement was obtained in comparison with the other two measuring methods. Discrepancies up to 50% were observed which are in an agreement with the recovery rate experiments but could also arise from insufficient oxidation due to the high monoterpene mixing ratio of

approximately 200 ppb. Nevertheless, the total NMOC analyzer was capable of following the diurnal course again. During night time the values were close to zero and showed that Quercus ilex has a light- and temperature-dependent behavior concerning VOC emission. The volatile organics originate from *de novo* biosynthesis during the day period. The temperature dependence was observed during the temperature increase on two measurement days. Experiments with ozone addition proved that the total NMOC analyzer was performing best compared to the GC-MS and the PTR-MS. The two instruments showed a significant signal decrease during ozone addition. The signal loss can be explained by a degradation of emitted compounds with ozone. The degradation products were not detected with the GC-MS or the PTR-MS. The total NMOC analyzer also showed a signal decrease during ozone addition but in comparison the signal loss was much lower than for the other two instruments. This showed that the reaction products from the degradation processes were partly still detected with the total NMOC analyzer. The assumption that the emission rates were influenced by the ozone addition also has to be considered for the interpretation of the signal decrease but could not be validated for sure. The total NMOC analyzer is capable to obtain good results when ozone was added to the chamber. Together with the fact that the CO_2 background signals were increased during the ozone addition, the results from the total NMOC analyzer during that period are definitely underestimated. The experiments showed a good performance of the analyzer concerning the ability to follow the diurnal course of plant emissions within an enclosure experiment. Nevertheless, quantitative analysis is difficult due to unknown recovery rates of the volatile organic compounds emitted by the biosphere and due to the high CO_2 background signals originating from sampled ambient CO_2 and from interferences from water vapor and possibly also from VOCs. Compared to other commercially available instruments the carbon mixing ratios obtained with the NMOC analyzer were most of the time lower than the results of the PTR-MS and the GC-MS analysis. For isoprene emitting plants a relatively good agreement was obtained but for monoterpene emitting species, discrepancies of up to 50% were found.

Summary and conclusion

A total NMOC analyzer was developed to determine the total organic carbon after catalytic oxidation to CO_2 and subsequent measurement by an infrared gas analyzer. Calibration of the total NMOC analyzer for carbon mixing ratios was performed with different CO_2 ratios which were injected into the instrument and measured with the infrared gas analyzer. Calibration via any other compound was difficult as oxidation efficiency and recovery rates might be different for each compound and cannot be used as a calibration factor for any other compound. A good reproducibility for the different CO_2 mixing ratios during calibration and of the single compound measurements were obtained with a precision of ±2.6% and ±3.5%. Zero air measurements containing ambient CO_2 mixing ratios showed a detection limit of 48 ng or 29 ppb carbon.

The presented experiments and results showed that the total NMOC analyzer was able to follow VOC emissions from plant enclosure measurements. However, various different factors influenced the total NMOC analyzer measurements. As pointed out in this thesis, the choice of the catalytic material turned out as a great problem. Different commonly used materials were tested. Most catalysts could not be used for the application of the instrument as they either released CO_2 when oxygen was added to the carrier gas stream or adsorbed and released CO_2 due to their large surface area despite the high temperatures used. The oxidation efficiency is the crucial factor of importance, but due to the behavior of the catalytic material concerning the CO_2 background, the right choice of the catalyst was rather difficult. A Pt-Rh wire achieved the best results with respect to the CO_2 behavior and was used as catalyst eventual. However, experiments with single VOC compounds injected into the oxidation unit to confirm the oxidation efficiency still have to be carried out.

So far only recovery rate tests of a few single compounds were executed with the instrument. Nevertheless, these results indicated that the oxidation efficiency was adequate for most mixing ratios which were applied. Another problem with the measurement of the single compounds was the recovery rates. Low molecular carbon compounds like isoprene were recovered to 100%. With α-pinene and nopinone only recovery rates of 61% and 68% were obtained. Additional tests with the solid NMOC adsorbent unit connected to the PTR-MS confirmed these results. However, because of the critical response of the PTR-MS under helium, synthetic air

was used as a carrier gas for these tests which supports oxidation and degradation reactions during thermal desorption. In general the experiments indicate that it is likely that the recovery rate for every volatile organic compound might be different especially for higher molecular compounds with C≥10 like α-pinene or for oxygenated compounds like nopinone that can interact with the solid adsorbent material and result in a nonlinear desorption.

As the ambient CO_2 was also sampled to a small amount on the solid adsorbent unit, different NMOC adsorbent unit settings were applied to minimize the background from ambient CO_2. Sampling temperature, sampling volume and flush volume of the NMOC solid adsorbent unit were varied to obtain ideal settings. The attempt to separate the sampled ambient CO_2 from the NMOC compounds failed as the solid adsorbent material released the CO_2 and the sampled compounds at the same time. Only a small part of the CO_2 could be separated. However, CO_2 background signals were still in the range of 100 – 400 ppb depending on the experiment setup. For plant chamber experiments the CO_2 background signal arriving at the detector of the total NMOC analyzer was increased, presumably caused by interferences from water vapor from plant transpiration but also sampled VOCs could have an impact on the detector.

Plant chamber measurements with *Pinus sylvestris* and *Popolus x canescens* showed relatively good agreements of the NMOC signal with the accompanying PTR-MS and GC-MS measurements under daylight conditions with isoprene as the main VOC emitted. High discrepancies occurred under night time conditions between the different instruments when the main compounds emitted were monoterpenes. With *Quercus ilex* which is a monoterpene emitter the discrepancies raised up to 50%. For the explanation also the recovery rate measurements of α-pinene and nopinone must be taken into account. Contrasting, when adding ozone into the plant chamber the total NMOC analyzer showed a good performance compared to the GC-MS and the PTR-MS. High compound losses were observed with the latter two instruments whereas the loss with the total NMOC analyzer was relatively small. However, it must be added that the carbon mixing ratios during ozone addition might be underestimated due to increased CO_2 background signals. This indicates a better sampling efficiency for monoterpene decomposition products. Nevertheless, the possible effect on physiology of emission rates due to ozone addition should also be kept in mind for the data interpretation.

The focus of the present total NMOC analyzer development was the size reduction of the instrumental setup, the decrease of the CO_2 background signal and the enhancement of the recovery rate. Dindorf (2006) obtained good results with the previous total NMOC analyzer setup for the carbon exchange rates from plant enclosure measurements compared to other analytical techniques but recovery rates were not exceeding 48%. The size reduction was accomplished by the new setup of the oxidation unit. Due to this essential step the size of the analyzer was halved. The new oxidation unit also led to a lower CO_2 background signal and also to more sufficient oxidation efficiencies as a different catalytic material was applied. However, CO_2 background signals were still in the range of a few 100 ppb. The high values were due to the fact that a part of the ambient CO_2 was sampled on the solid adsorbent unit. Also important for the CO_2 background signal are interferences originating from water vapor and possibly from VOCs. A significant reduction of the CO_2 background signal was not possible without the risk of losing NMOC compounds. The recovery rates for single compounds were enhanced. Isoprene was fully recovered. However, α-pinene and nopinone were only recovered to a percentage of 61% and 68% for the single compound measurements. In comparison with other analytical methods like PTR-MS and GC-MS discrepancies of up to 50% occurred for plant chamber experiments especially with monoterpene emitting plants. However a good performance was observed under ozone stress. The PTR-MS and the GC-MS measurements showed a large signal decrease during ozone addition due to degradation and oxidation of reactive VOCs, whereas the total NMOC analyzer only showed a slight drop of the carbon mixing ratio values. Nevertheless, a quantitative analysis is difficult with the present setup as recovery rates seem to vary for each compound. A quantitative total non-methane organic carbon analysis is not possible with this setup. However diurnal courses and VOC emissions in enclosure experiments can be monitored with the instrument.

Bibliography

Apel E.C., Calvert J.G., Gilpin T.M., Fehsenfeld F.C., Parrish D.D., Lonneman W.A.; 1999; The Nonmethane Hydrocarbon Intercomparison Experiment (NOMHICE): Task 3; Journal of Geophysical Research-Atmospheres 104: 26069-26086

Atkinson R.; 2000; Atmospheric chemistry of VOCs and NOx; Atmospheric Environment 34: 2063-2101

Atkinson R., Arey J.; 2003; Atmospheric degradation of volatile organic compounds; Chemical Reviews 103: 4605-4638

Baker A.K., Schuck T.J., Slemr F., van Velthoven P., Zahn A., Brenninkmeijer C.A.M.; 2011; Characterization of non-methane hydrocarbons in Asian summer monsoon outflow observed by the CARIBIC aircraft; Atmospheric Chemistry and Physics 11: 503-518

Bartram S., Jux A., Glelxner G., Boland W.; 2006; Dynamic pathway allocation in early terpenoid biosynthesis of stress-induced lima bean leaves (vol 67, pg 1661, 2006); Phytochemistry 67: 2512-2512

Bertoni G., Tappa R.; 1997; Improvement in breakthrough volume evaluation methods for light adsorbent traps employed for volatile organic compounds determination at atmospheric concentration levels; Journal of Chromatography A 767: 153-161

Blake R.S., Monks P.S., Ellis A.M.; 2009; Proton-Transfer Reaction Mass Spectrometry; Chemical Reviews 109: 861-896

Blanchard C.L., Hidy G.M., Tanenbaum S., Edgerton E.S.; 2011; NMOC, ozone, and organic aerosol in the southeastern United States, 1999-2007: 3. Origins of organic aerosol in Atlanta, Georgia, and surrounding areas; Atmospheric Environment 45: 1291-1302

Boschetti A., Biasioli F., van Opbergen M., Warneke C., Jordan A., Holzinger R., Prazeller P., Karl T., Hansel A., Lindinger W., Iannotta S.; 1999; PTR-MS real time monitoring of the emission of volatile organic compounds during postharvest aging of berryfruit; Postharvest Biology and Technology 17: 143-151

Bracho Núnez A.; 2010; Leaf level VOC emissions of single plants from Amazonian and Mediterranean ecosystems; Ontogeny and flooding as stress factor for VOC emission; Johannes Gutenberg University, Mainz

Brancaleoni E., Scovaventi M., Frattoni M., Mabilia R., Ciccioli P.; 1999; Novel family of multi-layer cartridges filled with a new carbon adsorbent for the quantitative determination of volatile organic compounds in the atmosphere; Journal of Chromatography A 845: 317-328

Cataldo F., Ursini O., Lilla E., Angelini G.; 2010; Ozonolysis of alpha-Pinene, beta-Pinene, d- and l- Turpentine Oil Studied by Chirooptical Methods: Some Implications

on the Atmospheric Chemistry of Biogenic Volatile Organic Compounds; Ozone-Science & Engineering 32: 274-285

Choi E., Choi K., Yi S.M.; 2011; Non-methane hydrocarbons in the atmosphere of a Metropolitan City and a background site in South Korea: Sources and health risk potentials; Atmospheric Environment 45: 7563-7573

Chung M.Y., Maris C., Krischke U., Meller R., Paulson S.E.; 2003; An investigation of the relationship between total non-methane organic carbon and the sum of speciated hydrocarbons and carbonyls measured by standard GC/FID: measurements in the Los Angeles air basin; Atmospheric Environment 37: S159-S170

Chung M.Y., Beene M., Ashkan S., Krauter C., Hasson A.S.; 2010; Evaluation of non-enteric sources of non-methane volatile organic compound (NMVOC) emissions from dairies; Atmospheric Environment 44: 786-794

de Gouw J., Warneke C.; 2007; Measurements of volatile organic compounds in the earths atmosphere using proton-transfer-reaction mass spectrometry; Mass Spectrometry Reviews 26: 223-257

Dindorf T.; 2006; Measurement of nonmethane organic carbon - Quality assurance, instrument design and enclosure studies; Johannes Gutenberg University, Mainz

Dindorf T., Kuhn U., Ganzeveld L., Schebeske G., Ciccioli P., Holzke C., Koble R., Seufert G., Kesselmeier J.; 2006; Significant light and temperature dependent monoterpene emissions from European beech (Fagus sylvatica L.) and their potential impact on the European volatile organic compound budget; Journal of Geophysical Research-Atmospheres 111

Dudareva N., Negre F., Nagegowda D.A., Orlova I.; 2006; Plant volatiles: Recent advances and future perspectives; Critical Reviews in Plant Sciences 25: 417-440

Fehsenfeld F., Calvert J., Fall R., Goldan P., Guenther A.B., Hewitt C.N., Lamb B., Liu S., Trainer M.; 1992; Emissions of volatile organic compounds from vegetation and the implications for atmospheric chemistry; Global Biogeochemical Cycles 6: 389-430

Feussner I., Wasternack C.; 2002; The lipoxygenase pathway; Annual Review of Plant Biology 53: 275-297

Finlayson-Pitts B., Pitts J.N.; 2000; Chemistry of the Upper and Lower Atmosphere, Theory, Experiments and Applications; San Diego, San Francisco, New York, Boston, London, Sydney, Tokyo: Academic Press

Fowler D., Pilegaard K., Sutton M.A., Ambus P., Raivonen M., Duyzer J., Simpson D., Fagerli H., Fuzzi S., Schjoerring J.K., Granier C., Neftel A., Isaksenm I.S.A., Laj P., Maione M., Monks P.S., Burkhardt J., Daemmgen U., Neirynck J., Personne E., Wichink-Kruit R., Butterbach-Bahl K., Flechard C., Tuovinen J.P., Coyle M., Gerosa G., Loubet B., Altimir N., Gruenhage L., Ammann C., Cieslik S., Paoletti E., Mikkelsen T.N., Ro-Poulsen H., Cellier P., Cape J.N., Horváth L., Loreto F., Niinemets Ü., Palmer P.I., Rinne J., Misztal P., Nemitz E., Nilsson D., Pryor S.,

Gallagher M.W., Vesala T., Skiba U., Brüggemann N., Zechmeister-Boltenstern S., Williams J., O'Dowd C., Facchini M.C., de Leeuw G., Flossman A., Chaumerliac N., Erisman J.W.; 2009; Atmospheric composition change: Ecosystems-Atmosphere interactions; Atmospheric Environment 43: 5193-5267

Fung I, Field C.B., Berry J.A., Thompson M.V., Randerson J.T., Malmström C.M., Vitousek P.M., James Collatz G., Sellers P.J., Randall D.A., Denning A.S., Badeck F. John J.; 1997; Carbon 13 exchanges between the atmosphere and biosphere; Global Biogeochemical Cycles 11: 507-533

Ghirardo A., Koch K., Taipale R., Zimmer I., Schnitzler J.P., Rinne J.; 2010; Determination of de novo and pool emissions of terpenes from four common boreal/alpine trees by $^{13}CO_2$ labelling and PTR-MS analysis; Plant Cell and Environment 33: 781-792

Grote R., Niinemets U.; 2008; Modeling volatile isoprenoid emissions - a story with split ends; Plant Biology 10: 8-28

Guenther A., Karl T., Harley P., Wiedinmyer C., Palmer P.I., Geron C.; 2006; Estimates of global terrestrial isoprene emissions using MEGAN (Model of Emissions of Gases and Aerosols from Nature); Atmospheric Chemistry and Physics 6: 3181-3210

Guenther A., Hewitt C.N., Erickson D., Fall R., Geron C., Graedel T., Harley P., Klinger L., Lerdau M., McKay W.A., Pierce T., Scholes B., Steinbrecher R., T allamraju R., Taylor J., Zimmerman P.; 1995; A global model of natural volatile organic compound emissions; Journal of Geophysical Research-Atmospheres 100: 8873-8892

Hansel A., Jordan A., Holzinger R., Prazeller P., Vogel W., Lindinger W.; 1995; Proton-Transfer Reaction Mass-Spectrometry – Online trace gas-analysis at the ppb level; International Journal of Mass Spectrometry 149: 609-619

Heiden A.C., Hoffmann T., Kahl J., Kley D., Klockow D., Langebartels C., Mehlhorn H., Sandermann H., Schraudner M., Schuh G., Wildt J.; 1999; Emission of volatile organic compounds from ozone-exposed plants; Ecological Applications 9: 1160-1167

Hewitt C.N., Hayward S., Tani A.; 2003; The application of proton transfer reaction-mass spectrometry (PTR-MS) to the monitoring and analysis of volatile organic compounds in the atmosphere; Journal of Environmental Monitoring 5: 1-7

Hewitt C.N., Karl T., Langford B., Owen S.M., Possell M.; 2011; Quantification of VOC emission rates from the biosphere; Trends in Analytical Chemistry 30: 937-944

Holzinger R., Sandoval-Soto L., Rottenberger S., Crutzen P.J., Kesselmeier J.; 2000; Emissions of volatile organic compounds from Quercus ilex L. measured by Proton Transfer Reaction Mass Spectrometry under different environmental conditions; Journal of Geophysical Research-Atmospheres 105: 20573-20579

IPCC 2001; "Intergovernmental Panel on Climate Change, Contribution of Working Group I to the Third Assessment Report (Houghton J.T., Ding Y., Griggs D.J., Noguer

M., van der Linden P.J, Dai X., Maskell K., Johnson C.A.)." Climate Change 2001: The Scientific basis, Cambridge University Press, Cambridge

IPCC 2007; "Climate Change 2007 – the Physical Science Basis; Working Group I, Contribution to the Fourth Assessment Report of the IPCC, Intergovernmental Panel on Climate Change." Cambridge University Press, Cambridge
.
Jordan A., Hansel A., Holzinger R., Lindinger W.; 1995; Acetonitrile and benzene in the breath of smokers and non-smokers investigated by Proton-Transfer Reaction Mass-Spectrometry (PTR-MS); International Journal of Mass Spectrometry 148: L1-L3

Karl T., Prazeller P., Mayr D., Jordan A., Rieder J., Fall R., Lindinger W.; 2001; Human breath isoprene and its relation to blood cholesterol levels: new measurements and modelling; Journal of Applied Physiology 91: 762-770

Kesselmeier J., Staudt M.; 1999; Biogenic volatile organic compounds (VOC): An overview on emission, physiology and ecology; Journal of Atmospheric Chemistry 33: 23-88

Kesselmeier J., Schafer L., Ciccioli P., Brancaleoni E., Cecinato A., Frattoni M., Foster P., Jacob V., Denis J., Fugit J.L., Dutaur L., Torres L.; 1996; Emission of monoterpenes and isoprene from a Mediterranean oak species Quercus ilex L measured within the BEMA (Biogenic Emissions in the Mediterranean Area) project; Atmospheric Environment 30: 1841-1850

Kesselmeier J., Ciccioli P., Kuhn U., Stefani P., Biesenthal T., Rottenberger S., Wolf A., Vitullo M., Valentini R., Nobre A., Kabat P., Andreae M.O.; 2002; Volatile organic compound emissions in relation to plant carbon fixation and the terrestrial carbon budget; Global Biogeochemical Cycles Vol.16, No. 4, 1126

Kesselmeier J., Bode K., Schäfer L., Schebeske G., Wolf A., Brancaleoni E., Cecinato A., Ciccioli P., Frattoni M., Dutaur L., Fugit J.L., Simon V., Torres L.; 1998; Simultaneous field measurements of terpene and isoprene emissions from two dominant Mediterranean oak species in relation to a North American species; Atmospheric Environment 32: 1947-1953

Kesselmeier J, Bode K., Hofmann U., Muller H., Schafer L., Wolf A., Ciccioli P., Brancaleoni E., Cecinato A., Frattoni M., Foster P., Ferrari C., Jacob V., Fugit J.L., Dutaur L., Simon V., Torres L.; 1997; Emission of short chained organic acids, aldehydes and monoterpenes from Quercus ilex L. and Pinus pinea L. in relation to physiological activities, carbon budget and emission algorithms; Atmospheric Environment 31: 119-133

Kim L., Galbally I.E., Porter N., Weeks I.A., Lawson S.J.; 2011a; BVOC emissions from mechanical wounding of leaves and branches of Eucalyptus sideroxylon (red ironbark); Journal of Atmospheric Chemistry 68: 265-279

Kim S., Guenther A., Karl T., Greenberg J.; 2011b; Contributions of primary and secondary biogenic VOC tototal OH reactivity during the CABINEX (Community

Atmosphere-Biosphere INteractions Experiments)-09 field campaign; Atmospheric Chemistry and Physics 11: 8613-8623

Kimmerer T.W., Kozlowski T.T.; 1982; Ethylene, ethane, acetaldehyde, and ethanol-production by plants under stress; Plant Physiology 69: 840-847

Kirstine W., Galbally I., Ye Y.R., Hooper M.; 1998; Emissions of volatile organic compounds (primarily oxygenated species) from pasture; Journal of Geophysical Research-Atmospheres 103: 10605-10619

Komenda M., Kobel K., Koppmann R., Wildt J.; 2003; Comparability of biogenic VOC emission rate measurements under laboratory and ambient conditions at the example of monoterpene emissions from Scots pine (Pinus sylvestris); Journal of Atmospheric Chemistry 45: 1-23

Kreuzwieser J., Scheerer U., Rennenberg H.; 1999; Metabolic origin of acetaldehyde emitted by poplar (Populus tremula x P-alba) trees; Journal of Experimental Botany 50: 757-765

Kuhn U., Rottenberger S., Biesenthal T., Wolf A., Schebeske G., Ciccioli P., Brancaleoni E., Frattoni M., Tavares T.M., Kesselmeier J.; 2002; Isoprene and monoterpene emissions of Amazonian tree species during the wet season: Direct and indirect investigations on controlling environmental functions; Journal of Geophysical Research-Atmospheres 107, 8071

Lanz V.A., Henne S., Staehelin J., Hueglin C., Vollmer M.K., Steinbacher M., Buchmann B., Reimann S.; 2009; Statistical analysis of anthropogenic non-methane VOC variability at a European background location (Jungfraujoch, Switzerland); Atmospheric Chemistry and Physics 9: 3445-3459

Laothawornkitkul J., Taylor J.E., Paul N.D., Hewitt C.N.; 2009; Biogenic volatile organic compounds in the Earth system; New Phytologist 183: 27-51

Larsen B., Bomboi-Mingarro T., Brancaleoni E., Calogirou A., Cecinato A., Coeur C., Chatzinestis I., Duane M., Frattoni M., Fugit J.-L., Hansen U., Jacob V., Mimikos N., Hoffmann T., Owen S., Perez-Pastor R., Reichmann A., Seufert G., Staudt M., Steinbrecher R.; 1997; Sampling and analysis of terpenes in air. An interlaboratory comparison; Atmospheric Environment 31: 35-49

Lerdau M., Gray D.; 2003; Ecology and evolution of light-dependent and light-independent phytogenic volatile organic carbon; New Phytologist 157: 199-211

Lichtenthaler H.K.; 1999; The 1-deoxy-D-xylulose-5-phosphate pathway of isoprenoid biosynthesis in plants; Annual Review of Plant Physiology and Plant Molecular Biology 50: 47-65

Lindfors V., Laurila T.; 2000; Biogenic volatile organic compound (VOC) emissions from forests in Finland; Boreal Environment Research 5: 95–113

Lindinger W., Hansel A., Jordan A.; 1998; On-line monitoring of volatile organic compounds at pptv levels by means of proton-transfer-reaction mass spectrometry

(PTR-MS) - Medical applications, food control and environmental research; International Journal of Mass Spectrometry 173: 191-241

Malmstrom C.M., Thompson M.V., Juday G.P., Los S.O., Randerson J.T., Field C.B.; 1997; Interannual variation in global-scale net primary production: Testing model estimates; Global Biogeochemical Cycles 11: 367-392

Maris C., Chung M.Y., Lueb R., Krischke U., Meller R., Fox M.J., Paulson S.E.; 2003; Development of instrumentation for simultaneous analysis of total non-methane organic carbon and volatile organic compounds in ambient air; Atmospheric Environment 37: S149-S158

Matsui K.; 2006; Green leaf volatiles: hydroperoxide lyase pathway of oxylipin metabolism; Current Opinion in Plant Biology 9: 274-280

Monks P.S., Granier C., Fuzzi S., Stohl A., Williams M.L., Akimoto H., Amanni M., Baklanov A., Baltensperger U., Bey I., Blake N., Blake R.S., Carslawn K., Cooper O.R., Dentener F., Fowler D., Fragkou E., Frost G.J., Generoso S., Ginoux P., Grewet V., Guenther A., Hansson H.C., Hennew S., Hjorth J., Hofzumahaus A., Huntrieser H., Isaksen I.S.A., Jenkin M.E., Kaiser J., Kanakidou M., Klimont i Z., Kulmala M., Laj P., Lawrence M.G., Lee J.D., Liousse C., Maione M., McFiggans G., Metzger A., Mieville A., Moussiopoulos N., Orlando J.J., O'Dowdmm C.D., Palmer P.I., Parrish D.D., Petzold A., Platt U., Pöschl U., Prévôt A.S.H., Reeves C.E., Reimann S., Rudich Y., Sellegri K., Steinbrecher R., Simpson D., ten Brink H., Theloke J., van der Werf G.R., Vautard R., Vestreng V., Vlachokostas Ch., von Glasow R.; 2009; Atmospheric composition change - global and regional air quality; Atmospheric Environment 43: 5268-5350

Müller J.-F.; 1992; Geographical distribution and seasonal variation of surface emissions and deposition velocities of atmospheric trace gases; Journal of Geophysical Research 97: 3787-3804

Park C.; 2001; The Environment; London, New York: Routledge, Taylor and Francis Group

Penuelas J., Staudt M.; 2010; BVOCs and global change; Trends in Plant Science 15: 133-144

Qualley A.V., Dudareva N.; 2008; Aromatic volatiles and their involvement in plant defense; Induced Plant Resistance to Herbivory, Part B, 409-432

Randerson J.T., Thompson M.V., Field C.B.; 1999; Linking C-13-based estimates of land and ocean sinks with predictions of carbon storage from CO_2 fertilization of plant growth; Tellus Series B-Chemical and Physical Meteorology 51: 668-678

Rinne H.J.I., Guenther A.B., Greenberg J.P., Harley P.C.; 2002; Isoprene and monoterpene fluxes measured above Amazonian rainforest and their dependence on light and temperature; Atmospheric Environment 36: 2421-2426

Roberts J.M., Bertman S.B., Jobson T., Niki H., Tanner R.; 1998; Measurement of total nonmethane organic carbon (C_y): Development and application at Chebogue

Point, Nova Scotia, during the 1993 North Atlantic Regional Experiment campaign; Journal of Geophysical Research-Atmospheres 103: 13581-13592

Rottenberger S., Kleiss B., Kuhn U., Wolf A., Piedade M.T.F., Junk W., Kesselmeier J.; 2008. The effect of flooding on the exchange of the volatile C-2-compounds ethanol, acetaldehyde and acetic acid between leaves of Amazonian floodplain tree species and the atmosphere; Biogeosciences 5: 1085-1100

Schimel D.S.; 1995; Terrestrial ecosystems and the carbon-cycle; Global Change Biology 1: 77-91

Schimel D.S., House J.I., Hibbard K.A., Bousquet P., Ciais P., Peylin P., Braswell B.H., Apps M.J., Baker D., Bondeau A., Canadell J., Churkina G., Cramer W., Denning A.S., Field C.B., Friedlingstein P., Goodale C., Heimann M., Houghton R.A., Melillo J.M., Moore III B., Murdiyarso D., Noble I., Pacala S.W., Prentice I.C., Raupach M.R., Rayner P.J., Scholes R.J., Steffen W.L., Wirth C.; 2001; Recent patterns and mechanisms of carbon exchange by terrestrial ecosystems; Nature 414: 169-172

Schuh G., Heiden A.C., Hoffmann T., Kahl J., Rockel P., Rudolph J., Wildt J.; 1997; Emissions of volatile organic compounds from sunflower and beech: Dependence on temperature and light intensity; Journal of Atmospheric Chemistry 27: 291-318

Seco R., Penuelas J., Filella I.; 2007; Short-chain oxygenated VOCs: Emission and uptake by plants and atmospheric sources, sinks, and concentrations; Atmospheric Environment 41: 2477-2499

Seinfeld J.H., Pandis S.N.; 1997; Atmospheric chemistry and physics: From air pollution to climate change; New York: John Wiley & Sons

Sharkey T.D., Yeh S.S.; 2001; Isoprene emission from plants; Annual Review of Plant Physiology and Plant Molecular Biology 52: 407-436

Shreffler J.H.; 1993; Comparison of nonmethane organic compound concentration data collected by two methods in Atlanta; Air and Waste 43: 1576-1584

Sidiropoulos C., Tsilingiridis G.; 2007; Biogenic emissions during a hot season day in Greece; Fresenius Environmental Bulletin 16: 465-471

Simpraga M., Verbeeck H., Demarcke M., Joó É., Pokorska O., Amelynck C., Schoon N., Dewulf J., van Langenhove H., Heinesch B., Aubinet M., Laffineur Q., Müller J.F., Steppe K.; 2011; Clear link between drought stress, photosynthesis and biogenic volatile organic compounds in Fagus sylvatica L.; Atmospheric Environment 45: 5254-5259

von Schneidemesser E., Monks P.S., Gros V., Gauduin J., Sanchez O.; 2011; How important is biogenic isoprene in an urban environment? A study in London and Paris; Geophysical Research Letters 38

Warneke C., Kuczynski J., Hansel A., Jordan A., Vogel W., Lindinger W.; 1996; Proton transfer reaction mass spectrometry (PTR-MS): Propanol in human breath; International Journal of Mass Spectrometry 154: 61-70

Warneke C., Karl T., Judmaier H., Hansel A., Jordan A., Lindinger W., Crutzen P.J.; 1999; Acetone, methanol, and other partially oxidized volatile organic emissions from dead plant matter by abiological processes: Significance for atmospheric HOx chemistry; Global Biogeochemical Cycles 13: 9-17

Wildt J., Kley D., Rockel A., Rockel P., Segschneider H.J.; 1997; Emission of NO from several higher plant species; Journal of Geophysical Research-Atmospheres 102: 5919-5927

Wolff E.W.; 2011; Greenhouse gases in the Earth system: a palaeoclimate perspective; Philosophical Transactions of the Royal Society a-Mathematical Physical and Engineering Sciences 369: 2133-2147

Xiang L., Milc J.A., Pecchioni N., Chen L.Q.; 2007; Genetic aspects of floral fragrance in plants; Biochemistry-Moscow 72: 351-358

Yang S.F., Hoffman N.E.; 1984; Ethylene biosynthesis and its regulation in higher plants; Annual Review of Plant Physiology and Plant Molecular Biology 35: 155-189

Yung-Chen Y., Liu P.W.G., Yi-Chyun H., Tzi-Chin C., Jiun-Horng T.; 2009; Characterisation of non-methane organic compounds collected in an industrial urban area; International Journal of Environment and Pollution 39

Appendix

A List of Abbreviations

acetyl CoA	activated acetic acid bound to Coenzyme A
BTV	breakthrough volume
BVOC	biogenic volatile organic compound
CSTR	continuously stirred tank reactor
DMAPP	dimethylallyl diphosphate
DOXP	1-Deoxy-D-xylulose-5-phosphate
GAP	glyceraldehydes-3-phosphate
GC-FID	gas chromatography-flame ionisation detector
GC-MS	gas chromatography-mass spectrometry
IPP	isopentenyl pyrophosphate
IRGA	infrared gas analyzer
JPAC	Jülich plant atmosphere chamber
LOD	limit of detection
MeJA	methyl jasmonate
MEP	2-C-methyl-D-erythritol-4-phosphate
MeSA	methyl salicylate
NDIR	non-dispersive infrared
NMHC	non-methane hydrocarbon
NMOC	non-methane organic compound
NMVOC	non-methane volatile organic compound
NO_x	nitrogen oxides
PAR	photosynthetic active radiation
ppb	parts per billion
ppm	parts per million
PTR-MS	proton transfer reaction-mass spectrometry
sccm	standard cubic centimetre per minute
SOA	secondary organic aerosol
VOC	volatile organic compound

B List of Figures

C List of Tables

D Software Settings for the external controller device of the NMOC Analyzer

Configuration file:

```
program main;

uses system,pidreg,vsio;

type
  offontype     =  (off,on);
  switchtype    =  (error,logperiod,Pump,
                    FlushValve,BypassValve,CalValve,SampleValve,VOCValve,
                    MFCCalHe,MFCCalCO2,MFCCarHe,MFCSample,MFCO2, MFCRefHe,
MFCQ0,

HeaterVOC,HeaterCO2,BaseStart,BaseEnd,Integration,SelSampValve,
                                                          CO2Valve);

  ReadStruct    =  object(AllInstanceRec)
                     RunTime      : TimeInst;     {show=timerel;wr=0}
                     ProcVar      : SwitchType;   {wr=0}
                     SetState     : offontype;    {wr=0}
                     SetValue     : SingleInst;   {wr=0;Dec=2}
                   end;

  RFNStruct    =  object(AllInstanceRec)
                     RunTime      : TimeInst;     {show=timerel;wr=0}
                     SetCtrlFile  : StringInst;   {wr=0}
                   end;

  LicorStruct   =  object(AllInstanceRec)
                     CO2_ppm      : SingleInst; {Wr=1; Dec=3}
                     H2O_ppm      : SingleInst; {Wr=0; Dec=3}
                     TLicor       : SingleInst; {Wr=0; Dec=3}
                   end;

  ControlStruct =  object(AllInstanceRec)
                     Process      : BoolInst;
{range=off,manual,standby,auto}
                     proctest     : offontype;
                     Host         : BoolInst; {range=off,on}
                     logger       : BoolInst; {range=off,on}
                     BlowerCO2    : BoolInst; {range=off,on}
                     Pump         : BoolInst; {range=off,on}
                     Valv14       : LongInst; {show=hex}
                     SelSamp      : OffOnType;
                                                          SelCO2Vlv1
      : OffOnType;
                                                          SelCO2Vlv2
      : OffOnType;
                     ParamSave    : BoolInst; {range=______,saving,loading}
                     ParamFile    : FileInst;
                     CtrlFile     : FileInst;
                     RFNFile      : FileInst;
                     LogDir       : FileInst; {wr=0}
                     LogFile      : FileInst; {wr=0}
                     DataFile     : FileInst; {wr=0}
                     SpecFile     : FileInst; {wr=0}
                     ReadRec      : structinst;
                     RFNRec       : structinst;
                   end;
```

```
  MksDataStruct  =  object(AllInstanceRec)
                      DateTime   : TimeInst;      {show=timesys}
                      MFC0       : SingleInst;    {wr=0;dec=1}
                      MFC1       : SingleInst;    {wr=0;dec=1}
                      MFC2       : SingleInst;    {wr=0;dec=1}
                      MFC3       : SingleInst;    {wr=0;dec=1}
                      MFC4       : SingleInst;    {wr=0;dec=1}
                      MFC5       : SingleInst;    {wr=0;dec=1}
                      TempBox    : SingleInst;    {wr=0;dec=1}
                      SetTempBox : SingleInst;    {dec=1}
                      BoxPower   : LongInst;      {wr=0}
                    end;

  DataStruct    =  object(AllInstanceRec)
                      TimeDate     : TimeInst;   {show=timesys}
                      CO2Licor     : SingleInst; {Wr=0; Dec=3}
                      H2OLicor     : SingleInst; {Wr=0; Dec=3}
                      TLicor       : SingleInst; {Wr=0; Dec=2}
                      TVOCTrap     : SingleInst; {Wr=0; Dec=1}
                      TCO2Trap     : SingleInst; {Wr=0; Dec=1}
                      FCalHe       : SingleInst; {Wr=0; Dec=1}
                      FCalCO2      : SingleInst; {Wr=0; Dec=1}
                      FCarHe       : SingleInst; {Wr=0; Dec=1}
                      FSmpl        : SingleInst; {Wr=0; Dec=1}
                      FO2          : SingleInst; {Wr=0; Dec=1}
                      FName1       : SingleInst; {Wr=0; Dec=1}
                      FName2       : SingleInst; {Wr=0; Dec=1}
                      FRefHe      : SingleInst; {Wr=0; Dec=1}
                      TempRef      : SingleInst; {Wr=0; Dec=2}
                      FlushValv    : BoolInst;   {range=off,on}
                      BypasValv    : BoolInst;   {range=off,on}
                      CalValv      : OffOnType;
                      SmplValv     : BoolInst;   {range=off,on}
                      VOCValv      : BoolInst;   {range=off,on}
                      MFC0       : SingleInst;    {wr=0;dec=1}
                      MFC1       : SingleInst;    {wr=0;dec=1}
                      MFC2       : SingleInst;    {wr=0;dec=1}
                      MFC3       : SingleInst;    {wr=0;dec=1}
                      MFC4       : SingleInst;    {wr=0;dec=1}
                      MFC5       : SingleInst;    {wr=0;dec=1}
                      TempBox    : SingleInst;    {wr=0;dec=1}
                      TTubeHeat  : SingleInst;    {wr=0;dec=1}
                      TTubeExt   : SingleInst;    {wr=0;dec=1}
                      TOven       : SingleInst;    {wr=0;dec=1}
                                                              SampValve
      : OffOnType;
                      CO2Valv    : OffOnType;
                    end;

   FastDataStruct = object(AllInstanceRec)
                      TimeDate     : TimeInst;   {show=timesys;
show=timemil}
                      CO2Licor     : SingleInst; {Wr=0; Dec=3}
                      H2OLicor     : SingleInst; {Wr=0; Dec=3}
                      TLicor       : SingleInst; {Wr=0; Dec=2}
                      TVOCTrap     : SingleInst; {Wr=0; Dec=1}
                      TCO2Trap     : SingleInst; {Wr=0; Dec=1}
                    end;

   SpecDataStruct = object(AllInstanceRec)
                      StartTime    : TimeInst;   {show=mil}
                      EndTime      : TimeInst;   {show=mil}
                      Duration     : TimeInst;   {show=timerel}
```

```
                    RFNFile      : StringInst; {wr=0}
                    CtrlFile     : StringInst; {wr=0}
                    Value        : SingleInst; {Wr=0; Dec=3}
                    BaseStart    : SingleInst; {Wr=0; Dec=3}
                    BaseStartT   : TimeInst;   {show=timemil}
                    BaseEnd      : SingleInst; {Wr=0; Dec=3}
                    BaseEndT     : TimeInst;   {show=timemil}
                    IntStartT    : TimeInst;   {show=timemil}
                    IntEndT      : TimeInst;   {show=timemil}
                    Datapoints   : LongInst;   {wr=0}
                  end;

FlowSubStruct = object(AllInstanceRec)
                    Flow         : SingleInst;  {wr=0;dec=1}
                    FlowSet      : SingleInst;  {dec=1; param=1}
                    FlowSize     : SingleInst;  {dec=1; param=1}
                    FlowOffs     : SingleInst;  {dec=4; param=1}
                    FlowGain     : SingleInst;  {dec=4; wr=1; param=1}
                  end;

TempSubStruct = object(AllInstanceRec)
                    Temp         : SingleInst;  {wr=0;dec=1}
                    TempOffs     : SingleInst;  {dec=4; param=1}
                    TempGain     : SingleInst;  {dec=4; param=1}
                  end;

MKSLocStruct   =  object(AllInstanceRec)
                     FCalHe       : FlowSubStruct; {param=1}
                     FCalCO2      : FlowSubStruct; {param=1}
                     FCarHe       : FlowSubStruct; {param=1}
                     FSmpl        : FlowSubStruct; {param=1}
                     FO2          : FlowSubStruct; {param=1}
                     FName1       : FlowSubStruct; {param=1}
                     FName2       : FlowSubStruct; {param=1}
                     FRefHe       : FlowSubStruct; {param=1}
                  end;

RemoteStruct =  object(AllInstanceRec)
                    Command      : StringInst;
                    num             : LongInst;
                    Value        : SingleInst;
                  end;

MKSCalibStruct   =  object(AllInstanceRec)
                      SetMFC0       : SingleInst;    {dec=1}
                      SetMFC1       : SingleInst;    {dec=1}
                      SetMFC2       : SingleInst;    {dec=1}
                      SetMFC3       : SingleInst;    {dec=1}
                      SetMFC4       : SingleInst;    {dec=1}
                      SetMFC5       : SingleInst;    {dec=1}
                      Remote        : RemoteStruct;
                  end;


ParamStruct   =  object(AllInstanceRec)
                    AutoStart    : BoolInst;   {range=off,on; param=1}
                    SetVOCTrap   : SingleInst; {Dec=1; Max=350; param=1}
                    SetCO2Trap   : SingleInst; {Dec=1; Max=250; param=1}
                    SetTLicor    : SingleInst; {Dec=1; Max=250; param=1}
                    SetTTubeHeat : SingleInst; {Dec=1; Max=250; param=1}
                    SetMksLoc    : MKSLocStruct;
                    SetMksCalib  : MKSCalibStruct;
                    SetFCar      : SingleInst; {dec=1; param=1}
```

```
                    SetO2P       : SingleInst; {dec=1;min=0;max=100;
param=1}
                    TVOCTrap     : TempSubStruct; {param=1}
                    TCO2Trap     : TempSubStruct; {param=1}
                    TOven          : TempSubStruct; {param=1}
                    FiltTemp     : SingleInst; {param=1}
                    LogPeriod    : LongInst;   {min=1; param=1}
                    RegVOCTrap   : StructInst; {param=1}
                    RegCO2Trap   : StructInst; {param=1}
                    RegTLicor    : StructInst; {param=1}
                    RegTTubeHeat : StructInst; {param=1}
                    Com2         : SIO;
                    Com3         : SIO;
                    File3        : FileInst,
                    IntegOffs    : SingleInst; {dec=3; param=1}
                    IntegSpan    : SingleInst; {dec=3; param=1}
                  end;

  UserStructP   =  ^UserStruct;
  UserStruct    =  object(AllInstanceRec)
                    Data      : StructInst;
                    FastData  : StructInst;
                    SpecData  : StructInst;
                    Param     : StructInst;
                    Control   : StructInst;
                    LicorData : LicorStruct;
                    MksCalib  : StructInst;
                  end;

  Workstruct    = object(AllInstanceRec)
                    WTempOven      : LongInst;
                    WTempOvenI     : LongInst;
                    WTVOCTrap      : LongInst;
                    WTVOCTrapI     : LongInst;
                    WTempRef       : LongInst;
                    WTempRefI      : LongInst;
                    WTube       : LongInst;
                    WTubeI      : LongInst;
                    DiodeTabl      : ArrayInst;   {Typ=Integer; NData=50}
                    ThermistTabl   : ArrayInst;   {Typ=Integer; NData=200}
                    ThermCoupTemp  : ArrayInst;   {Typ=Integer; NData=180}
                    IntegRunning   : BoolInst;    {range=off,on}
                    DataFileOpen   : offontype;
                    SpecFileOpen   : offontype;
                    LogFileOpen    : offontype;
                    Integration    : offontype;
                    Baseline       : offontype;
                  end;

const

  TamaraNum      =  2150745;

  TVOCTrapAddr   =  $A480;
      TOvenAddr              =  $A482;
  TempRefAddr    =  $A486;
  TCO2TrapAddr   =  $A488;
  TTubeHeatAddr  =  $A48D;
  TTubeExtAddr   =  $A48E;

  FCalHeAddr     =  $A4A0;
  FCalCO2Addr    =  $A4A2;
  FCarHeAddr     =  $A4A4;
```

```
  FSmplAddr      =  $A4A6;

  FO2Addr        =  $A4C0;
  FName1Addr     =  $A4C2;
  FName2Addr     =  $A4C4;
  FRefHeAddr     =  $A4C6;

  DACTimBasAddr  =  $A404;

  SetFCalHeAddr  =  $A440;
  SetFCalCO2Addr =  $A442;
  SetFCarHeAddr  =  $A444;
  SetFSmplAddr   =  $A446;

  SetFO2Addr     =  $A448;
  SetFName1Addr  =  $A44A;
  SetFName2Addr  =  $A44C;
  SetFRefHeAddr  =  $A44E;

  HeatCO2Addr    =  $A410;
  HeatVOCAddr    =  $A412;
  TubeHeatAddr   =  $A414;

  SelSampAddr    =  $A460;
  SelSampVoltHigh  =  24;
  SelSampVoltLow   =  18;

  CO2Valv1Addr    =  $A462;
  CO2Valv2Addr    =  $A464;

  BlowLicAddr    =  $A46C;
  PumpAddr       =  $A46E;

  Valv14PowAddr  =  $A478;
  Valv14OutAddr  =  $A408;

  FlushValvMask  = $0001;
  BypasValvMask  = $0018;
  VOCValvMask    = $0006;
  CalValvMask    = $0080;
  SmplValvMask   = $0200;
  BlowerCO2Mask  = $0020;

  Mux0          =  $0;
  Mux1          =  $1;
  Mux2          =  $2;
  Mux3          =  $3;
  Mux4          =  $4;
  Mux5          =  $5;
  Mux6          =  $6;
  Mux7          =  $7;
  BridgeEn      =  $8;
  Gain1         =  $0;
  Gain10        =  $10;
  Gain100       =  $20;
  Gain1000      =  $30;
  Offs0         =  $0;
  Offs1         =  $40;
  Offs2         =  $80;
  Offs3         =  $C0;

  work     :  workstruct = (ThermistTabl :
```

```
    ( 11132 -5000 11119 -4800 11104 -4600 11087 -4400 11068 -4200 11047 -
4000 11023 -3800 10996 -3600 10967 -3400
      10933 -3200 10896 -3000 10856 -2800 10811 -2600 10762 -2400 10709 -
2200 10651 -2000 10588 -1800 10521 -1600
      10448 -1400 10371 -1200 10289 -1000 10202 -800  10111 -600  10016 -
400  9916  -200  9813  0     9707  200
      9598  400    9486 600    9373 800   9259  1000   9144 1200  9028
1400  8913  1600  8799  1800  8686  2000
      8575  2200   8466 2400   8359 2600  8255  2800   8155 3000  8057
3200  7963  3400  7873  3600  7786  3800
      7703  4000   7623 4200   7548 4400  7476  4600   7407 4800  7343
5000  7281  5200  7223  5400  7168  5600
      7116  5800   7068 6000   7022 6200  6978  6400   6937 6600  6899
6800  6863  7000  6829  7200  6797  7400
      6767  7600   6739 7800   6712 8000  6687  8200   6664 8400  6642
8600  6621  8800  6602  9000
    );
  );

  UserData :  UserStruct = (Data : DataStruct;
                            FastData : FastDataStruct;
                            SpecData : SpecDataStruct;
                            Param : ParamStruct =
                             (SetMksLoc    : MKSLocStruct =
                               (FCalHe       : FlowSubStruct =
                                 (FlowSize :  73;
                                  FlowGain : 1.0;
                                  FlowOffs : 0.0);
                                FCalCO2      : FlowSubStruct =
                                 (FlowSize :  10;
                                  FlowGain : 1.0;
                                  FlowOffs : 0.0);
                                FCarHe       : FlowSubStruct =
                                 (FlowSize :  725;
                                  FlowGain : 1.0;
                                  FlowOffs : 0.0);
                                FSmpl        : FlowSubStruct =
                                 (FlowSize :  500;
                                  FlowGain : 1.0;
                                  FlowOffs : 0.0);
                                FO2          : FlowSubStruct =
                                 (FlowSize :  50;
                                  FlowGain : 1.0;
                                  FlowOffs : 0.0);
                                FName1       : FlowSubStruct =
                                 (FlowSize :  100;
                                  FlowGain : 1.0;
                                  FlowOffs : 0.0);
                                FName2       : FlowSubStruct =
                                 (FlowSize :  100;
                                  FlowGain : 1.0;
                                  FlowOffs : 0.0);
                                FRefHe       : FlowSubStruct =
                                 (FlowSize :  100
                                  FlowGain : 1.0;
                                  FlowOffs : 0.0);
                               );
                              SetMksCalib  : MKSCalibStruct =
                               (Remote     : RemoteStruct;
                               );

                              TVOCTrap     : TempSubStruct =
                               (TempOffs     : 0.0;
```

```
                                TempGain     : 1.0);
                              TCO2Trap     : TempSubStruct =
                               (TempOffs     : 0.0;
                                TempGain     : 1.0);
                              FiltTemp    : 10.0;

                              RegVOCTrap : PID =
                               (PropBand : 200;
                                IntTime  : 5000;
                                DiffTime : 1000;
                                SamplePeriod : 500;
                                OutMax       : 255;
                                OutMin       : 0);
                              RegCO2Trap : PID =
                               (PropBand : 200;
                                IntTime  : 15000;
                                DiffTime : 5000;
                                SamplePeriod : 500;
                                OutMax       : 255);
                              RegTLicor : PID =
                               (PropBand : 200;
                                IntTime  : 120000;
                                DiffTime : 5000;
                                SamplePeriod : 500;
                                OutMax       : 3500);
                              RegTTUbeHeat : PID =
                               (PropBand : 200;
                                IntTime  : 120000;
                                DiffTime : 5000;
                                SamplePeriod : 500;
                                OutMax    : 255;
                                OutMin    : 0);
                              COM2            : SIO = (
                                PortAddr : 0; Baud     : 9600;
                                Bits     : 8; StopBits : 1;
                                Parity   : none;
                                Handshake : NoHandShake;
                                Protocol : MultiFile);
                              COM3            : SIO = (
                                PortAddr : $640; Baud     : 9600;
                                Bits     : 8; StopBits : 1;
                                Parity   : none;
                                Handshake : NoHandShake;
                                Protocol : MultiFile);
                              IntegSpan : 1;
                              IntegOffs : 0;
                            );
                            Control : ControlStruct =
                              (ParamFile  : 'mc:\tvoce.ini';
                               CtrlFile   : 'mc:\dummy.txt';
                               RFNFile    : 'mc:\method.txt';
                               ReadRec    : ReadStruct;
                               RFNRec     : RFNStruct);
                            LicorData : LicorStruct;
                            MksCalib  : MksDataStruct;
                            );

procedure Clock;
var Hour : Longinst; loctime : TimeInst;
begin
  with Userdata,Data,Control do begin
    loctime := Now;
    while 0 = 0 do begin
```

```
      loctime := loctime + 500;
      waitfor(loctime);
      TimeDate := loctime;
    end;
  end;
end;

procedure RemoteInOut;
var LocTimer : TimeInst;

begin
  with UserData, Control, Param, SetMksCalib, Remote  do begin

    File3 := 'Com3';
    if Open(File3,ReadMode or WriteMode) <> 0 then File3 := '---';
    SetDelimiter(File3,$000D);

    On SetMFC0 do begin
      Command := 'FS'; Num := 0; Value := SetMFC0;
      WriteRecord (File3, Remote, 32);
    end;
    On SetMFC1 do begin
      Command := 'FS'; Num := 1; Value := SetMFC1;
      WriteRecord (File3, Remote, 32);
    end;
    On SetMFC2 do begin
      Command := 'FS'; Num := 2; Value := SetMFC2;
      WriteRecord (File3, Remote, 32);
    end;
    On SetMFC3 do begin
      Command := 'FS'; Num := 3; Value := SetMFC3;
      WriteRecord (File3, Remote, 32);
    end;
    On SetMFC4 do begin
      Command := 'FS'; Num := 4; Value := SetMFC4;
      WriteRecord (File3, Remote, 32);
    end;
    On SetMFC5 do begin
      Command := 'FS'; Num := 5; Value := SetMFC5;
      WriteRecord (File3, Remote, 32);
    end;

    On LocTimer do begin
      StartTimer (LocTimer,1000,fromTime);
      WriteLn (File3, 'D');
      while ReadRecord (File3,MksCalib,100) = 0 do begin
        Data.MFC0       := MksCalib.MFC0;
        Data.MFC1       := MksCalib.MFC1;
        Data.MFC2       := MksCalib.MFC2;
        Data.MFC3       := MksCalib.MFC3;
        Data.MFC4       := MksCalib.MFC4;
        Data.MFC5       := MksCalib.MFC5;
        Data.TempBox    := MksCalib.TempBox;
      end;
    end;

    LocTimer := now;
    while 0 = 0 do HandleEvents(1);

  end;
end;

procedure ReceiveLicor;
```

```
var LicorFile  : FileInst;
begin
  with UserData,LicorData,work,Control,Param do begin
    LicorFile := 'Com2';
    Open(LicorFile,ReadMode or WriteMode);
    SetDelimiter(LicorFile,$0D0A);
    while 0 = 0 do begin
      if ReadRecord(LicorFile,LicorData,1500) = 0 then begin
        Data.TimeDate := now;
        Data.CO2Licor := CO2_ppm;
        Data.H2OLicor := H2O_ppm;
        Data.TLicor   := TLicor;

        FastData.TimeDate := Data.TimeDate;
        FastData.CO2Licor := CO2_ppm;
        FastData.H2OLicor := H2O_ppm;
        FastData.TLicor   := TLicor;
        FastData.TVOCTrap := Data.TVOCTrap;
        FastData.TCO2Trap := Data.TCO2Trap;
        if (Integration = on) then with Specdata do begin
          Value := Value + (CO2_ppm-IntegOffs) * IntegSpan;
          Datapoints := Datapoints + 1;
        end;
        if (SpecFileOpen = on) then WriteRecord(SpecFile,FastData,9);
      end;
    end;
  end;
end;

procedure FlowCalib (var FlowCtrl : FlowSubStruct; SetAddr : LongInst);
var  dummy : SingleInst;
begin
  with Userdata, Control, FlowCtrl do begin
    If Process <> manual then begin
                  if (1 = 0) then begin
            dummy := FlowSize * 0.996;
            if FlowSet > dummy then FlowSet := dummy;
            if FlowSet < -FlowOffs then FlowSet := -FlowOffs;
            FlowGain := FlowSize / (FlowSize + FlowOffs);
                        WriteWord(SetAddr, round ((FlowSet + FlowOffs) *
FlowGain / FlowSize * 256));
                  end;
                  WriteWord(SetAddr, round (FlowSet / FlowSize * 255));
    end;
  end;
end;

procedure HandleMulIO;
var LocTime : TimeInst;
begin
  with Userdata,Control,Param,SetMksLoc,Data,work do begin

    On SetFCar do with Param.SetMksLoc.FCarHe do begin
      if SetFCar > FlowSize then SetFCar := FlowSize;
      if SetFCar < 0 then SetFCar := 0;
      FlowSet := SetFCar * (100 - SetO2P) * 0.01;
      Param.SetMksLoc.FO2.FlowSet := SetFCar * SetO2P * 0.01;
    end;

    On SetO2P do begin
      Param.SetMksLoc.FCarHe.FlowSet  := SetFCar * (100 - SetO2P) * 0.01;
      Param.SetMksLoc.FO2.FlowSet     := SetFCar * SetO2P * 0.01;
    end;
```

```
    On Param.SetMksLoc.FCalHe.FlowSet   do FlowCalib
(Param.SetMksLoc.FCalHe, SetFCalHeAddr);
    On Param.SetMksLoc.FCalCO2.FlowSet  do FlowCalib
(Param.SetMksLoc.FCalCO2,SetFCalCO2Addr);
    On Param.SetMksLoc.FCarHe.FlowSet   do FlowCalib
(Param.SetMksLoc.FCarHe, SetFCarHeAddr);
    On Param.SetMksLoc.FSmpl.FlowSet    do FlowCalib
(Param.SetMksLoc.FSmpl,  SetFSmplAddr);
    On Param.SetMksLoc.FO2.FlowSet      do FlowCalib (Param.SetMksLoc.FO2,
SetFO2Addr);
    On Param.SetMksLoc.FName1.FlowSet   do FlowCalib
(Param.SetMksLoc.FName1, SetFName1Addr);
    On Param.SetMksLoc.FName2.FlowSet   do FlowCalib
(Param.SetMksLoc.FName2, SetFName2Addr);
    On Param.SetMksLoc.FRefHe.FlowSet   do FlowCalib
(Param.SetMksLoc.FRefHe, SetFRefHeAddr);


    WriteWord (TVOCTrapAddr + $10 ,Mux0 + Gain100);
    WriteWord (TOvenAddr + $10 ,Mux1 + Gain10);
    WriteWord (TCO2TrapAddr + $10 ,Mux4 + Gain100);
    WriteWord (TempRefAddr  + $10 ,Mux3 + Gain1);
    WriteWord (TTubeHeatAddr+ $10 ,Mux6 + Gain1);
    WriteWord (TTubeExtAddr + $10 ,Mux7 + Gain1);
            if (0=1) then begin
          WriteWord (FCalHeAddr  + $10 ,Mux0 shl 8);
          WriteWord (FCalCO2Addr + $10 ,Mux1 shl 8);
          WriteWord (FCarHeAddr  + $10 ,Mux2 shl 8);
          WriteWord (FSmplAddr   + $10 ,Mux3 shl 8);
          WriteWord (FName1Addr  + $10 ,Mux5 shl 8);
          WriteWord (FName2Addr  + $10 ,Mux6 shl 8);
          WriteWord (FRefHeAddr  + $10 ,Mux7 shl 8);
            end;
            WriteWord (FCalHeAddr  + $10 ,Mux0);
            WriteWord (FCalCO2Addr + $10 ,Mux1);
            WriteWord (FCarHeAddr  + $10 ,Mux2);
            WriteWord (FSmplAddr   + $10 ,Mux3);

            WriteWord (FO2Addr       + $10 ,Mux0);
            WriteWord (FName1Addr  + $10 ,Mux1);
            WriteWord (FName2Addr  + $10 ,Mux2);
            WriteWord (FRefHeAddr  + $10 ,Mux3);
    LocTime := now + 2000;
    while now < LocTime do HandleEvents(0);
    InterPol(Readword(TempRefAddr),ThermistTabl,WTempRef,WTempRefI);
    TempRef := WTempRef / 100;
    with Param.TVOCTrap do Data.TVOCTrap := (Readword(TVOCTrapAddr) -
10000) * TempGain + TempRef + TempOffs;
    with Param.TCO2Trap do Data.TCO2Trap := (Readword(TCO2TrapAddr) -
10000) * TempGain + TempRef + TempOffs;

    while 0 = 0 do begin

      InterPol(Readword(TempRefAddr),ThermistTabl,WTempRef,WTempRefI);
      if WTempRef < -5000 then
       TempRef := 9999.00
      else TempRef := WTempRef / 100;

      InterPol(Readword(TTubeHeatAddr),ThermistTabl,WTube,WTubeI);
      if WTube < -5000 then
        TTubeHeat := 9999.00
      else TTubeHeat := WTube / 100;
```

```
      InterPol(Readword(TTubeExtAddr),ThermistTabl,WTube,WTubeI);
      if WTube < -5000 then
        TTubeExt := 9999.00
      else TTubeExt := WTube / 100;

      with Param.TVOCTrap do begin
        if ((TempRef = 9999.00) or ((Readword(TVOCTrapAddr) < 9700) or
(Readword(TVOCTrapAddr) > 12000)))
        then begin
          Temp := 9999.00;
          Data.TVOCTrap:= Temp;
        end else begin
          Temp := (Readword(TVOCTrapAddr) - 10000) * TempGain + TempRef +
TempOffs;
          if (Temp < (Data.TVOCTrap + FiltTemp)) and (Temp > (Data.TVOCTrap
- FiltTemp)) then
            Data.TVOCTrap:= Temp;
        end;
      end;

      with Param.TOven do begin
        if ((TempRef = 9999.00) or ((Readword(TOvenAddr) < 9700)))
        then begin
          Temp := 9999.00;
          Data.TOven:= Temp;
        end else begin
          Temp := (Readword(TOvenAddr) - 10000) * TempGain + TempRef +
TempOffs;
          Data.TOven:= Temp;
        end;
      end;

      with Param.TCO2Trap do begin
        if ((TempRef = 9999.00) or ((Readword(TCO2TrapAddr) < 9700) or
(Readword(TCO2TrapAddr) > 12000)))
        then begin
          Temp := 9999.00;
          Data.TCO2Trap:= Temp;
        end else begin
          Temp := (Readword(TCO2TrapAddr) - 10000) * TempGain + TempRef +
TempOffs;
          if (Temp < (Data.TCO2Trap + FiltTemp)) and (Temp > (Data.TCO2Trap
- FiltTemp)) then
            Data.TCO2Trap:= Temp;
        end;
      end;

      LocTime := LocTime + 200;
      while now < LocTime do HandleEvents(0);

      with Param.SetMksLoc.FCalHe do begin
        if (1=0) then Flow := (((ReadWord (FCalHeAddr) - 10000) / 1495) *
FlowSize) / FlowGain - FlowOffs;
                      Flow := (((Readword(FCalHeAddr) - 10000) / 1500) *
FlowGain * FlowSize) + FlowOffs;
        Data.FCalHe := Flow;
      end;

      with Param.SetMksLoc.FCalCO2 do begin
        if (1=0) then Flow := (((ReadWord (FCalCO2Addr) - 10000) / 1495) *
FlowSize) / FlowGain - FlowOffs;
```

```
                        Flow := (((Readword(FCalCO2Addr) - 10000) / 1500) *
FlowGain * FlowSize) + FlowOffs;
        Data.FCalCO2 := Flow;
      end;

      with Param.SetMksLoc.FCarHe do begin
        if (1=0) then Flow := (((ReadWord (FCarHeAddr) - 10000) / 1495) *
FlowSize) / FlowGain - FlowOffs;
                        Flow := (((Readword(FCarHeAddr) - 10000) / 1500) *
FlowGain * FlowSize) + FlowOffs;
        Data.FCarHe := Flow;
      end;

      with Param.SetMksLoc.FSmpl do begin
        if (1=0) then Flow := (((ReadWord (FSmplAddr) - 10000) / 1495) *
FlowSize) / FlowGain - FlowOffs;
                        Flow := (((Readword(FSmplAddr) - 10000) / 1500) *
FlowGain * FlowSize) + FlowOffs;
        Data.FSmpl := Flow;
      end;

      with Param.SetMksLoc.FO2 do begin
        if (1=0) then Flow := (((ReadWord (FO2Addr) - 10000) / 1495) *
FlowSize) / FlowGain - FlowOffs;
                        Flow := (((Readword(FO2Addr) - 10000) / 1500) *
FlowGain * FlowSize) + FlowOffs;
        Data.FO2 := Flow;
      end;

      with Param.SetMksLoc.FName1 do begin
        if (1=0) then Flow := (((ReadWord (FName1Addr) - 10000) / 1495) *
FlowSize) / FlowGain - FlowOffs;
                        Flow := (((Readword(FName1Addr) - 10000) / 1500) *
FlowGain * FlowSize) + FlowOffs;
        Data.FName1 := Flow;
      end;

      with Param.SetMksLoc.FName2 do begin
        if (1=0) then Flow := (((ReadWord (FName2Addr) - 10000) / 1495) *
FlowSize) / FlowGain - FlowOffs;
                        Flow := (((Readword(FName2Addr) - 10000) / 1500) *
FlowGain * FlowSize) + FlowOffs;
        Data.FName2 := Flow;
      end;

      with Param.SetMksLoc.FRefHe do begin
        if (1=0) then Flow := (((ReadWord (FRefHeAddr) - 10000) / 1495) *
FlowSize) / FlowGain - FlowOffs;
                        Flow := (((Readword(FRefHeAddr) - 10000) / 1500) *
FlowGain * FlowSize) + FlowOffs;
        Data.FRefHe := Flow;
      end;

      WriteWord(DACTimBasAddr,255);

      LocTime := LocTime + 200;
      while now < LocTime do HandleEvents(0);
    end;
  end;
end;

procedure LogProc;
var LocTime : TimeInst; Day : LongInst;
```

```
begin
  with Userdata,Control,Param,Work do begin
    while 0 = 0 do begin
      while (logger = off) do waitfor(logger);

      LocTime := now;
      If logPeriod < 1 then logperiod := 1;

      LogDir := 'mc:\' + JulianDate(BinDate(LocTime),'_');
      MkDir(LogDir);

      LogFile := LogDir + '\' + JulianTime(BinTime(LocTime,0),'_',0) +
'.log';
      Open(LogFile,WriteMode);
      Writeln(LogFile,'.dataset');
      Writeln(LogFile,'.data');
      WriteHeader(LogFile,Data,9);
      LogFileOpen := on;

      DataFile := LogDir + '\' + JulianTime(BinTime(LocTime,0),'_',0) +
'.dat';
      Open(DataFile,WriteMode);
      WriteHeader(DataFile,SpecData,9);
      DataFileOpen := on;

      Day := BinDate(LocTime);
      while logger = on do begin
        If BinDate(now) <> Day then break;
        WriteRecord(LogFile,Data,9);
        LocTime := LocTime + (LogPeriod * 1000);
        waitfor(LocTime);
      end;

      LogFileOpen := off;
      Close(LogFile);

      DataFileOpen := off;
      Close(DataFile);
      end;
  end;
end;

procedure ProcessProc;
var LocTime : TimeInst; StartCTRLTime : TimeInst; EndTime : TimeInst;
    StartRFNTime : TimeInst; EndRFNTime : TimeInst; sdummy1: SingleInst;
sdummy2 : SingleInst;
           long1 : LongInst; long2 : LongInst;
begin
  with UserData,Control,Data,Param,SetMksLoc,ReadRec do begin
    while 0 = 0 do begin
      logger  := off;
      pump    := off;
      FCalHe.FlowSet  := 0;
      FCalCO2.FlowSet := 0;
      FCarHe.FlowSet := 50;
      FSmpl.FlowSet  := 0;
      FRefHe.FlowSet := 50;
      FlushValv := off;
      CalValv   := off;
      SmplValv  := off;
      BypasValv := off;
      VOCValv   := off;
      SetVocTrap := 30;
```

```
      SetCO2Trap := 20;
      SelSamp := off;
                  SelCO2Vlv1 := off;
                  SelCO2Vlv2 := off;

      while process <> auto do waitfor(process);

      logger := on;
      pump := on;

      Loctime := now + 1000;
      waitfor(LocTime);

      SpecData.RFNFile := RFNFile;

      while process = auto do begin
        LocTime := now;
        StartRFNTime := LocTime;
        Open(RFNFile,ReadMode);
        while ReadRecord(RFNFile,RFNRec,200) = 0 do begin
          FCalHe.FlowSet  := 0;
          FCalCO2.FlowSet := 0;
          FCarHe.FlowSet := 50;
          FSmpl.FlowSet  := 25;
          FRefHe.FlowSet := 50;
          FlushValv := on;
          CalValv   := off;
          SmplValv  := off;
          BypasValv := off;
          VOCValv   := off;
          SetVocTrap := 30;
          SetCO2Trap := 20;
                               CO2Valv := off;
          EndRFNTime := StartRFNTime + RFNRec.RunTime;
          If EndRFNTIme < Loctime then EndRFNTime := LocTime;
          If proctest = on then begin
            If EndRFNTime > LocTime + 5000 then EndRFNTime := LocTime +
5000;
          end;
          while LocTime < EndRFNTime do begin
            LocTime := LocTime + 1000;
            waitfor(LocTime);
            RFNRec.RunTime := EndRFNTime - LocTime;
            If process <> auto then break;
          end;
          If process <> auto then break;
          if RFNRec.SetCTRLfile <> 'loop' then begin
            StartCTRLTime := LocTime;

            SpecData.StartTime := LocTime;
            SpecData.EndTime := 0;
            SpecData.Duration := 0;
            SpecData.RFNFile := Control.RFNfile;
            SpecData.CtrlFile := RFNRec.SetCtrlfile;
            SpecData.Value :=-999;
            SpecData.BaseStart := -999;
            SpecData.BaseStartT := 0;
            SpecData.BaseEnd :=-999;
            SpecData.BaseEndT := 0;
            SpecData.IntStartT := 0;
            SpecData.IntEndT := 0;
            SpecData.Datapoints := 0;
```

```
            CtrlFile := 'mc:\' + RFNRec.SetCtrlfile + '.txt';
            Open(CtrlFile,ReadMode);
            ReadRecord(CtrlFile,ReadRec,100);

            SpecFile := LogDir + '\' +
JulianTime(BinTime(StartCTRLTime,0),'_',0) + '.spc';
            Open(SpecFile,WriteMode);
            WriteHeader(SpecFile,FastData,9);
            work.SpecFileOpen := on;

            while ReadRecord(CtrlFile,ReadRec,200) = 0 do begin
              EndTime := StartCTRLTime + RunTime;
              If proctest = on then begin
                If EndTime > LocTime + 5000 then EndTime := LocTime + 5000;
              end;
              while LocTime < EndTime do begin
                LocTime := LocTime + 1000;
                waitfor(LocTime);
                RunTime := EndTime - LocTime;
                If process <> auto then break;
              end;
              If process <> auto then break;
              if ProcVar = logperiod then logperiod := round(SetValue)
              else if ((1=2) and (ProcVar = BaseStart))   then begin
Specdata.BaseStartT := now; Specdata.BaseStart := CO2Licor; end
              else if ((1=2) and (ProcVar = BaseEnd))     then begin
Specdata.BaseEndT := now; Specdata.BaseEnd := CO2Licor; end
              else if ProcVar = Integration then begin
                                  if SetState = on then begin
                                      Specdata.BaseStartT := now;
Specdata.BaseStart := CO2Licor;
                  Specdata.IntStartT := Specdata.BaseStartT;
                  Specdata.Value := 0;
                  work.Integration := on;
                end else begin
                  Specdata.IntEndT := now;
                  work.Integration := off;
                                  Specdata.BaseEndT := Specdata.IntEndT;
Specdata.BaseEnd := CO2Licor;
                end;
              end
              else if ProcVar = FlushValve  then FlushValv := SetState
              else if ProcVar = BypassValve then BypasValv := SetState
              else if ProcVar = CalValve    then CalValv   := SetState
              else if ProcVar = SampleValve then SmplValv  := SetState
              else if ProcVar = VOCValve    then VOCValv   := SetState
              else if ProcVar = MFCCalHe    then FCalHe.FlowSet  :=
SetValue
              else if ProcVar = MFCCalCO2   then FCalCO2.FlowSet :=
SetValue
              else if ProcVar = MFCCarHe    then FCarHe.FlowSet  :=
SetValue
              else if ProcVar = MFCSample   then FSmpl.FlowSet   :=
SetValue
              else if ProcVar = MFCO2         then FO2.FlowSet     :=
SetValue
                                          else if ProcVar = MFCRefHe
      then FRefHe.FlowSet  := SetValue
              else if ProcVar = MFCQ0         then SetMksCalib.SetMFC0 :=
SetValue
              else if ProcVar = HeaterVOC   then SetVOCTrap := SetValue
              else if ProcVar = HeaterCO2   then SetCO2Trap := SetValue;
              else if ProcVar = SelSampValve then SampValve := SetState;
```

```
              else if ProcVar = CO2Valve then CO2Valv := SetState;
            end;
                        with SpecData do begin
              EndTime := now;
              Duration := EndTime - StartTime;
              sdummy1 := value;
                              value := (sdummy1 - (Datapoints *
(BaseStart+BaseEnd) / 2));
                              sdummy2 := value;
                                          long1 := IntStartT;
                                          long2 := IntEndT;
                    value := (((long2-long1)/1000) / Datapoints);
                    sdummy1 := value;
                    value:= sdummy2 * sdummy1;
                          end;
            work.SpecFileOpen := off;
            Close(SpecFile);
            SpecFile := ' ';
            Close(CtrlFile);
            CtrlFile := ' ';
            if work.DataFileOpen then WriteRecord(DataFile,SpecData,9);
          end;
        end;
        Close(RFNFile);
        if RFNRec.SetCTRLfile <> 'loop' then Process := standby;
      end;
    end;
  end;
end;

procedure HdlSelValve (ValveAddr : LongInst; var SelValve : OffOnType);
var LocTimer : TimeInst;
begin
  with UserData, Control do begin

    On SelValve do begin
      if (SelValve  = on) then begin
        if (ReadWord (ValveAddr) = 0) then begin
          StartTimer(LocTimer,2000,fromNow);
          WriteWord (ValveAddr, SelSampVoltHigh * 140);
        end;
      end
      else WriteWord (ValveAddr, 0);
    end;

    On LocTimer do begin
      if SelValve   = off then WriteWord (ValveAddr, 0);
      else if SelValve   = on then WriteWord (ValveAddr, SelSampVoltLow *
140);
    end;
  end;

  while 0 = 0 do HandleEvents (1);
end;


begin
  with UserData,Param,Control,Data,Work do begin

    with RegVOCTrap do begin
      On TVOCTrap do Input := round(TVOCTrap * 10);
      On SetVOCTrap do SetPoint := round(SetVOCTrap * 10);
      On OutPut do begin
```

```
        If (Process = off) or (Process = manual) or (TVOCTrap  < -200) then
begin
          WriteWord(HeatVOCAddr,0)
        end
        else WriteWord(HeatVOCAddr,OutPut);
      end;
    end;

    with RegCO2Trap do begin
      On TCO2Trap do Input := round(TCO2Trap * 10);
      On SetCO2Trap do SetPoint := round(SetCO2Trap * 10);
      On OutPut do begin
        If (Process = off) or (Process = manual) or (TCO2Trap  < -200) then
begin
          WriteWord(HeatCO2Addr,0);
          SetBit(Valv14,BlowerCO2Mask,0);
        end
        else begin
          WriteWord(HeatCO2Addr,OutPut);
          SetBit(Valv14,BlowerCO2Mask,OutPut=0);
        end;
      end;
    end;

    with RegTLicor do begin
      On TLicor do Input := round(TLicor * 10);
      On SetTLicor do SetPoint := round(SetTLicor * 10);
      On OutPut do If Process <> manual then WriteWord(BlowLicAddr,OutMax-
OutPut);
    end;

    with RegTTubeHeat do begin
      On TTubeHeat do Input := round(TTubeHeat * 10);
      On SetTTubeHeat do SetPoint := round(SetTTubeHeat * 10);
      On OutPut do If Process <> manual then
WriteWord(TubeHeatAddr,OutPut);
    end;

    On CalValv do begin
      If CalValv = on then
        Valv14 := Valv14 and not CalValvMask or (CalValvMask shl 1);
      else
        Valv14 := Valv14 and not (CalValvMask shl 1) or CalValvMask;
    end;

    On SmplValv do begin
      If SmplValv = on then
        Valv14 := Valv14 and not SmplValvMask or (SmplValvMask shl 1);
      else
        Valv14 := Valv14 and not (SmplValvMask shl 1) or SmplValvMask;
    end;

    On FlushValv do begin
      SetBit (Valv14,FlushValvMask,FlushValv);
    end;
    On BypasValv do begin
      SetBit (Valv14,BypasValvMask,BypasValv);
    end;
    On VOCValv do begin
      SetBit (Valv14,VOCValvMask,VOCValv);
    end;
    On BlowerCO2 do begin
      SetBit (Valv14,BlowerCO2Mask,BlowerCO2);
```

```
    end;

    On Pump do begin
      WriteWord(PumpAddr,12 * 140 * (Pump = on));
    end;

    On Valv14 do begin
      WriteWord(Valv14PowAddr,20 * 140 * (Process > off));
      WriteWord(Valv14OutAddr,Valv14);
    end;

            On CO2Valv do begin
                  SelCO2Vlv1 := CO2Valv;
                  SelCO2Vlv2 := CO2Valv;
            end;

            On SampValve do SelSamp := SampValve;

    On ParamSave do begin
      If ParamSave = saving then begin
        ParamSave := _______;
        writetree(ParamFile,Param);
      end;
      If ParamSave = loading then begin
        ParamSave := _______;
        readtree(ParamFile,Param);
      end;
    end;
    WriteWord ($1004,1);

    Logperiod := 10;

    readtree(ParamFile,Param);

    CreateThread('Clock',2048,Clock);

    CreateThread ('RemoteInOut', 2048, RemoteInOut);

    CreateThread('Process',4096,ProcessProc);

    CreateThread('Logger',3072,LogProc);

    CreateThread('HandleMulIO',2048,HandleMulIO);

    CreateThread('ReceiveLicor',4096,ReceiveLicor);

    CreateThread('HdlSelSampValve', 2048, HdlSelValve,SelSampAddr,
SelSamp);
    CreateThread('HdlCO2Valve1', 2048,          HdlSelValve,CO2Valv1Addr,
SelCO2Vlv1);
    CreateThread('HdlCO2Valve2', 2048,          HdlSelValve,CO2Valv2Addr,
SelCO2Vlv2);

    while 0 = 0 do HandleEvents(0);
  end;
end;
```

Parameter file:

```
AutoStart  off
SetVOCTrap  35.0
SetCO2Trap  30.0
```

```
SetTLicor   38.0
SetTTubeHeat  50.0

SetMksLoc >

FCalHe   >
FlowSet     50.0
FlowSize    154.7
FlowOffs    0.0000
FlowGain    1.0000

FCalCO2  >
FlowSet     0.0
FlowSize    11.2
FlowOffs    0.0000
FlowGain    1.0000

FCarHe   >
FlowSet     50.0
FlowSize    780.3
FlowOffs    1.2000
FlowGain    1.0000

FSmpl    >
FlowSet     0.0
FlowSize    515.6
FlowOffs   -0.2000
FlowGain    1.0600

FO2      >
FlowSet     0.0
FlowSize    55.2
FlowOffs    0.1800
FlowGain    1.0400

FName1   >
FlowSet     0.0
FlowSize    100.0
FlowOffs    0.0000
FlowGain    1.0000

FName2   >
FlowSet     0.0
FlowSize    100.0
FlowOffs    0.0000
FlowGain    1.0000

FRefHe   >
FlowSet     50.0
FlowSize    768.7
FlowOffs    0.0000
FlowGain    0.9900

SetMksCalib >

Remote   >
SetFCar     0.0
SetO2P      0.0

TVOCTrap >
TempOffs   -4.0000
TempGain    0.1620
```

```
TCO2Trap >
TempOffs   -34.0000
TempGain    0.1620

TOven    >
TempOffs    14.0000
TempGain    1.5100
FiltTemp    11000.0
LogPeriod  1

RegVOCTrap >
PropBand   200
IntTime    5000
DiffTime   1000
SamplePeriod 500
OutMax     255
OutMin     0
IntBrake   0

RegCO2Trap >
PropBand   200
IntTime    15000
DiffTime   5000
SamplePeriod 500
OutMax     255
OutMin     0
IntBrake   0

RegTLicor >
PropBand   200
IntTime    120000
DiffTime   5000
SamplePeriod 500
OutMax     3500
OutMin     0
IntBrake   0

RegTTUbeHeat >
PropBand   200
IntTime    120000
DiffTime   5000
SamplePeriod 500
OutMax     255
OutMin     0
IntBrake   0

Com2     >

Com3     >
IntegOffs   0.000
IntegSpan   1.000
```

Method file:

NMOC sampling:

```
00:00:00    HeCO2
00:17:00    TestCO2
00:52:00    SYSCO2
01:09:00    KatCO2
01:31:00    TestSam
02:06:00    loop
```

Calibration with a carrier gas flow of 50 ml min^{-1}

```
00:00:00    Cal8
00:17:00    Cal7
00:34:00    Cal6
00:51:00    Cal5
01:08:00    Cal4
01:25:00    Cal3
01:42:00    Cal2
01:59:00    Cal1
02:16:00    HeCO2
02:33:00    loop
```

Program file:

TestSam (=$area_{NMOCSample}$):

```
time        variable    state value
00:00:00    CalValve    off
00:00:00    FlushValve  off
00:00:00    MFCSample   on    285
00:00:01    HeaterVOC   on    35
00:00:01    HeaterCO2   on    30
00:01:00    VOCValve    on
00:10:00    MFCO2       on    5
00:11:00    FlushValve  on
00:11:00    MFCSample   on    500
00:14:00    SampleValve on
00:14:00    MFCSample   on    25
00:14:01    HeaterVOC   on    35
00:19:00    CO2Valve    on
00:19:00    HeaterVOC   on    250
00:27:00    HeaterVOC   on    35
00:27:00    MFCO2       off   0
00:27:01    CalValve    on
00:27:01    Integration on
00:27:02    HeaterCO2   on    200
00:33:02    HeaterCO2   off   30
00:34:30    Integration off
00:34:59    SampleValve off
00:34:59    VOCValve    off
00:34:59    CO2Valve    off
```

TestCO2 (=$area_{CO2Sample}$):

```
time        variable    state value
00:00:00    CalValve    on
00:00:00    FlushValve  off
00:00:00    MFCSample   on    285
00:00:01    HeaterVOC   on    35
00:00:01    HeaterCO2   on    30
00:01:00    VOCValve    on
00:10:00    MFCO2       on    5
00:11:00    FlushValve  on
00:11:00    MFCSample   on    500
00:14:00    SampleValve on
00:14:00    MFCSample   on    25
00:14:01    HeaterVOC   on    35
00:19:00    CO2Valve    on
00:19:00    HeaterVOC   on    250
```

```
00:27:00    HeaterVOC   on    35
00:27:00    MFCO2       off   0
00:27:01    Integration on
00:27:02    HeaterCO2   on    200
00:33:02    HeaterCO2   off   30
00:34:30    Integration off
00:34:59    SampleValve off
00:34:59    VOCValve    off
00:34:59    CO2Valve    off
```

HeCO2

```
time        variable          state value
00:00:00    CalValve          on
00:01:00    CO2Valve          on
00:01:01    HeaterVOC         on    35
00:01:01    HeaterCO2         on    30
00:09:01    Integration       on
00:09:02    HeaterCO2         on    200
00:15:02    HeaterCO2         off   30
00:16:30    Integration       off
00:16:59    CO2Valve          off
```

SysCO2

```
time        variable          state value
00:00:00    CalValve          off
00:01:00    CO2Valve          on
00:01:01    HeaterVOC         on    35
00:01:01    HeaterCO2         on    30
00:09:01    CalValve          on
00:09:01    Integration       on
00:09:02    HeaterCO2         on    200
00:15:02    HeaterCO2         off   30
00:16:30    Integration       off
00:16:59    CO2Valve          off
```

KatCO2

```
time        variable          state value
00:00:00    CalValve          off
00:00:00    MFCO2             on    5
00:06:00    CO2Valve          on
00:06:01    HeaterVOC         on    35
00:06:01    HeaterCO2         on    30
00:14:00    MFCO2             off   0
00:14:01    CalValve          on
00:14:01    Integration       on
00:14:02    HeaterCO2         on    200
00:20:02    HeaterCO2         off   30
00:21:30    Integration       off
00:21:59    CO2Valve          off
```

Calibration (example file: Cal3):

```
time        variable          state value
00:00:00    HeaterCO2         on    30
00:00:00    MFCCalCO2         on    10
00:00:01    MFCCalHe          on    50.1
00:01:00    CO2Valve          on
```

```
00:03:00    CalValve          on
00:04:00    CalValve          off
00:09:01    Integration       on
00:09:02    HeaterCO2         on    200
00:09:03    MFCCalHe          off   0
00:09:04    MFCCalCO2         off   0
00:15:02    HeaterCO2         off   30
00:16:30    Integration       off
00:16:59    CO2Valve          off
```